

INFORMATION TO USERS

This manuscript has been reproduced from the microfilm master. UMI films the text directly from the original or copy submitted. Thus, some thesis and dissertation copies are in typewriter face, while others may be from any type of computer printer.

The quality of this reproduction is dependent upon the quality of the copy submitted. Broken or indistinct print, colored or poor quality illustrations and photographs, print bleedthrough, substandard margins, and improper alignment can adversely affect reproduction.

In the unlikely event that the author did not send UMI a complete manuscript and there are missing pages, these will be noted. Also, if unauthorized copyright material had to be removed, a note will indicate the deletion.

Oversize materials (e.g., maps, drawings, charts) are reproduced by sectioning the original, beginning at the upper left-hand corner and continuing from left to right in equal sections with small overlaps.

Photographs included in the original manuscript have been reproduced xerographically in this copy. Higher quality 6" x 9" black and white photographic prints are available for any photographs or illustrations appearing in this copy for an additional charge. Contact UMI directly to order.

Bell & Howell Information and Learning
300 North Zeeb Road, Ann Arbor, MI 48106-1346 USA
800-521-0600

UMI[®]

**GPS 3-D COCKPIT DISPLAYS:
SENSORS, ALGORITHMS, AND FLIGHT TESTING**

A DISSERTATION

SUBMITTED TO THE DEPARTMENT OF AERONAUTICS AND ASTRONAUTICS

AND THE COMMITTEE ON GRADUATE STUDIES

OF STANFORD UNIVERSITY

IN PARTIAL FULFILLMENT OF THE REQUIREMENTS

FOR THE DEGREE OF

DOCTOR OF PHILOSOPHY

Andrew Kevin Barrows

May 2000

UMI Number: 9986061

Copyright 2000 by
Barrows, Andrew Kevin

All rights reserved.

UMI[®]

UMI Microform 9986061

Copyright 2000 by Bell & Howell Information and Learning Company.
All rights reserved. This microform edition is protected against
unauthorized copying under Title 17, United States Code.

Bell & Howell Information and Learning Company
300 North Zeeb Road
P.O. Box 1346
Ann Arbor, MI 48106-1346

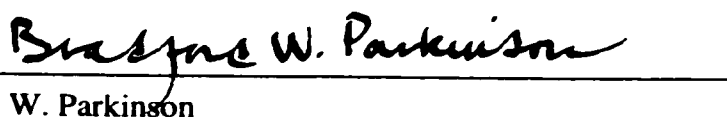
© Copyright by Andrew Kevin Barrows 2000

All Rights Reserved

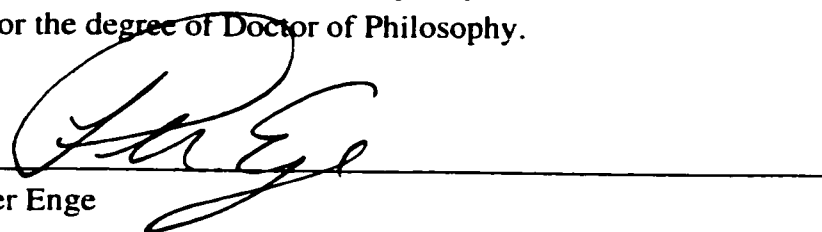
I certify that I have read this dissertation and that in my opinion it is fully adequate, in scope and quality, as a dissertation for the degree of Doctor of Philosophy.


J. David Powell, Principal Adviser

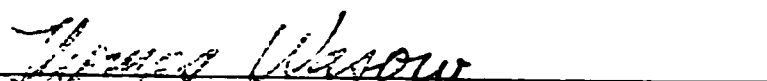
I certify that I have read this dissertation and that in my opinion it is fully adequate, in scope and quality, as a dissertation for the degree of Doctor of Philosophy.


Bradford W. Parkinson

I certify that I have read this dissertation and that in my opinion it is fully adequate, in scope and quality, as a dissertation for the degree of Doctor of Philosophy.


Per Enge

Approved for the University Committee on Graduate Studies:



Abstract

Tunnel-in-the-Sky 3-D flight displays have been investigated for several decades as a means of enhancing aircraft safety and utility. However, high costs have prevented commercial development and seriously hindered research into their operational benefits. The rapid development of Differential Global Positioning Systems (DGPS), inexpensive computing power, and ruggedized displays is now changing this situation. A low-cost prototype system was built and flight tested to investigate implementation and operational issues. The display provided an “out the window” 3-D perspective view of the world, letting the pilot see the horizon, runway, and desired flight path even in instrument flight conditions. The flight path was depicted as a tunnel through which the pilot flew the airplane, while predictor symbology provided guidance to minimize path-following errors. Positioning data was supplied by various DGPS sources including the Stanford Wide Area Augmentation System (WAAS) testbed. A combination of GPS and low-cost inertial sensors provided vehicle heading, pitch, and roll information.

Architectural and sensor fusion tradeoffs made during system implementation are discussed. Computational algorithms used to provide guidance on curved paths over the

earth geoid are outlined along with display system design issues. It was found that current technology enables low-cost Tunnel-in-the-Sky display systems with a target cost of \$20,000 for large-scale commercialization. Extensive testing on Piper Dakota and Beechcraft Queen Air aircraft demonstrated enhanced accuracy and operational flexibility on a variety of complex flight trajectories. These included curved and segmented approaches, traffic patterns flown on instruments, and skywriting by instrument reference. Overlays to existing instrument approaches at airports in California and Alaska were flown and compared with current instrument procedures. These overlays demonstrated improved utility and situational awareness for non-precision procedures, operations to closely spaced parallel runways, and noise abatement. A database of inflight path-following errors on straight and curved segments of varying radius was developed to aid Tunnel-in-the-Sky instrument approach procedure design. The aggregate results demonstrate that low-cost Tunnel-in-the-Sky primary flight displays can provide intuitive landing guidance, precision navigation on complex flight paths, and increased safety through improved situational awareness.

Acknowledgments

Foremost thanks go to my dissertation adviser, Prof. J. David Powell, for his outstanding mentoring offered with a healthy dose of enthusiasm. “Professor Powder’s” balanced outlook on research, teaching, and life in general made my Ph.D. experience highly enjoyable and rewarding. This project would never have “taken off” without his patience as owner and test pilot of Dakota N434IM.

Prof. Brad Parkinson’s keen insights into complex projects were instrumental in guiding my approach to this research. His allowing me to impersonate an AA242 professor was a highlight in my development as a teacher. Prof. Per Enge’s leadership of the WADGPS Lab, willingness to let me manage a flight test program, and careful reading of this dissertation greatly added to the end result. The GPS program these three educators have created at Stanford is an incredibly fertile and stimulating environment.

By its nature, this systems engineering project relied on the efforts of many people in the Stanford GPS Lab. Work by members of the Wide Area Differential GPS and Integrity Beacon Landing System groups led to the remarkable navigation systems used for the flight tests. Keith Alter and Chad Jennings supported this work and later

propelled it in new directions. Roger Hayward and Demoz Gebre-Egziabher created the GPS/rate gyro attitude system that was the final technology piece in the Tunnel-in-the-Sky puzzle. Awele Ndili and Demoz Gebre-Egziabher produced the Hollywood-quality videos documenting the experiments, and Sharon Houck kept flight tests productive with her Navy jet experience. Tom Langenstein shepherded me through setting up flight test funding, and Jeff Wade worked all hours to keep the computers at GP-B functional. Sincere thanks go to Jock Christie and Glenn Lightsey who kept me sane and endured disorganization in my half of the cubicle. Working with such top-notch people was a joy!

I'm indebted to Sky, Kevin McCoy, and Ben Hovelman of Sky Research, Inc. for first-rate flight test services onboard Queen Air N6890Q and for their encouragement of Stanford's research. Palo Alto Airport management, the Palo Alto Civil Air Patrol, and Moffett Field flight operations all provided invaluable support of flight testing.

I gratefully acknowledge the support of the FAA Satellite Program Office and of NASA. Their willingness to sponsor forward-looking university research is a valued long-term investment. Trimble Navigation graciously donated a TANS Vector GPS receiver used in flight testing.

Thanks to my many friends - especially FAT-FARM alumni past and present - who made the last several years fun as well as educational. For his sage advice on writing this dissertation, Glenn Marcus has earned tenure on my personal faculty!

Finally, deepest thanks go to my family. Sitting on my father's shoulders at Cape Canaveral to watch the Apollo 17 liftoff launched a five-year-old's fascination with things that fly. In my pursuit of that fascination, my mother Nancy and sister Kris have always given me their unending love and support. I dedicate this dissertation to them.

Table of Contents

Abstract iv

Acknowledgments vi

Table of Contents viii

List of Tables xii

List of Figures..... xiii

Chapter 1: Introduction..... 1

 1.1 Novel Aspects of This Work 3

 1.1.1 Identification of Fundamental Systems Engineering
 Tradeoffs and Building a Low-Cost Tunnel-in-the-Sky
 Display 3

 1.1.2 Flight Tests of a Tunnel-in-the-Sky Display on a Single-
 Engine Piston Airplane 4

 1.1.3 Extensive Flight Test Campaign in a Variety of Operational
 Environments 4

 1.1.4 Tunnel-in-the-Sky Overlay Approaches Compatible with
 the Current Air Traffic Control System..... 5

1.2	Overview	5
Chapter 2: Background		8
2.1	Current Instrument Flying Practice.....	8
2.1.1	Primary Flight Instruments	9
2.1.2	Radio Navigation Aids	11
2.1.3	Instrument Approaches	13
2.1.4	Motivation.....	16
2.2	Objectives.....	17
2.2.1	Increased Safety through Situational Awareness	17
2.2.2	Enhanced Utility through Flight-Path Flexibility.....	18
2.3	Tunnel-in-the-Sky Display Concept	19
2.4	Previous Simulation Studies.....	21
2.5	Previous Inflight Demonstrations	23
2.6	Enabling Technologies.....	27
2.6.1	Global Positioning System.....	27
2.6.2	Low-Cost Inertial Sensors.....	28
2.6.3	Computers	28
2.6.4	Graphics Hardware	28
2.6.5	Flat-Panel Displays.....	29
2.7	Systems Engineering Approach of This Work.....	29
Chapter 3: Sensor Fusion.....		32
3.1	Sensor Accuracy	32
3.2	Sensor Responsiveness	33
3.2.1	Bandwidth	33
3.2.2	Sensor Sample Rate and Latency	34
3.2.3	Display Framerate and Latency.....	34
3.2.4	System Latency	35
3.3	Sensor Jitter	37
3.4	Position Sensors.....	37
3.4.1	Inertial Navigation Systems	38
3.4.2	Global Positioning System.....	39
3.4.3	Positioning for the Prototype System	41
3.5	Attitude Sensors.....	43
3.5.1	Attitude Heading Reference Systems	44

3.5.2	GPS Attitude	45
3.5.3	Integrated GPS and Inexpensive Inertial Sensors	45
3.5.4	Attitude for the Prototype System	46
3.6	Other Sensors.....	47
3.7	Display Domain Errors	48
Chapter 4: Algorithms		53
4.1	Segmented Flight Path Representation	53
4.2	Geoid Earth Model.....	55
4.3	Realtime Segment Computations	58
4.3.1	Geodetic Path Segments	59
4.3.2	Cartesian Path Segments.....	62
4.4	Compensation for Numerically Induced Jitter	63
Chapter 5: Display Design		69
5.1	Design Philosophy	69
5.2	Display Elements	71
5.2.1	Frame of Reference	71
5.2.2	Tunnel Depiction.....	74
5.2.3	Predictive Guidance Symbolology	75
5.2.4	Other Information.....	78
5.3	Evolution of Display in Response to Pilot Evaluations	79
5.3.1	Added Horizontal and Vertical Deviation Indicators.....	80
5.3.2	Tightened Hoop Spacing	81
5.3.3	Added Predictor Guidance Symbolology	81
5.3.4	Moved Guidance Symbolology into Central Field of View	81
5.3.5	Eliminated Gradient Horizon and Increased Contrast.....	83
5.3.6	Increased Symbol Size and Added Shadowing.....	83
5.3.7	Decluttered Center of Display	84
5.4	Display Hardware	84
Chapter 6: Piloted Simulation Tests.....		87
6.1	Experimental Simulator	87
6.2	Methodology.....	89
6.3	Straight-In Approaches with Varying Winds.....	89
6.4	Curved and Segmented Approaches	95

6.5	ILS Approaches Flown by a Student Pilot	102
6.6	Skywriting with GPS	103
6.7	General Discussion	104
Chapter 7: Flight Tests		105
7.1	Flight Test Aircraft	105
7.1.1	Piper Dakota.....	106
7.1.2	Beechcraft Queen Air	107
7.2	Methodology	108
7.3	Initial Flight Testing	109
7.3.1	Straight-In Approaches.....	110
7.3.2	Approaches with GPS as the Sole Sensor.....	113
7.4	Expanded Flight Operations.....	114
7.4.1	Curved and Segmented Approaches.....	114
7.4.2	Flying Traffic Patterns on Instruments	117
7.4.3	Skywriting Using GPS.....	119
7.5	Operating Within the Current Airspace System	120
7.5.1	Precision Approaches for a Non-Precision Airport.....	120
7.5.2	Approaches for Closely-Spaced Parallel Runways	124
7.5.3	Noise Abatement Approaches.....	129
7.6	Generating a Prototype Flight Technical Error Dataset.....	132
7.7	General Discussion	136
Chapter 8: Conclusion		138
8.1	Summary of Results.....	138
8.1.1	Human-Machine Interface Results	139
8.1.2	Implementation Results	140
8.1.3	Operations Results.....	141
8.2	Project Conclusions	143
8.3	Related and Future Work	144
8.4	Future Synthetic Vision Applications.....	146
8.5	Epilogue	147
References.....		149

List of Tables

Table 3.1	Candidate Tunnel-in-the-Sky Position Sensors.....	42
Table 3.2	Candidate Tunnel-in-the-Sky Attitude Sensors.....	46
Table 6.1	Wind Conditions for Straight-In Approaches	90
Table 6.2	Wind Conditions for Curved and Segmented Approaches	96
Table 7.1	Prototype FTE Dataset Results.....	135

List of Figures

Figure 1.1	Stanford Tunnel-in-the-Sky Display	1
Figure 1.2	Tunnel-in-the-Sky System Overview	6
Figure 2.1	Light Aircraft Instrument Panel	9
Figure 2.2	Boeing 777 Primary Flight Display.....	10
Figure 2.3	Instrument Landing System Needle Display	12
Figure 2.4	Three Supporting Pillars for Tunnel-in-the-Sky Systems	31
Figure 3.1	Angular Mapping of Perspective Projection.....	49
Figure 3.2	Effect of Attitude Error on Onscreen Position.....	49
Figure 3.3	Effect of Position Error on Onscreen Position.....	51
Figure 4.1	Linked Segment Flight Path Description (Overhead View).....	54
Figure 4.2	Flat Plate Earth Model	55
Figure 4.3	Geodetic Path Segment.....	60
Figure 4.4	Cartesian Path Segment	63
Figure 4.5	Viewer and World Coordinate Systems	64
Figure 4.6	Addition of a Local Coordinate System	67
Figure 5.1	Final Stanford Tunnel-in-the-Sky Display Configuration.....	72
Figure 5.2	Initial Stanford Tunnel-in-the-Sky Display Configuration.....	80
Figure 5.3	Intermediate Stanford Tunnel-in-the-Sky Display Configuration	82
Figure 6.1	Experimental Simulator Setup	88
Figure 6.2	Overhead View of Straight-In Test Procedure.....	91
Figure 6.3	Vertical FTE on Straight-In Approaches	92
Figure 6.4	Lateral FTE on Straight-In Approaches	92

Figure 6.5	Lateral Flight Path Intercept on Straight-In Approaches.....	93
Figure 6.6	Overhead View of Straight-In Approaches	94
Figure 6.7	Overhead View of Curved Approaches (Pilots A and B).....	97
Figure 6.8	FTE on Curved Approaches (Pilot A, Student Pilot)	98
Figure 6.9	FTE on Curved Approaches (Pilot B, 210-Hour Instrument Pilot).....	99
Figure 6.10	Overhead View of Segmented Approaches (Pilots A and B)	99
Figure 6.11	FTE on Segmented Approaches (Pilot A, Student Pilot)	100
Figure 6.12	FTE on Segmented Approaches (Pilot B, 210-Hour Instrument Pilot).....	101
Figure 6.13	Skywriting with GPS (Piloted Simulation).....	104
Figure 7.1	Piper Dakota N4341M Test Aircraft	106
Figure 7.2	Beechcraft Queen Air N6890Q Test Aircraft	107
Figure 7.3	Queen Air Instrument Panel with Tunnel-in-the-Sky Display	108
Figure 7.4	Straight-In Approaches Vertical FTE.....	111
Figure 7.5	Straight-In Approaches Lateral FTE	112
Figure 7.6	Overshoot Using ILS Needles for Lateral Flight Path Intercept.....	112
Figure 7.7	Segmented Approaches	115
Figure 7.8	FTE on Segmented Approaches.....	115
Figure 7.9	Curved Approaches	116
Figure 7.10	Traffic Patterns Flown on Instruments	118
Figure 7.11	Tight Traffic Patterns on Instruments.....	118
Figure 7.12	Skywriting with GPS (Beechcraft Queen Air).....	119
Figure 7.13	VOR/DME Approach Plate for Palo Alto, California Runway 30	122
Figure 7.14	Profile View of Palo Alto VOR/DME Approach.....	124
Figure 7.15	LOC/DME Approach Plate for Moffett Field, California Runway 32R	126
Figure 7.16	Overhead View of Moffett Field LOC/DME Approach.....	127
Figure 7.17	Profile View of Moffett Field LOC/DME Approach	128
Figure 7.18	Profile View of Moffett Field Noise-Reducing Approaches	131
Figure 7.19	Prototype FTE Dataset Patterns (Actual Flight Data)	134

Chapter 1:

Introduction

The primary flight display of the future will be based on a 50-year-old idea enabled by present-day technology:

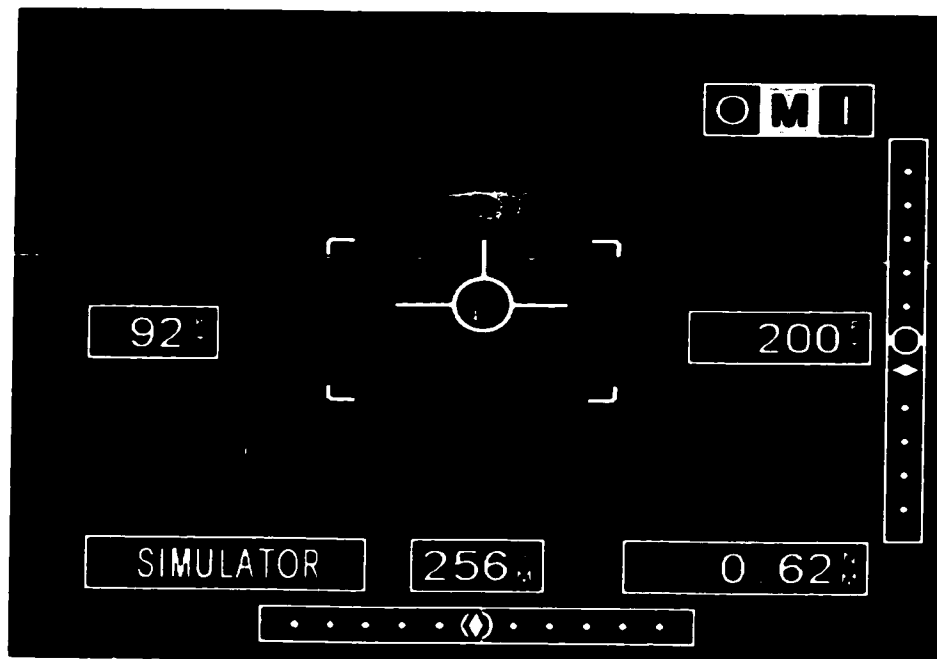


Figure 1.1 Stanford Tunnel-in-the-Sky Display

Today's civil aircraft fly with cockpit display concepts that are half a century old - in the form of a loosely integrated set of indicators, dials, and gauges. Instrument flying is therefore not an easy task. The rigors of initial training, the cost of maintaining instrument currency, and the persistence of accidents involving loss of situational awareness remain major concerns for instrument pilots in every segment of aviation. Advances such as the Global Positioning System (GPS) and electronic displays can improve this situation. To date, however, GPS positioning has typically been used in conventional bearing/distance formats or with a moving map. With few exceptions, the flat panel displays on airline flight decks are computer-generated versions of roughly the same instrument information found in personal aircraft. In this sense, *commercial avionics have barely begun to take advantage of the full 3-D sensing and display capabilities offered by modern technology.*

Another 50-year-old idea, the *Tunnel-in-the-Sky display*, promises safety and operational benefits for instrument flight. This concept, sometimes referred to as *synthetic vision*, uses a cockpit display to present an "out the window" view of the world, allowing the horizon, runway, and desired flight path to be seen even in instrument flying conditions. Tunnel-in-the-Sky research and development has been underway for more than five decades. Despite promising workload and path-following accuracy results on hand-flown procedures, these systems have not yet found their way into commercial or private aviation. However, rapid development of such technologies as GPS, inexpensive embeddable computers, and flat panel displays is now enabling this cockpit revolution.

To address commercialization and widespread use of the technology, a Tunnel-in-the-Sky prototype was developed. The display (shown in Figure 1.1) was tested in piloted simulation and extensive real-world flight testing on small aircraft. The approach of this effort was to complement previous work on the human-machine interface with a

low-cost and operationally oriented approach to flight testing. This research demonstrated that Tunnel-in-the-Sky displays can offer significant safety and operational benefits over conventional displays, and that the technology now exists for viable production systems.

1.1 Novel Aspects of This Work

The contributions of this research are as follows:

1.1.1 Identification of Fundamental Systems Engineering Tradeoffs and Building a Low-Cost Tunnel-in-the-Sky Display

In light of previous emphasis on simulation and sparseness of real flight experience, an overriding project goal was to test a Tunnel-in-the-Sky system on a light aircraft. The assumption was that a system that meets the budget, power, and form-factor constraints of light aircraft could meet those constraints in larger aircraft. A low-cost approach was adopted in building the Tunnel-in-the-Sky system, using commodity hardware wherever feasible. (Based on the successful flight program and continuing cost trends, synthetic vision systems costing \$20,000 or less appear to be a reasonable target for commercialization.)

Sensor tradeoffs were identified based on requirements of the pilot and the flying task involved. Techniques for realtime data fusion using the selected GPS and inertial sensors were developed. The need to accurately model the earth's true shape for takeoff-to- touchdown systems was identified, leading to development of realtime algorithms for guidance on curved paths over the earth geoid. Results of previous human factors work were incorporated into a display design that evolved during continuing flight testing. A computer, 3-D graphics hardware, and a flat panel display were integrated into a Tunnel-in-the-Sky prototype.

1.1.2 Flight Tests of a Tunnel-in-the-Sky Display on a Single-Engine Piston Airplane

In 1995, the first known flight of a digital 3-D Tunnel-in-the-Sky system on a single-engine airplane (a Piper Dakota) was made with the Stanford display. Considering the sensor suite and aircraft type chosen, *this was also the lowest-cost Tunnel-in-the-Sky prototype and flight test demonstration to date.*

In 1996, the system was flown using GPS positioning and multiple-antenna GPS attitude determination with no other inertial, air data, magnetic, or radionavigation sensors. This is the first known flight of a Tunnel-in-the-Sky display driven solely by GPS.

1.1.3 Extensive Flight Test Campaign in a Variety of Operational Environments

After straight-in instrument approaches on the Piper Dakota, a wide variety of tests on a Beechcraft Queen Air demonstrated situational awareness and operational benefits of practical Tunnel-in-the-Sky displays. The system's capabilities were investigated on closed patterns including curved and segmented approaches. Additional close-in work included visual traffic patterns flown solely by instrument reference. GPS-guided skywriting demonstrated enhanced pilot situational awareness on extremely complex flight paths. Feedback from the seven project pilots (ranging from a 210-hour Private Pilot to a 15,000-hour Airline Transport Pilot) was incorporated into the evolving display design.

The test program ultimately achieved 115 Tunnel-in-the-Sky approaches, five of which were flown in actual instrument conditions (with a safety pilot monitoring certified navigation instruments). Operations were conducted at six different airports in California

and Alaska. *This Tunnel-in-the-Sky flight test program encompassed the widest range of procedure types, operational environments, airports, and pilots to date.*

1.1.4 Tunnel-in-the-Sky Overlay Approaches Compatible with the Current Air Traffic Control System

A transition to the operational flexibility of Tunnel-in-the-Sky instrument flying will require extensive cultural changes within aviation. New certification, training, and operational procedures will be required. Based on prior aviation history, the changeover could last decades and will require new Tunnel-in-the-Sky operational concepts to coexist with legacy Air Traffic Control (ATC) procedures. To demonstrate the necessary compatibility, *Tunnel-in-the-Sky overlay approaches* were designed to allow use of the new technology within today's airspace system.

The procedures were flown on the Beechcraft Queen Air in the busy airspace of the San Francisco Bay area. Vertical guidance was added to a non-precision approach to reduce workload and enhance safety. Accurate GPS guidance overlaid on a long straight-in final approach demonstrated accuracy required for instrument operations on parallel runways. The ability to reduce ground noise exposure through flexible vertical guidance overlaid on an existing non-precision approach was illustrated. Air traffic controllers noted nothing atypical, except - perhaps - that the procedures were flown more accurately than usual!

1.2 Overview

Figure 1.2 shows the Tunnel-in-the-Sky display system architecture in schematic form. Chapter 2 provides background on instrument flying and previous work done with Tunnel-in-the-Sky displays. An integrated approach to system development based on three "pillars" (human-machine interface, implementation, and operations) is introduced.

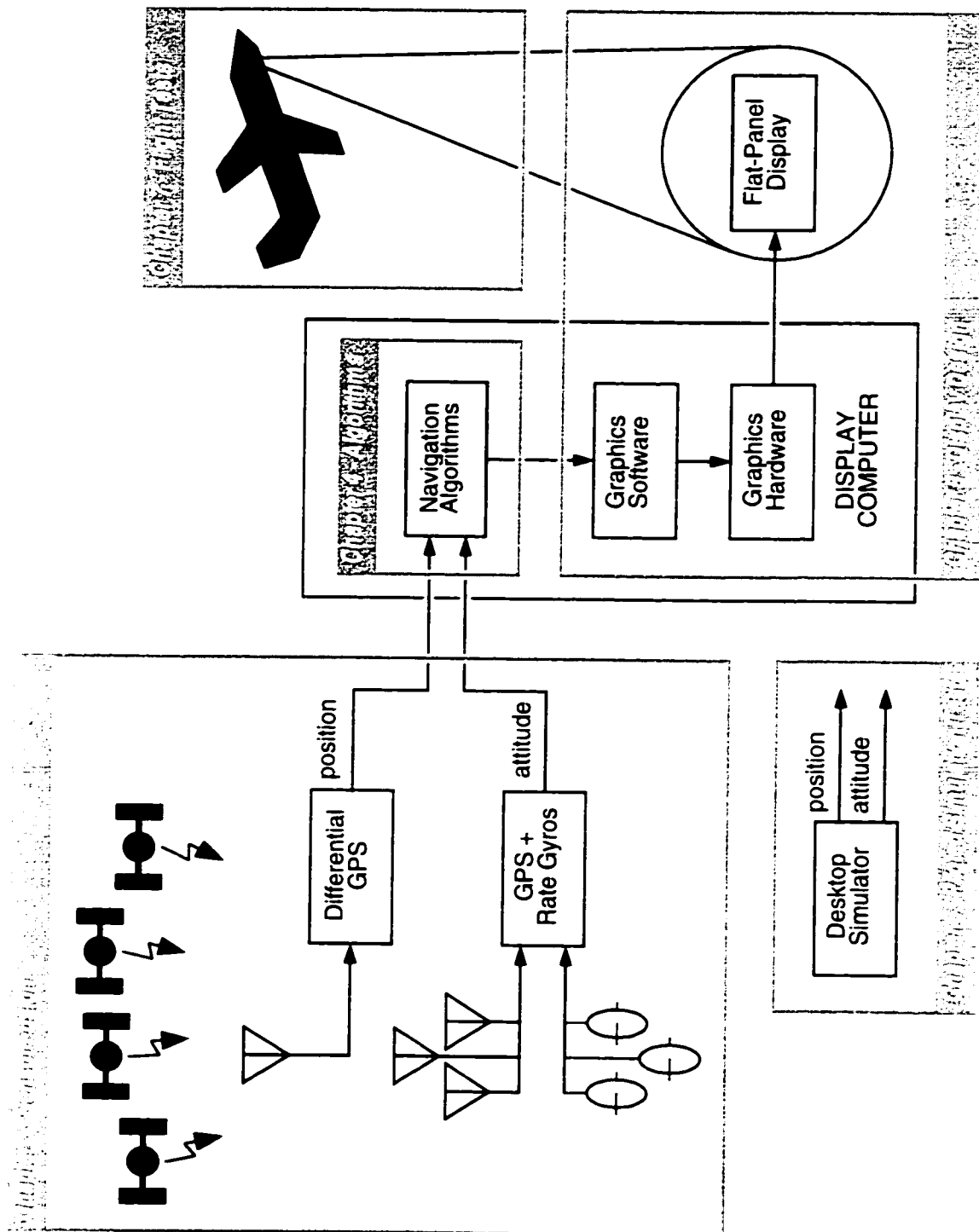


Figure 1.2 Tunnel-in-the-Sky System Overview

Requirements for and fusion of the GPS and inertial sensor data are described in Chapter 3. Algorithms for Tunnel-in-the-Sky navigation and guidance over the earth's curved surface are discussed in Chapter 4. Design of the display and computer hardware is treated in Chapter 5.

Chapter 6 describes the piloted simulation trials used to develop and refine the display prototype, and Chapter 7 documents flight testing on Piper Dakota and Beechcraft Queen Air aircraft. Chapter 8 summarizes the conclusions of this work.

Chapter 2:

Background

This chapter describes current problems in instrument flying and introduces the Tunnel-in-the-Sky display concept intended to address them. Sections 2.1 and 2.2 outline instrument flying practice and motivate the need for better instrumentation. Previous Tunnel-in-the-Sky display work and enabling technology developments are covered in Sections 2.3 through 2.6. Section 2.7 describes the systems engineering approach used in this research.

2.1 Current Instrument Flying Practice

Flying in poor weather solely by instrument reference is one of the most critical challenges faced by pilots. The cockpits of today's large and small aircraft are based on instruments invented 50 years ago. Pilots integrate information from these varied sources to form a mental picture of where the aircraft is and where it should be going. A significant amount of training and skill is required to maintain this "big picture" awareness and to fly instrument procedures smoothly by hand.

2.1.1 Primary Flight Instruments

During instrument flight, the pilot looks at separate instruments and integrates the information into awareness of the overall situation. This information fusion is called an *instrument scan*. Figure 2.1 shows a typical light aircraft instrument panel.

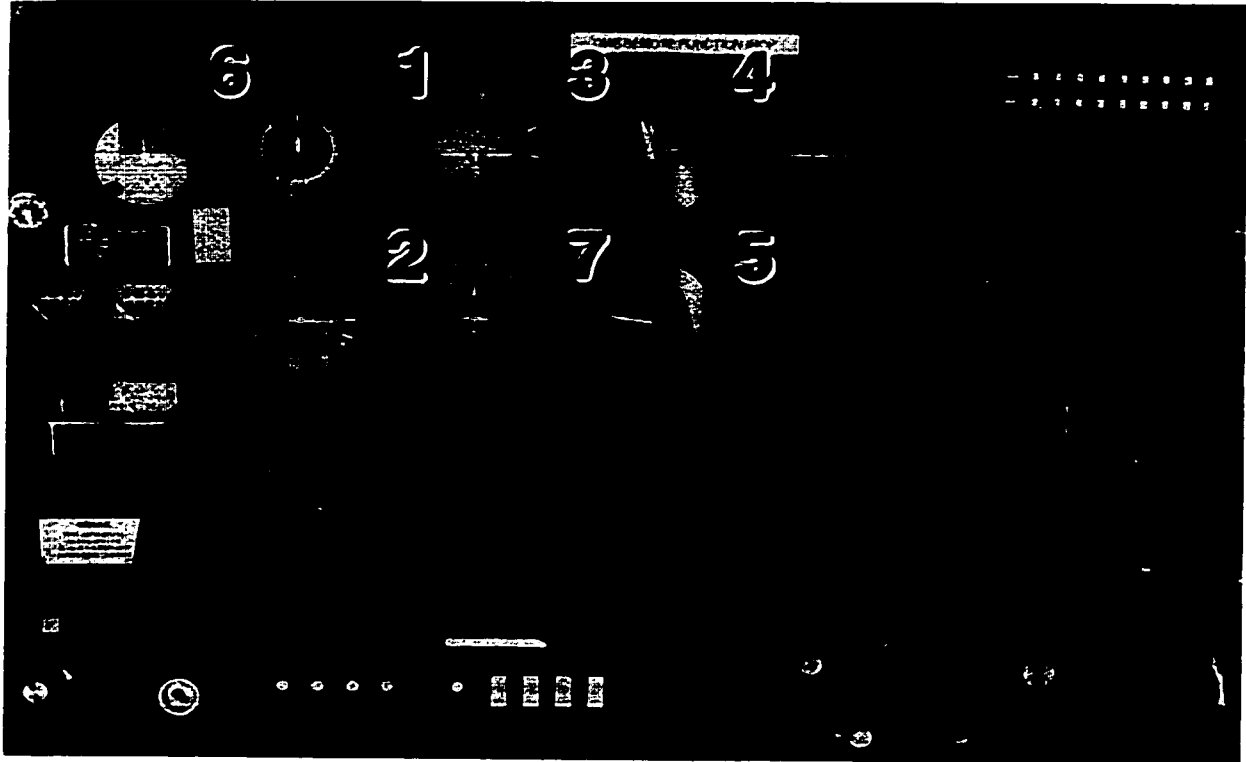


Figure 2.1 Light Aircraft Instrument Panel

Basic pitch and roll information appears on the attitude indicator (also called an artificial horizon) at (1) in Figure 2.1. Since it represents the tightest level of inner-loop flight dynamics, it is the focal point of the instrument scan. The heading indicator (2) presents the third element of aircraft attitude.

The barometric altimeter (3) conveys vertical location information. Horizontal location (and vertical information if a glideslope is being received) is inferred from radionavigation instruments (4 and 5) described in the next subsection. Although the

pictured instrument panel does not contain a GPS receiver, this is now standard on new aircraft. Altitude and horizontal location combine to form position in three dimensions.

The airspeed indicator (6) and the vertical speed indicator (7) combine with aircraft direction (2) to provide 3-D velocity data from the instrument panel above.

Flight decks of modern airliners employ Electronic Flight Information System (EFIS) technology that presents primary and navigational flight data on reconfigurable displays. The Primary Flight Display (PFD) for the Boeing 777 is shown in Figure 2.2 (courtesy of Honeywell) as an example.

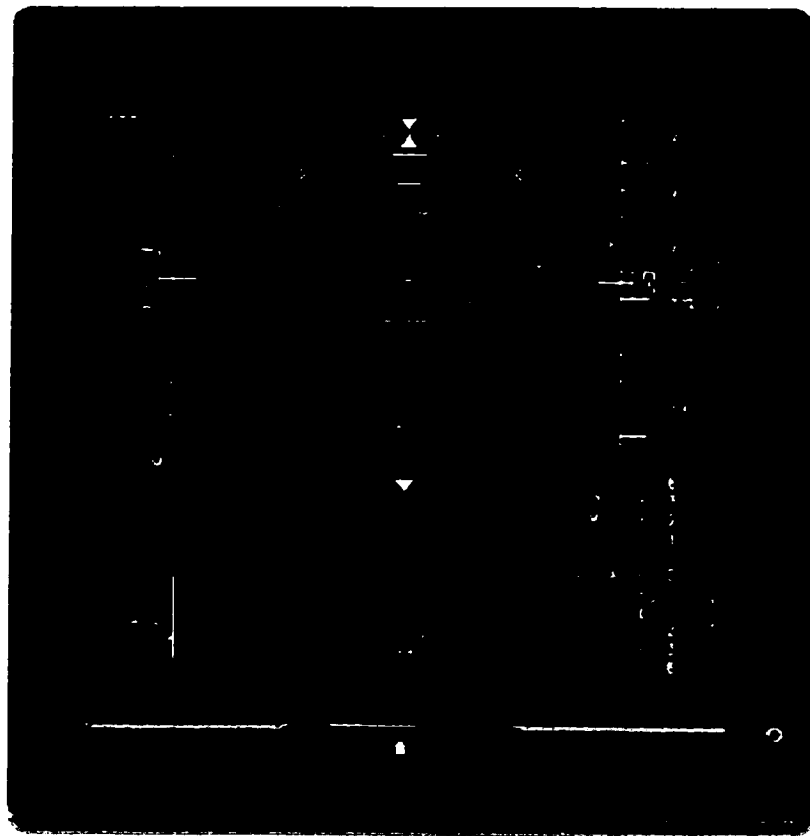


Figure 2.2 Boeing 777 Primary Flight Display

This PFD incorporates many improvements to the light aircraft cockpit above. Airspeed and altitude “tapes” facilitate the instrument scan while flight director guidance

provides steering commands. The companion Navigation Display (ND) depicts weather and terrain on a moving map. However, these modern instruments still present attitude, position, and velocity in a format requiring additional interpretation by the pilot.

The instruments in both classes of aircraft convey at least nine dynamic quantities: 3-D attitude, 3-D position, and 3-D velocity. On a clear day, the pilot instinctively extracts many of these cues from the visual scene. During instrument flight, assessing this “big picture” from a collection of indicators becomes a much more demanding task.

2.1.2 Radio Navigation Aids

Radio navigation aids (or *navaids*) provide electronic signals for navigation without visual ground contact. The navaids in current use have one common characteristic: *they all employ primitive indicators that require pilot interpretation*. They include (in rough order of date of introduction and increasing accuracy):

Automatic Direction Finder (ADF)

ADF provides relative bearing to a non-directional radio beacon (NDB), with output displayed by a needle on a compass card. Bearings to two stations can be combined to estimate position. Antenna characteristics, sensitivity to atmospheric conditions, and radio interference limit the accuracy of the system.

Very High Frequency Omnidirectional Range (VOR)

A VOR receiver provides an accurate absolute bearing to or from a station on the ground. Angular deviation from the selected course is presented on a Course Deviation Indicator (CDI) that consists of a needle moving over a scale marked with several dots.

Each dot represents approximately 2 deg, so that position offset from the selected course varies with distance from the VOR ground station.

Distance Measuring Equipment (DME)

DME provides distance to a ground station based on timing, and displays it to within 0.1 NM in a digital format. When used with VOR, range and bearing from a station uniquely locate the aircraft in the horizontal plane.

Instrument Landing System (ILS)

ILS provides both horizontal and vertical guidance and is the most accurate landing aid in regular use. The *localizer* provides lateral deviation from a predefined horizontal course line over the ground, while the *glideslope* provides vertical deviation from a constant-gradient approach path (normally having a slope of 3 deg) down to the runway. The ILS cockpit display shown in Figure 2.3 (also as (4) in Figure 2.1) consists of two needles that indicate lateral and vertical angular glidepath deviations. The CDI needle is approximately twice as sensitive to localizer deviations as it is to VOR deviations

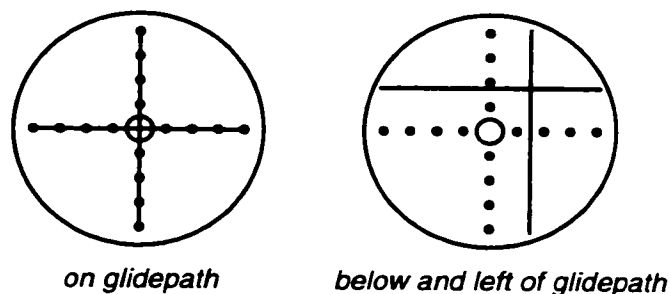


Figure 2.3 Instrument Landing System Needle Display

Area Navigation (RNAV)

The RNAV designation applies to systems that explicitly calculate 2-D position. For example, two DME signals or two VOR signals can be combined to calculate position. LORAN (LONg RANGE Navigation) and GPS are also RNAV sensors. (As detailed in chapter 3, GPS also provides altitude information that can be used for vertical approach guidance through differential operation.) Course deviations are displayed with a CDI needle or pointer moving over a scale.

One additional concept characterizes the performance of these navigation systems:

Navigation Sensor Error (NSE)

Navigation Sensor Error is the difference between the aircraft's actual position and the position measured by the navigation sensor. This positioning error is a function of the navigation equipment both onboard and external to the aircraft. The concept of NSE applies whether or not the aircraft is trying to follow a specified path. NSE's relationship to Total System Error (which applies only when attempting to follow a desired trajectory) is discussed in Subsection 2.2.2.

2.1.3 Instrument Approaches

An instrument approach procedure brings an aircraft from the enroute or terminal airspace structure down to a point near the runway from which a landing can be made. The textual information required to fly instrument approaches is printed in small type on a paper approach plate that lists relevant navaid frequencies, times, headings, altitudes, and distances. Two examples are shown in Figures 7.13 and 7.15. Instrument approaches fall into one of two categories depending on whether electronic vertical guidance is used.

Precision Approaches

In addition to using lateral radionavigation, precision approaches employ a radio navaid for vertical glidepath guidance. ILS is the most accurate landing system normally used in light aircraft and permits precision approaches down to a low decision height (DH) where the pilot must see the runway environment or abort the approach [FAA-AIM90]. If the aircraft is significantly off the intended approach path, one or both of the deviation needles will “peg” at full deflection. Beyond this point, the ILS provides no indication of the magnitude of the lateral or vertical deviation. A significant amount of training and skill is required to smoothly fly an ILS approach by hand. The pilot must mentally integrate information from many sources (artificial horizon, airspeed indicator, altimeter, vertical speed indicator, ILS needles, and often DME for distance to touchdown) in order to follow the ILS signal with the desired damped behavior. Category I ILS approaches have a minimum DH of 200 ft and minimum visibility of 1/2 mile while the most accurate ILS variant, Category III (requires a radar altimeter), permits automatic landing and rollout with zero ceiling and zero visibility. ILS does not allow for curved instrument approaches since the localizer and glideslope beams are fixed in space.

If the pilot cannot see the runway at the DH or if the approach must be aborted for another reason, the published *missed approach procedure* is executed. This is designed to maneuver the aircraft back into position to make another approach and therefore typically includes curved segments. Because the missed approach leads the aircraft away from the straight-in approach path, the ILS is of no use during this procedure. *The pilot can be without positive course guidance during one of the most critical phases of flight.* Due to varying aircraft performance, pilot performance, and wind conditions, large obstacle-free areas must exist around the approach and missed approach paths [FAA-TERPS93]. Local terrain determines how much clearance is available, which influences

the minimum DH. For airports surrounded by terrain, this ultimately limits the utility of the instrument approach and the airport that it serves.

Non-Precision Approaches

The term *non-precision* refers to an instrument approach that lacks positive vertical flightpath guidance. These include VOR, localizer, and NDB approaches along with their DME-aided counterparts. GPS has also come into use recently as a non-precision approach sensor. These approach types are limited to straight segments between waypoints. A barometric altimeter is used to remain at or above *minimum descent altitude* (MDA) at various approach stepdown fixes for terrain and obstruction clearance. Progress along the approach - and also the relevant MDA at each point - is monitored using DME, VOR cross radials, GPS, marker beacons, or stopwatch timing. This requires a skilled instrument scan and integration of various information sources to remain aware of the relationship between the aircraft, MDA, and terrain in the vertical dimension. Multiple pitch and power changes are typically required as the aircraft transitions from level flight on one approach segment to descent to the next segment's MDA.

In the worst cases of pilot failure to integrate the information correctly, a perfectly functioning aircraft descends below MDA on a non-precision approach and strikes terrain. These so-called *Controlled Flight into Terrain* (CFIT) accidents continue as a major accident category across a range of aircraft types. Even experienced airline flight crews fall into this CFIT trap; in August 1997, a Korean Air Boeing 747 impacted terrain while on a non-precision approach to Agana, Guam. (The ILS glideslope was out of service, forcing use of a localizer-only approach.) Indications are that confusion over applicable stepdown altitudes along the approach led to this CFIT accident which resulted in 228 fatalities. The increased workload associated with such stepdown configuration

changes on non-precision approaches has led to a safety record five times worse than for precision approaches [NTSB2000].

2.1.4 Motivation

The limitations of the above approach types and their cockpit displays may be summarized as follows:

1. A significant degree of pilot training and continuing skill is required to smoothly fly instrument approaches.
2. Changes in flight condition, such as intercepting a localizer or transitioning between visual and instrument references, present extra challenges.
3. Current procedures in normal use provide only straight segments on approach to a runway. Curving approaches are not available.
4. If the aircraft is not near the desired course or glidepath, current cockpit instruments yield limited information about where the pilot should fly.
5. Missed approach procedures typically include portions with no positive vertical or course guidance.

These characteristics all contribute to a more fundamental problem: that it is possible to lose awareness of the spatial and navigational situation, especially if the aircraft is not stabilized on the approach. Such situational awareness is critical in a demanding phase of flight such as instrument approach. The continuing existence of accidents involving loss of the “big picture” motivates the need for better display technologies. Additional benefits are increases in aircraft and airport utility enabled by all-weather curved approaches.

2.2 Objectives

The dual operational goals of this work were to demonstrate increased safety (through situational awareness) and enhanced utility (through flexibility in defining flight paths). Both objectives can be achieved by cockpit displays that allow intuitive interpretation, reduced workload, and high accuracy in instrument flying.

2.2.1 *Increased Safety through Situational Awareness*

Situational awareness is a concept so encompassing that experts seldom agree on its definition. It can range from knowledge of position and orientation, to comprehension of procedures required by ATC, to understanding of aircraft system status, to knowing about deteriorating weather at the destination. The concept is therefore often broken down into positional, navigational, spatial, and other varieties of situational awareness. For the purposes of this research, situational awareness refers to knowledge of aircraft position, velocity, and attitude; understanding of the intended instrument flight path; and comprehension of the actions needed to intercept and remain on the desired path.

Loss of aircrew situational awareness is a contributing factor in accidents across many segments of aviation. The CFIT accident in Guam illustrates that situational awareness remains an issue even for the crews of well-equipped transport aircraft. Current instrument flight rules rely heavily on *procedural safety*. This notion guarantees safe terrain clearance as long as the aircraft flies the altitudes and ground tracks designated by the certified approach procedure. Direct awareness of threatening factors such as terrain below MDA can also enhance safety in the event of a deviation from the published procedure. The Enhanced Ground Proximity Warning System [Proctor97] is a good example of non-procedural safety through threat awareness. This level of aircrew situational awareness is needed *even when the aircraft is being flown by the autopilot*.

Pilots performing this supervisory control function must know what the automation is doing at all times.

This research sought to enhance procedural safety by allowing the pilot to hand fly instrument approaches with greater ease and accuracy. The required increase in situational awareness was achieved through use of intuitive cockpit displays.

2.2.2 Enhanced Utility through Flight-Path Flexibility

Increased flexibility in defining instrument procedures can greatly enhance aircraft and airport utility. Curved approaches and missed approaches can be flown at airports with high instrument minimums due to localized high terrain. Noise abatement departures and arrivals can be tailored to noise-sensitive areas on the ground. Dynamic curved missed approach procedures based on other traffic, along with the ability to fly very accurate straight-in approaches, could enable instrument approaches to closely spaced parallel runways. Complex pattern flying capability can even benefit specialized aviation operators.

A goal of this research was to demonstrate operational benefits of being able to accurately fly complex ground tracks and variable climb/descent gradients. The desired flexibility required enhanced displays for flight path awareness and workload reduction. The ultimate metric of accuracy on complex paths is Total System Error.

Total System Error (TSE)

Total System Error is the difference between the aircraft's actual position and the desired position (as defined by a flight path or nominal flight condition in an autopilot). Unlike Navigation Sensor Error, the concept of TSE is valid only if the aircraft is trying to follow a specified path. TSE describes the accuracy with which a path is flown; reduction of TSE is important to safe implementation of complex procedures. Even

accidents that represent gross loss of situational awareness (such as CFIT) start out as an increase in TSE.

Flight Technical Error (FTE)

TSE lumps Navigation Sensor Error and path-following errors into one quantity that indicates whether the procedure was flown as specified. The path-following metric is called Flight Technical Error. FTE is the difference between the position measured by the navigation sensor and the desired position, and as such applies only when the aircraft is trying to follow a specified path. Since the aircraft's sensors are not perfect, NSE (and therefore TSE) is not observable to the pilot; the best a pilot or autopilot can do is attempt to drive FTE to zero. Even if this is achieved, nonzero navigational sensor error (NSE) results in nonzero TSE because $TSE = NSE + FTE$.

As an example, the horizontal and vertical deviation signals generated by the ILS represent FTE. If the pilot keeps the needles centered, the FTE is zero, even though navigation errors (NSE) may place the aircraft off the true desired path through space. NSE in this case could be caused by variations in ILS ground transmitting equipment and by errors in the onboard electronics. The (slightly corrupted) navigation signal is then sent to the needle indicators, which display deviations from the desired flight path.

2.3 Tunnel-in-the-Sky Display Concept

Shortcomings of conventional instruments have led to work on displays to enhance situational awareness. Since flight is a three-dimensional activity, significant work has centered on providing elements of a 3-D perspective view of the outside world. Integrating this view with additional data sources results in a single display from which the pilot can obtain all primary flight data. A common goal of these systems has been to give the pilot a natural representation of the aircraft's situation within the world.

Enhanced vision systems augment the outside view with symbology generated onboard the aircraft. [Bray81] discusses a Head-Up Display (HUD) format that depicts a 3-D extended runway centerline for lining up on approach. [Yang94] presents simulations of a wireframe runway displayed on a HUD. Flight tests of a similar concept based on radar sensors are described in [Nordwall94], and [Proctor94] details a commercially available HUD system that displays two lines representing the sides of the runway.

Synthetic vision systems recreate the outside view based on a stored database - both of real objects and of additional task symbology. A logical symbolic extension for 3-D perspective view displays is an intuitive depiction of the desired flight path. Work in this area has used familiar analogies to roads and tunnels with such names as *Highway-in-the-Sky*, *Pathway-in-the-Sky*, and *Tunnel-in-the-Sky*. This format depicts the desired flight path as a tunnel or series of symbols for the aircraft to fly through or over. The pilot can intuitively infer where the aircraft is relative to the desired flight path and what action should be taken to stay on this trajectory. Being able to see the path ahead gives a "preview" of the trajectory forcing function, thus aiding the pilot in following curved flight paths.

Pilot guidance using perspective flight path displays is not a new idea. The concept was formulated beginning in 1946 by a United States Navy study of the human-machine interface [Filarsky83]. Later work has its roots in the US Army Navy Instrumentation Program (ANIP) directed by George Hoover beginning in 1952. Military work on format concepts and laboratory simulation continued throughout the 1960s and 1970s [Watler81]. First flights published in the literature occurred in the 1980s. (It is likely - in this author's opinion - that additional classified work remains unpublished.) The advent of enabling technologies for commercially feasible Tunnel-in-the-Sky displays triggered more work in the 1990s. However, *work to date has focused on*

laboratory simulation and non-consumer hardware. The use of expensive turbine aircraft for demonstration programs has severely limited the amount of flight testing to date.

Sections 2.4 through 2.6 detail previous work in the field and technologies that will enable widespread use of Tunnel-in-the-Sky displays.

2.4 Previous Simulation Studies

Simulator studies of performance parameters, workload, and situational awareness have been underway for some time. Due to limitations of sensor and computer hardware, studies of dynamic perspective displays were constrained to simulation until the 1980s.

[Wilckens70] describes tests of a “Boulevard” display channel composed of moving dots to guide the pilot down an ILS approach. He concludes that presentation of flight data in an intuitive analog form greatly reduced the need for scanning and transition between different information elements.

[Watler81] discusses the “Maneuvering Flight Path Display” investigated for use on military head-down and head-up displays. Simulator work included a lead aircraft flying over a tiled, road-like surface.

[Grunwald81] describes evaluations of a perspective tunnel display for steep, curved approaches for helicopters. The displayed tunnel was composed of five connected squares with predictor symbology. An exploratory flight test for this effort is discussed in the next section. [Grunwald84] introduces an aircraft-shaped predictor symbol displayed in 3-D perspective with velocity cues for a fourth dimension of control. Larger tunnel widths were shown to result in lower control activity levels. [Grunwald96a] discusses an updated predictor guidance scheme to improve transitions between straight and curved portions of the flight trajectory. Simulation results are reported in

[Grunwald96b] and indicate improved performance on path transitions and with slowly varying crosswinds.

[Reising95] provides an extension of US Air Force simulation work dating back to the mid-1980s. This study compared standard HUD symbology to a HUD display incorporating a tiled pathway and a “follow-me” aircraft for formation-like guidance. Pilots preferred the pathway HUD format because it afforded them a preview of the upcoming curved approach trajectory.

[Wickens89] discusses fundamental psychological principles that influence perspective display design. Reference frame compatibility, consistency of display features with previous experience, and situational awareness were investigated in a simulation environment. The display consisted of three flight-path boxes and a predictor symbol with airspeed commands. These tests also indicated the advantages of aircraft state prediction and trajectory preview.

[Dorhigi93] investigates effects of display format on spatial awareness. During manual piloting conditions, a Tunnel-in-the-Sky format reduced directional uncertainty to designated geographical targets as compared to a standard Electronic Attitude Direction Indicator (EADI). An unexpected increase in directional uncertainty was noted when the display was used with an autopilot.

[Theunissen94] introduces the concept of Time-to-Wall Crossing (TWC - the time remaining until the aircraft will penetrate the tunnel wall) as an important parameter in predicting pilot control actions using a Tunnel-in-the-Sky display. He notes that ability to assess TWC enhances pilot supervisory control in cooperation with an autopilot or Flight Management System (FMS). [Theunissen95] demonstrated in simulation that as tunnel size was decreased, control activity increased and FTE decreased. Predictor symbology tended to reduce the effects of tunnel size on control activity. [Theunissen97]

gives a comprehensive overview of these results and their relation to display design and human performance issues.

[Parrish94] presents a comparison of a standard EFIS cockpit with a pictorial synthetic vision display. Simulation experiments included curved approaches and traffic incursions. Objective and subjective results indicate that spatial awareness was improved by the pictorial display, which depicted the approach as a tiled roadway. Pilot comments indicated a strong preference for the synthetic vision display, especially the large-screen wide-field-of-view version.

[Regal95] examined piloted simulation performance with a display composed of rectangular tunnel cross sections with lines connecting their corners. A flight path vector symbol displayed predicted aircraft position. Workload was measured using pilot performance on a secondary task. Comparisons with a flight director on complex curved trajectories indicated reduced flight path violations, reduced workload, and greater spatial awareness using the perspective display.

This varied history of simulation experiments, including additional work documented in Chapter 6, demonstrate significant advantages of the Tunnel-in-the-Sky format for primary flight displays. The ultimate proof of operational utility, however, lies in flight testing.

2.5 Previous Inflight Demonstrations

The limited amount of published Tunnel-in-the-Sky flight testing to date has centered on turbine research aircraft using non-consumer display hardware. The use of specialized graphics computers (typically dedicated workstations) and inertial navigation systems has resulted in useful research tools, but not in systems suitable for widespread use in small aircraft. Although the total cost of navigation and graphics hardware is not

published for the following efforts, the use of inertial navigation systems and graphics workstations drives system price into the range of \$100,000 and higher.

As indicated above, [Grunwald81] conducted exploratory flight testing of a Tunnel-in-the-Sky display on a fully instrumented Boeing CH-47 Chinook transport helicopter (twin rotors, twin turbine engines, gross weight >33,000 lbs). National Aeronautics and Space Administration (NASA) flight testing occurred at Wallops Island, Virginia. Images were generated by an Adage Graphics AGT 130 graphics terminal *located on the ground (!)* Sensor information included telemetered data from the helicopter as well as positioning from a ground-based laser tracker. Images were then transmitted to the cockpit via a scan-converted television uplink. Despite very limited flight testing, the test pilot commented that the display provided sufficient information for following the curved trajectory. That this complex system even functioned is a tribute to the researchers' tenacity!

In February 1983, the "Command Flight Path Display," a descendant of the original Army Navy Instrumentation Program work introduced in Section 2.3, was flown by the US Naval Air Development Center on the Calspan Total In-Flight Simulator [Filarsky83]. This aircraft is a highly modified NC-131H variable-stability transport research aircraft (twin turboprop engines, gross weight >46,900 lbs). The sensor suite included an inertial navigation platform. The report states that the display enhanced pilots' ability to conduct flight operations in zero visibility conditions. This system was also demonstrated in 1985 onboard a Navy F-14A Tomcat jet fighter (twin turbofan engines, gross weight 74,300 lbs) at Point Mugu, California [Brooks97]. A synthetic lead aircraft flying over a tiled roadway conveyed guidance information.

[Swenson93] describes a system developed by the United States Army and NASA for low-altitude helicopter guidance. This system was first flight tested in July 1992 on a

Sikorsky NUH-60A military helicopter (single rotor, twin turbine engines, gross weight 20,250 lbs). Testing occurred in a mountainous region of Pennsylvania. Onboard hardware included a VME flight computer, a Collins GPS receiver, a Litton Inertial Navigation Unit, a Silicon Graphics 4D/120 graphical workstation, a Honeywell helmet mounted display, and fiber optic and military 1553B networks for system integration. The display presented a flight channel with a lead aircraft and flight path predictor symbol for guidance. Results indicated an increase in situational awareness and decreased training time for all-weather flight near terrain.

[Sachs98] documents flight demonstrations performed by the Technical Universities at Munich and Braunschweig in Germany. First tests of this system occurred in October 1994 onboard a Dornier 128 airplane (twin turboprop engines, gross weight 9,570 lbs). Flight hardware included an integrated DGPS/Inertial Navigation System, a Silicon Graphics Onyx graphics workstation, and a head mounted display with head tracker. The flight test program included demonstrations at locations in Germany and Switzerland, including curved approaches flown to airports in mountainous regions. The head mounted synthetic vision display presented a channel through which the pilot flew the airplane. The powerful graphics computer allowed for perspective drawing of terrain on the display. Database requirements for drawing terrain and cultural features are discussed in [Möller94]. Additional “height bar” symbology allowed the pilot to land the aircraft using the synthetic vision display.

[Theunissen97] describes an inflight demonstration performed on a Delft University of Technology Cessna Citation II jet aircraft (twin turbofan engines, gross weight 13,300 lbs). Flight hardware included GPS, a Microwave Landing System receiver for the approaches, an analog attitude determination system, and novel use of a low-cost PC computer driving a graphics engine based on the TMS 34020 chip (an early device used for 3-D graphics). This demonstration in December 1994 comprised several

successful straight-in approaches to Aberdeen. A square channel with an open top was displayed to the pilot. A lack of inertial velocity information on the display made staying inside the tunnel difficult in the presence of a crosswind. [Theunissen97] also refers to plans for an inflight concept demonstration onboard a Douglas DC-3 aircraft at Ohio University.

[Below97] and [von Viebahn98] describe work jointly performed by the VDO avionics company and the Darmstadt University of Technology in Germany. This program utilized a modified Fokker VFW 614 variable-stability jet transport research aircraft (twin jet engines, gross weight 43,890 lbs) for flight testing between 1995 and 1997. Flight hardware included an integrated DGPS/Inertial Navigation System, a high-performance Symbol Generation Unit graphics processor custom developed by VDO, and a flat-panel cockpit display. Flight tests included ILS and non-precision approaches, low-level following of displayed terrain, and taxi guidance. The perspective display depicted the flight path as a rectangular channel and was accompanied by a navigation display presenting the view from above.

The remaining chapters describe work performed by this author. In June 1995, the Stanford Tunnel-in-the-Sky display was first flown on a Piper Dakota four-place airplane (single piston engine, gross weight 3,000 lbs). Using consumer hardware wherever possible, the system cost was less than \$25,000 (includes a ruggedized cockpit display but not the specialized GPS attitude receiver used for the flight tests). Flight testing was then performed on a Beechcraft Queen Air (twin piston engine, gross weight 8,000 lbs) at several airports in California and Alaska. A wide variety of procedure types was flown during this test program. This research effort aimed to integrate enabling technologies into a *low-cost* and *operationally oriented* approach to system development.

2.6 Enabling Technologies

This section outlines the emerging technologies of GPS, inertial sensors, embeddable computers, and flat panel displays that will enable commercialization of synthetic vision technology. Specific descriptions of the Stanford test system are reserved for Chapters 3 through 5.

2.6.1 Global Positioning System

The advent of GPS has made accurate and inexpensive 3-D worldwide positioning data available for the first time. The cost is now low enough that many light aircraft are equipped with GPS for enroute and non-precision approach navigation. With differential GPS (DGPS) techniques, accuracy can be improved to sub-meter levels while providing integrity needed for critical flight operations such as precision approach. Wide Area Augmentation System DGPS navigation (described in Chapter 3) will enable entire-flight coverage within the United States. Accuracy is good enough that synthetic vision scenes generated using GPS data very closely match the actual view out the cockpit window.

Meter-level positioning heralds a turning point in the history of instrument flight. Navigation Sensor Error historically has been larger than Flight Technical Error. NDB and VOR approaches, for example, might have worst-case NSE measured in fractions of a kilometer or more, while FTE can be less than a few tens of meters. But DGPS navigation systems will be more accurate than the precision with which pilots fly; FTE will likely become the dominant source of Total System Error for hand-flown approaches. In fact, for many aviation uses of DGPS, we can approximate TSE with FTE. This was the approach taken in interpreting flight test results.

2.6.2 Low-Cost Inertial Sensors

Attitude sensors remain expensive relative to other display system components. Inertial Navigation Systems cost more (\$50,000 - \$120,000 in 1996 [Kayton97]) than many used general aviation aircraft. Attitude Heading Reference Systems with digital interfaces for turbine aircraft typically cost more than \$25,000, while lower cost instruments for personal aircraft lack the necessary interface electronics. As discussed in Chapter 3, innovative uses of inexpensive accelerometers and rate gyroscopes are making low-cost attitude systems a reality.

2.6.3 Computers

As the personal computer (PC) has become a commodity product, the price of computing power has dropped dramatically. PCs are finding increased use in embedded and industrial applications and are now available in ruggedized and low-power versions. Rising floating-point math performance of new microprocessors allows these devices to generate 3-D graphics available only on expensive workstations a few years ago.

2.6.4 Graphics Hardware

Performing 3-D graphics is computationally expensive. Each point in the database - including vertices of all lines and polygons - must undergo a perspective transformation and projection using floating-point 4x4-matrix arithmetic. Additional integer math is required to actually draw polygons or lines on the screen. High bandwidth to video memory is required to achieve sufficient frame refresh rates. It has been estimated that a person using a calculator to perform all the computations in a complex scene could complete *two frames* in his lifetime! A new generation of 3-D rendering chips, developed in response to demand from PC multimedia and gaming markets, are making sophisticated graphics possible at favorable price/performance

levels. The power of a \$10,000 graphics machine ten years ago can now be found on a \$100 add-in video board.

2.6.5 Flat-Panel Displays

Active-matrix liquid crystal displays (AMLCDs) are the leading choice for cockpit computer screens due to their light weight and minimum depth. Popularity of laptop computers has driven down the cost of AMLCDs over the past several years. Consumer laptop displays are not suitable for use in aircraft due to the high ambient lighting of an aircraft cockpit in daytime. Wide temperature variations can also render consumer displays unusable. For these reasons, aviation AMLCDs are typically fitted with powerful backlights and heaters. Although availability of reasonably-priced ruggedized flat panel displays is limited for light aircraft, this is changing as demand is fueled by other mobile electronics and outdoor kiosk applications.

2.7 Systems Engineering Approach of This Work

The novel balanced approach of this work is based on three interrelated “pillars”: the human-machine interface, implementation, and operations.

A sound basis in human factors is a crucial ingredient in design and certification to the highest levels for commercial aircraft. Design methodologies for non-certified use should similarly be based on a scientific approach to refining the human-machine interface. Otherwise, design according to mere designer or pilot preference can produce problematic displays. Accordingly, this work made extensive use of previous research successes and incorporated feedback from continuing implementation and flight test operations.

A major barrier to widespread use of perspective displays has been difficulty in implementing practical hardware. It has simply been too expensive for anyone but a few

institutionally funded programs to build and fly such a system. The advent of low cost sensors, graphics hardware, and flat panel displays will improve this condition. An important driver of continuing hardware development is increased understanding of the operational and human factors requirements involved.

Operational issues such as integration with current air traffic control schemes, performance under extreme circumstances, feedback from pilots, and regression in case of failure are critical in creating systems that satisfy the overall need. Integration with current instrument and navigation systems will also be necessary for a shift to a Tunnel-in-the-Sky paradigm. This research focused on minimizing hardware and aircraft operations cost to allow for more extensive flight testing than previous efforts. An important reason for studying such operational issues is to provide feedback into the human factors knowledge base.

An integrated approach to understanding and fostering this young, human-centered and systems-oriented technology must address all three of the pillars. As idealized in Figure 2.3, this work leveraged previous human factors work with a low-cost and operationally oriented approach to flight testing.

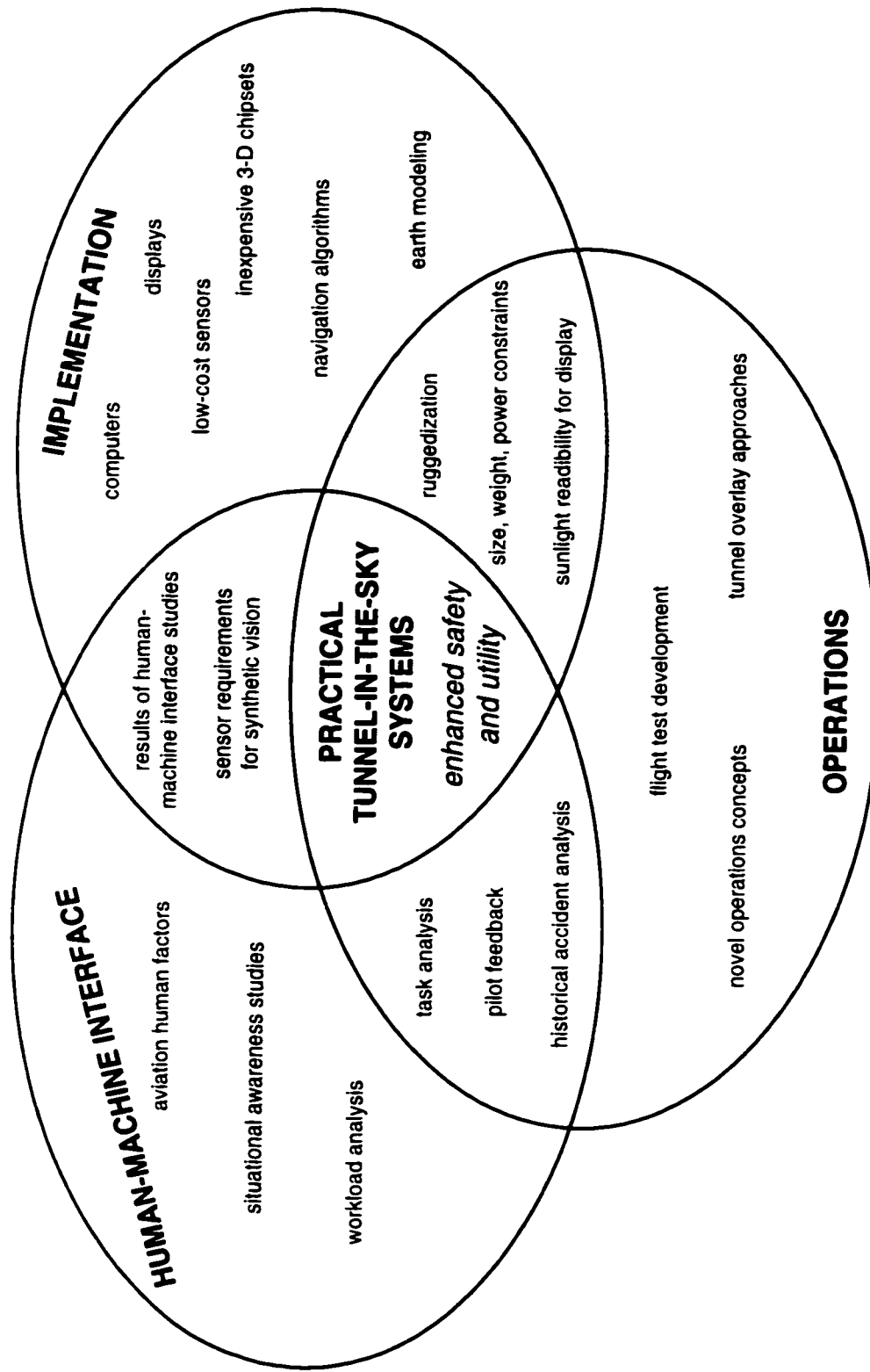


Figure 2.4 Three Supporting Pillars for Tunnel-in-the-Sky Systems

Chapter 3:

Sensor Fusion

A Tunnel-in-the-Sky display needs continuous 3-D positioning and attitude information to create its representation of the outside world. High accuracy is required for instrument approaches, while navigation signal integrity is needed for safety. Beyond these task domain requirements, additional data rate and bandwidth needs must be met when there is a human in the loop looking at a 3-D display. This must be achieved at reasonable cost for production systems. Sensor accuracy, responsiveness, and jitter properties are discussed in Sections 3.1 through 3.3. Sections 3.4 and 3.5 detail sensors chosen for the prototype system, and Section 3.6 suggests other aviation sensors that could be incorporated. Section 3.7 relates sensor errors to their onscreen effects.

3.1 Sensor Accuracy

Sensor accuracy requirements are determined by the flying task being performed. For example, required accuracy for an aircraft landing system is dictated by the size of the landing zone, aircraft dynamics, worst-case disturbances, etc. Accordingly, these

specifications on position and attitude accuracy (heading, pitch, and roll) exist in the *task domain*. A related quantity is *integrity*, which describes the probability with which the system meets its stated accuracy. Certified aircraft landing systems require high integrity because the consequences of a landing aid's not meeting its stated accuracy could be catastrophic. Specific accuracy and integrity requirements for aircraft are discussed later in this chapter. Sensor errors in 3-D perspective systems have specific effects on displayed images; these *display domain* effects are discussed in Section 3.7.

3.2 Sensor Responsiveness

An overall goal for primary flight display performance is to convey physical events to the pilot's eyes in minimum time. This section makes a general argument for fast system responsiveness (introduced as high "bandwidth") and then outlines effects of sensor lags. Although the topic of this chapter is Sensor Fusion, the responsiveness of the display hardware and the complete system are also discussed.

3.2.1 Bandwidth

As a framework for discussion, this subsection addresses relationships between display responsiveness, operator responsiveness, and system motions. The term *bandwidth* is used somewhat loosely here to describe "responsiveness" and was chosen to echo fundamental notions of classical control theory. This theory developed around continuous-time analog components characterized by frequency response that dropped off above a certain bandwidth. As used here, high bandwidth corresponds to high sample rate and low latency.

A perspective display for human-in-the-loop aircraft control can require responsiveness beyond that of a typical autopilot. For classical automatic control, a control system should be capable of sensing bandwidths higher - ideally several times

higher - than 1) the bandwidths of the motions being controlled, and 2) the disturbances being rejected. That is, automatic control requires:

$$BW_{sensors} > BW_{motions}, BW_{disturbances} \quad (3.1)$$

Human-in-the-loop control (or what should really be called *human-in-the-plant* control when the pilot is *inside* the moving vehicle) imposes requirements beyond automatic machine control. In civilian aircraft this results from the human optical and vestibular systems' having higher bandwidths than most of the motions encountered. While a given sensor accuracy and bandwidth may be sufficient for an automatic control loop, a human placed in that loop (either as manipulator of the controls or as a supervisor of automation) can dictate more stringent requirements. To satisfy the human along with the machine in such cases, the sensor bandwidth (and display hardware framerate) may need to be raised. So for human-in-the-plant control it is proposed that:

$$BW_{sensors}, BW_{display} > BW_{motions}, BW_{disturbances}, BW_{optical}, BW_{vestibular} \quad (3.2)$$

To illustrate the ideas expressed in Equations 3.1 and 3.2, consider a light aircraft subjected to turbulence that occasionally disturbs the aircraft with greater authority than its own controls. Recognizing this, an autopilot may justifiably be designed with cutoff frequencies (say 5 Hz) that leave significant (but infrequent) higher-frequency disturbances unrejected. However, introducing a human-in-the-plant display may require that the sensors detect aircraft response to disturbances (say a sharp-edged gust with 15-Hz frequency content) that the controls are not intended to reject. The pilot can become sick if the displays lag behind the optical view out the window. Even in instrument conditions with no outside view, the displays can still lag behind the pilot's vestibular system enough to be noticeable. Such human-centered considerations can elevate sensor and display bandwidth requirements, bringing required sampling frequencies from several Hz into the tens-of-Hz range as described below.

3.2.2 *Sensor Sample Rate and Latency*

Sample rate and latency are important descriptors of the time responsiveness of sampled data systems. *Sample rate* describes the number of datapoints measured by a sensor per unit time. *Latency*, or transport lag time, includes analog conversion, processing, and communication times. Latency for well-designed sensors is typically less than the inverse of the sample rate. Based on the bandwidth arguments above, maximizing sample rate and minimizing sensor latency aids perspective display system performance.

3.2.3 *Display Framerate and Latency*

Related to sample rate is the *framerate*, the number of display frames drawn per second. Again, maximizing framerate is beneficial to overall system performance although the boundary between “fast enough” and “not fast enough” is not well defined or agreed upon. The framerates used in visual media can lend some insight here: videotape standards specify 25 or 30 frames per second, while motion picture film uses 24 frames per second. Commercial flight simulator framerates range from 20 Hz to 120 Hz. A GPS-based backup attitude indicator has been successfully flown at framerates as low as 10 Hz by [Kornfeld98].

The speed at which display frames can be generated is limited by the computer graphics hardware and software. The display technology used also influences the framerate. For example, video display boards used to drive Cathode Ray Tube (CRT) displays normally have a fixed vertical refresh frequency. If such a system has a 60 Hz refresh rate, new images may only appear on the screen at rates of 60 Hz, 30 Hz, 15 Hz, 12 Hz, etc. Waiting for the next CRT vertical retrace to reveal a newly drawn frame can thereby introduce latency. Although the rods in the human eye can detect CRT flicker

above 60 Hz, it is doubtful that information beyond this frequency is useful for manual flight control.

Based on the above examples for visual media, a 24 Hz framerate was considered a goal for commercial systems with fluid onscreen movements. Although maximum framerates for this project were around 20 Hz, this was considered acceptable for an experimental effort.

3.2.4 System Latency

Latency effects are additive in systems with multiple elements. The entire chain can include sensor conversion and processing, communication between sensors and display hardware, data processing in the display, and generation of display frames by the video hardware. Because of the serial buildup of system latency, one slow component can limit system performance despite otherwise fast components. Since the internal clocks of the various components are often not synchronized, additional latency is incurred as downstream elements wait for samples from upstream elements. A fully synchronized, “pipelined” architecture can reduce latency to a minimum, but at the expense of additional complexity.

Overall display system requirements can be stated as limits on system latency. For example, a maximum attitude display latency of 100 msec is specified by Federal Aviation Administration (FAA) standards for transport aircraft [Kayton97]. Studies have shown that system latencies as small as 40 msec can cause degraded compensatory tracking performance [Wickens86]. A rigorous process for balancing the many factors contributing to Tunnel-in-the-Sky system latency remains a subject for further research.

Based on the above, 100 msec total system latency seems to be a reasonable upper limit for commercial systems to produce images that closely match the real world. Lower

latencies of 40 msec or less will be desirable for enhanced vision systems where synthetic symbology is fused directly on top of sensor images. Although system latency was in the range of 100 msec to 150 msec for the prototype described herein, it provided images that were adequate for the flying tasks involved.

3.3 Sensor Jitter

An additional quantity related to both accuracy and responsiveness is *jitter* - high-frequency sensor error content that makes objects shake on the screen. Even if small jitter errors are negligible in the task domain (e.g. 10-cm positioning errors are insignificant on initial instrument approach) they may be annoying or distracting to the pilot if they produce noticeable jitter on the display. Fatigue may result after long periods of use. Even worse, the pilot may lose trust in the instrumentation. "After all," the thinking goes, "the real world doesn't rattle around like that." For some applications, one degree of pitch jitter may be more noticeable than five degrees of pitch bias error. Perhaps a new term, *perceived credibility*, could be added to the standard navigation system metrics of accuracy, integrity, availability, and continuity.

Computationally, sensor jitter makes itself visible through perspective projection matrices used by the graphics algorithms. These matrices are built up from sensor data for each displayed frame. However, even with no sensor error, the matrices can still acquire *numerical* error that also appears as jitter. An algorithm for mitigating such numerically caused jitter is discussed in Chapter 4.

3.4 Position Sensors

For simplified integration, only navigation sensors that output a 3-D positioning signal were considered for this system. A byproduct of the systems considered is that they provide 3-D velocity and hence ground track. Feasibility of systems based on fusing

multiple 1-D and 2-D sensors such as VOR, ILS, DME, LORAN, and barometric altimetry is discussed in Section 3.7. Although the tradeoff with such sensors has historically been cost and complexity versus accuracy and integrity, GPS has enabled new levels of capability for a given cost.

Most of the task domain accuracy requirements for instrument approach are dictated by governing civil aviation authorities. The accuracy requirement at decision height can be inferred from specifications for current ILS systems. For Category I systems (200-ft DH) the 95% vertical accuracy requirement is 4.4 m when 200 ft above the runway, while for Category III (zero visibility landings) it is 2.0 m when 100 ft above the runway [RTCA98]. Specified Category III integrity requirements are as low as 10^{-9} integrity failures per approach.

Acceptable performance at minimum cost was the tradeoff philosophy for the Tunnel-in-the-Sky sensors. For the purposes of this work, vertical accuracy commensurate with the Category I requirement was deemed acceptable. This is achievable with most DGPS systems. Since no aviation-certified DGPS systems are yet in wide use, a hard integrity requirement was not set, although emphasis was placed on using a system designed for Category I integrity. A minimum position update rate of 10 Hz (or 100 msec maximum latency) was desired for creating fluid images on the synthetic vision display.

3.4.1 Inertial Navigation Systems

Modern strapdown Inertial Navigation Systems (INSs) employ high-quality accelerometers and rate gyroscopes to integrate a high-bandwidth position and attitude solution for output to cockpit instruments. The inertial sensors drift and must be occasionally corrected (aided) by an external navigation source. This drift makes them unsuitable for sole-means instrument approaches in civil aircraft. INSs are also

expensive (typically ranging from \$50,000-\$120,000 in 1996 [Kayton97]), costing more than many used single-engine general aviation aircraft! They can be augmented with GPS [Cramer96], but even this is not certified for precision instrument approaches below a 200-ft decision height. The high cost of INS prevented its being considered for this project, whose goal was to demonstrate a *practical* Tunnel-in-the-Sky display for *all* classes of aircraft.

3.4.2 Global Positioning System

The advent of the Global Positioning System has made accurate, low-cost 3-D positioning a reality. The nominal GPS space segment consists of 24 satellites that provide stand-alone GPS accuracy of better than 100 m horizontal (approximately 95% of the time) for civilian receivers [Parkinson96]. When the Selective Availability signal used by the U. S. Department of Defense to degrade accuracy is turned off (slated to occur before 2006), this number improves to approximately 20 m. Vertical errors are typically larger by a factor of two or three. GPS is used today for aircraft enroute navigation and non-precision instrument approaches. Stand-alone accuracy and integrity, however, are inadequate for precision vertical approach guidance.

Differential GPS can reduce the vertical error to a few meters or smaller. DGPS augments stand-alone GPS with ground-based reference receivers at known locations. Measurements made at these receivers are used to form corrections to the GPS signals that are broadcast to moving GPS users. Those user receivers then apply the broadcast corrections to improve the accuracy of their 3-D position estimates. The next three Subsections discuss the three DGPS variants considered.

Local Area Differential GPS

This concept uses a local reference receiver near the landing airport and a local datalink to send DGPS corrections to moving users near the airport. The FAA's GPS Local Area Augmentation System (LAAS) will provide positioning for precision approaches in all weather [Enge99]. This system uses the code phase of the GPS signal for raw ranging information. Vertical accuracy specified for the stringent Category III case is 2.0 m [RTCA98]. Future production LAAS receivers for transport aircraft are expected to be priced in the tens of thousands of dollars.

Even higher accuracy can be achieved with local DGPS systems that use the carrier phase of the GPS signal for ranging. Although carrier phase DGPS is more difficult to implement and certify than code phase DGPS, the Category III Stanford Integrity Beacon Landing System (IBLS) prototype uses this technique [Cohen94b]. This system achieves high integrity [Pervan96] by using ground-based pseudolites (pseudo-satellites) to augment the GPS satellite constellation.

Wide Area Differential GPS

Rather than place a reference receiver at each airport needing an instrument approach, Wide Area DGPS (WADGPS) uses a sparse network of reference stations to create a correction signal usable over a large geographical area [Kee91]. The correction signal contains *vector* differential corrections that separate the GPS error components into clock error (mostly Selective Availability), ionosphere, and ephemeris error. Utilizing this concept, the FAA's Wide Area Augmentation System (WAAS) is scheduled to begin operational capability in 2001. Corrections from the WAAS reference receiver network (20 receivers in the continental U. S., three in Alaska, one in Hawaii, and one in Puerto Rico) will be broadcast on GPS frequencies from geostationary satellites. The system is designed to provide 95% vertical accuracy of from 4.0 m to 7.7

m (depending on type of approach and certifying body) for near-Category I approaches. Entry-level aviation GPS receivers capable of decoding and using WAAS corrections will likely cost less than \$5,000.

Low-Frequency DGPS Beacons

The reception distance for local area DGPS corrections can be increased by lowering the datalink transmit frequency. Low-frequency radiobeacons in the 300 kHz range have been successfully operated for maritime applications by the U. S. Coast Guard and other worldwide government agencies. Signals can be received as far away as 280 miles. Accuracy of less than 3 m horizontal is regularly achieved within 50 miles of the reference station [CSI98], and receiver prices are less than \$5,000. Ongoing plans call for at least two low-frequency transmitters in each of the United States. No FAA certification of system integrity or accuracy for aviation use is planned.

3.4.3 Positioning for the Prototype System

A summary of the position sensors considered for flight test use is presented in Table 3.1. The first row contains the rough requirements for the Tunnel-in-the-Sky display, and sensor data rate is expressed in terms of latency. The last two sensors are not currently in active FAA certification for DGPS instrument approaches.

Based on its ability to provide continuous enroute navigation and precision approach guidance during an entire flight, WAAS DGPS was identified as the preferred position sensor to complement the Tunnel-In-the-Sky display's operational flexibility. A prototype WAAS receiver created by Stanford researchers was used [Walter94]. This system exceeded WAAS accuracy requirements by providing 2 m 95% vertical accuracy [Enge96].

Table 3.1 Candidate Tunnel-in-the-Sky Position Sensors

	Installed Cost	Vertical Accuracy (95%) [m]	Integrity	Latency [msec]
PROTOTYPE REQUIREMENTS	minimum	5.0	CAT I desired	100
FAA Wide Area Augmentation System	~ \$5k	4.0 - 7.7	CAT I to be certified	100
FAA Local Area Augmentation System	~ \$7k	2.0	CAT III to be certified	100
Integrity Beacon Landing System	? prototype	0.1	designed for CAT III	100
Low-Frequency DGPS Beacons	< \$5k	3.0	unmonitored for aviation	100

WAAS corrections were generated at the Stanford Master Station using data from the National Satellite Test Bed (NSTB) reference network. (The FAA's NSTB was conceived as a WAAS prototype to reduce technical risk.) These corrections were sent to the aircraft through 9600-baud VHF radio modems using an FAA-authorized VOR-band frequency. Raw GPS measurements were made by a PC-based GPS receiver on the aircraft and corrected with the WAAS signal. Finally, serial position and velocity messages were sent to the Tunnel-in-the-Sky display at 10 Hz. During initial development, positioning data at rates as low as 5 Hz was found to be flyable (although this made lags more noticeable) when combined with 10-Hz or greater attitude information.

In its early development, the Tunnel-in-the-Sky display was also used with Stanford's IBLs prototype described above, with the first operational success of the system occurring using IBLs. (Multi-antenna GPS with no inertial sensors was used on one of these flights in May 1996 at Palo Alto, California, marking the only known flight of a Tunnel-in-the-Sky system using GPS as the *sole* sensor for position and true attitude.) A system based on low-frequency Coast Guard DGPS corrections was occasionally used as a backup when the Stanford WAAS hardware was unavailable. Although this system's integrity is not certified for aviation use, it was acceptable for testing under visual flight conditions. The IBLs and Coast Guard sensors both provided data at 10 Hz. Accuracy of all positioning sources flown was good enough that the scene reconstructed from the internal database closely matched the actual view from the cockpit.

Sensor data was processed by the display computer at the graphics framerate, usually 15 or 20 Hz. Data was used unfiltered, meaning that the 10-Hz position was periodically used for two successive display frames. Positioning data was used to create a software state estimate containing aircraft position in an Earth-Centered, Earth-Fixed (ECEF) coordinate system. For the tunnel navigation algorithms and pilot altitude display, this was also converted to WGS-84 latitude, longitude, and ellipsoidal altitude. The significance of this to practical Tunnel-in-the-Sky displays is discussed in Chapter 4.

3.5 Attitude Sensors

Although attitude instruments (employing spinning mass gyroscopes for aircraft heading, pitch, and roll) have existed far longer than 3-D navigation electronics, integrated sensors with digital interfaces remain relatively expensive at greater than \$25,000. While tradeoffs exist between cost and accuracy, the driving issue for light aircraft is simply the existence of an affordable sensor with a digital interface.

Task domain attitude requirements were estimated by examining performance of current attitude sensors. The overriding requirement was for displayed Tunnel-in-the-Sky imagery to match the outside world. General aviation attitude and directional gyros typically perform with better than 1-2 deg of accuracy. Therefore, achieving 1 deg of accuracy about all three attitude axes was considered sufficient. All currently certified attitude sensors very likely have the required accuracy and integrity. Latency of less than 100 msec (as specified for transport aircraft) was desired to avoid display lag.

3.5.1 Attitude Heading Reference Systems

An inertial Attitude Heading Reference System (AHRS) simply provides heading, pitch, and roll through an interface to a remote attitude display or autopilot. The simplest systems are based on electric or vacuum-driven spinning-mass gyroscopes, with gyro costs reaching into the \$15,000 range. Since the electrical interfaces are typically analog (3-wire synchro or similar), additional synchro/resolver interface electronics are used for interface to the digital display. Add to this additional power supply and space requirements, and the result is a system too large and expensive for light aircraft.

Modern strapdown AHRSs are based on accelerometers and rate sensors, making some of them small enough to be used on large single-engine aircraft. Current rate sensor technologies for AHRS applications include ring laser gyros, fiber optic gyros, and quartz tuning forks. Prices for certified units start at \$25,000 for an AHRS with fiber optic gyros, micromachined accelerometers, and attitude output at 64 Hz. If a currently available AHRS is used, it can easily become the most expensive component of a Tunnel-in-the-Sky display system. An INS provides high-quality inertial AHRS data, but this option was considered prohibitively expensive.

3.5.2 *GPS Attitude*

GPS can be used to measure aircraft attitude through the use of multiple antennas and specialized receiver hardware [van Grass91, Cohen94a]. Since differential carrier phase error between antenna pairs is roughly constant, system accuracy improves as the antenna baseline lengths are increased. Achieving sub-degree accuracy has required spacing the antennas over at least several 19-cm GPS wavelengths. This requirement for an array of multiple antennas spread out over more than a meter creates installation difficulties, especially for light aircraft with their small fuselages. Commercial GPS-only attitude receivers are currently limited to 10 Hz sampling, too slow to smoothly drive a graphical display in dynamic environments. The long baselines required for accuracy result in increased computational burden and occasional solution dropouts during maneuvering.

3.5.3 *Integrated GPS and Inexpensive Inertial Sensors*

The limitations of GPS as a stand-alone attitude source can be countered by combining it with low-cost inertial sensors. Inexpensive rate gyros provide good high-frequency information but have poor long-term stability and bias drift. GPS has absolute long-term stability, but with a low data rate, occasional dropouts, and excessive noise for short baselines on the fuselage of a light aircraft. Using a Kalman filter, these sensors can be combined to achieve the best qualities of both [Hayward97]. AHRS units (< 1 deg error) that combine three angular rate sensors, three accelerometers, and a GPS receiver are becoming available and will cost less than \$5,000 [Hayward99]. The high-bandwidth information provided by the rate gyros allows slow GPS sampling, thus permitting use of a standard GPS navigation receiver.

3.5.4 Attitude for the Prototype System

A summary of the attitude sensors examined for flight test use is presented in Table 3.2. The first row is the rough requirements for the Tunnel-in-the-Sky display, and sensor data rate is expressed in terms of latency.

Table 3.2 Candidate Tunnel-in-the-Sky Attitude Sensors

	Cost	Accuracy [deg]	Latency [msec]
PROTOTYPE REQUIREMENTS	minimum	1.0	100
Inertial Navigation System (INS)	> \$50k	0.2	< 25
Attitude Heading Reference System (AHRS)	~ \$25k	0.5	< 25
GPS Attitude + Rate Gyros	< \$10k projected	0.25 pitch & heading 0.5 roll	50

In keeping with the philosophy of acceptable performance at minimum cost, flight test attitude data was derived by filtering of GPS attitude with inexpensive inertial sensors. This system built by Stanford researchers used a small array of three GPS antennas on top of the aircraft fuselage to provide carrier phase differential attitude measurements [Hayward97]. The left/right “roll baseline” was 36 cm in length and the third antenna was placed 50 cm forward to form the “yaw baseline.” The array was kept small (the longest baseline was approximately 53 cm in length - less than three GPS wavelengths) to limit computational load and to keep the array small enough for installation on top of the small test aircraft. Inexpensive quartz tuning fork rate gyros

were integrated using a Kalman filtering scheme. This system achieved pitch and heading accuracy better than 0.25 deg and roll accuracy better than 0.5 deg. Sensor jitter was estimated to be 0.1 deg. Serial attitude messages containing roll, pitch, and true heading were sent to the Tunnel-in-the-Sky display at 20 Hz.

Attitude data was used unfiltered, meaning that if the display was running at 24 Hz for example, the 20 Hz attitude was periodically used for two successive display frames. The different data rates for position and attitude presented no difficulty for display implementation or use. Attitude data was used to form a 3x3 direction cosine matrix relating aircraft body coordinates to the ECEF coordinate system. Magnetic heading was calculated for display to the pilot using a regional magnetic variation model.

3.6 Other Sensors

Although three-axis acceleration was not directly measured, this information can be used for autopilot control and driving display symbology. Airspeed was also not measured, but is required on a complete Primary Flight Display (PFD). Angle of attack measurements could also be presented as on some (HUD) formats. An outside air temperature sensor would complete an air data system for reporting quantities such as in-situ wind speed and direction.

Although all positioning hardware for this work was based on DGPS, it is not the only sensor that can be used. Localizer, glideslope, VOR, DME, ADF, and LORAN can be employed as 1-D or 2-D observables in a multi-sensor system. The first five have the advantage of already being certified for aviation approaches. Barometric and radar altimetry can provide vertical measurements. (Barometric altimetry has already been proposed as an aid to improving WAAS approach performance.) These positioning sensors may be integrated with inertial sensors and processed with a Kalman filter to estimate the full aircraft state. Except for the localizer and glideslope, none of these

sensors will likely offer the seamless precision of DGPS. For accuracy, wide-area navigation, low cost, and ease of interfacing, GPS is the current sensor of choice for Tunnel-in-the-Sky displays.

3.7 Display Domain Errors

Additional insight can be gained by looking at impacts of sensor errors in the *display domain*. Considered mathematically, the displayed image is simply a mapping of the 3-D world onto a small (as of this writing) 2-D display surface. When there is error in measuring the position or attitude of the vehicle, objects are displaced on the screen by a distance (measured in length or pixels) related to the sensor error. Understanding this relationship can help focus the inevitable cost and accuracy tradeoffs made by designers.

The mapping of real-world objects or their constituent points onto a flat screen is governed by projective geometry. Figure 3.1 presents a simplified geometry determined by the screen size, field of view, and the vertex V of the implied *viewing frustum*. (This *eyepoint* position V and distance s are determined by the viewing projection used and do not necessarily represent the actual location of the pilot's head.) For a point A , the onscreen distance from the screen center d_{screen} is determined by similar triangles:

$$d_{screen} = s \frac{d_{actual}}{a} \quad (3.3)$$

This results in an *angular* mapping of 3-D objects onto the display screen. This mapping is stored as a projection matrix in the 3-D display software and/or hardware, and is one component of the *graphics pipeline* that turns objects in computer memory into pixels on the display.

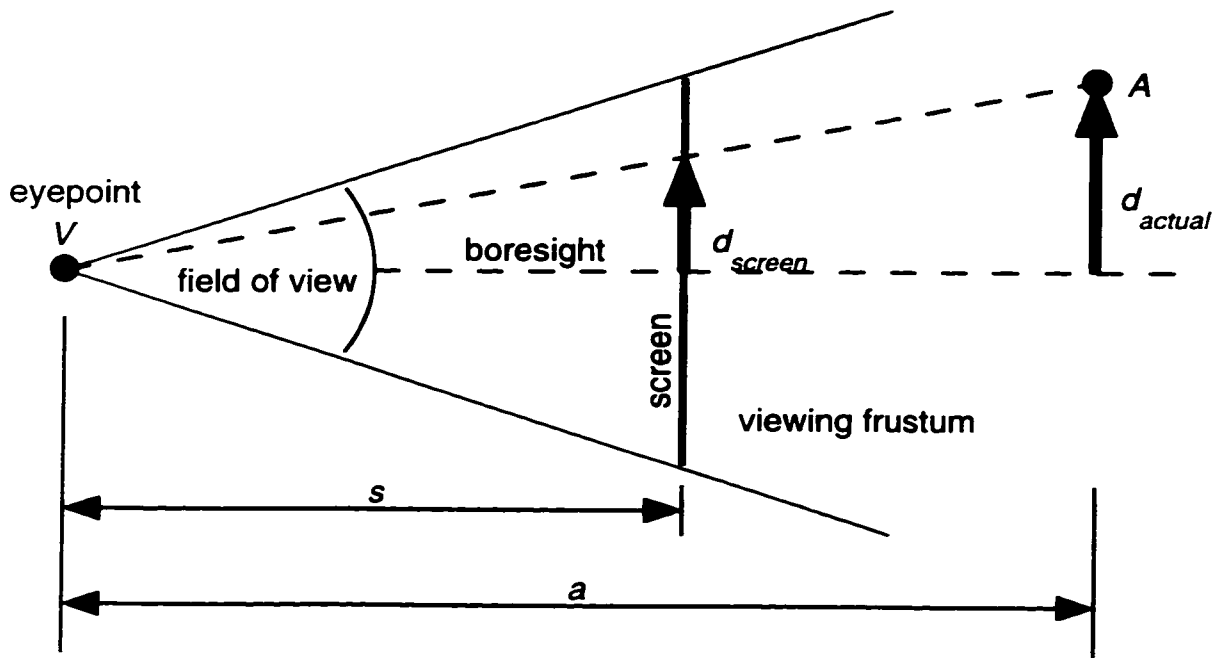


Figure 3.1 Angular Mapping of Perspective Projection

An attitude sensor error has the effect of moving objects through an angle in the viewing frustum's reference frame. Consider a point A that should map to the center of the display in Figure 3.2, but with an attitude error $e_{attitude}$ introduced that shifts the viewing projection (and the projection matrix in the graphics pipeline).

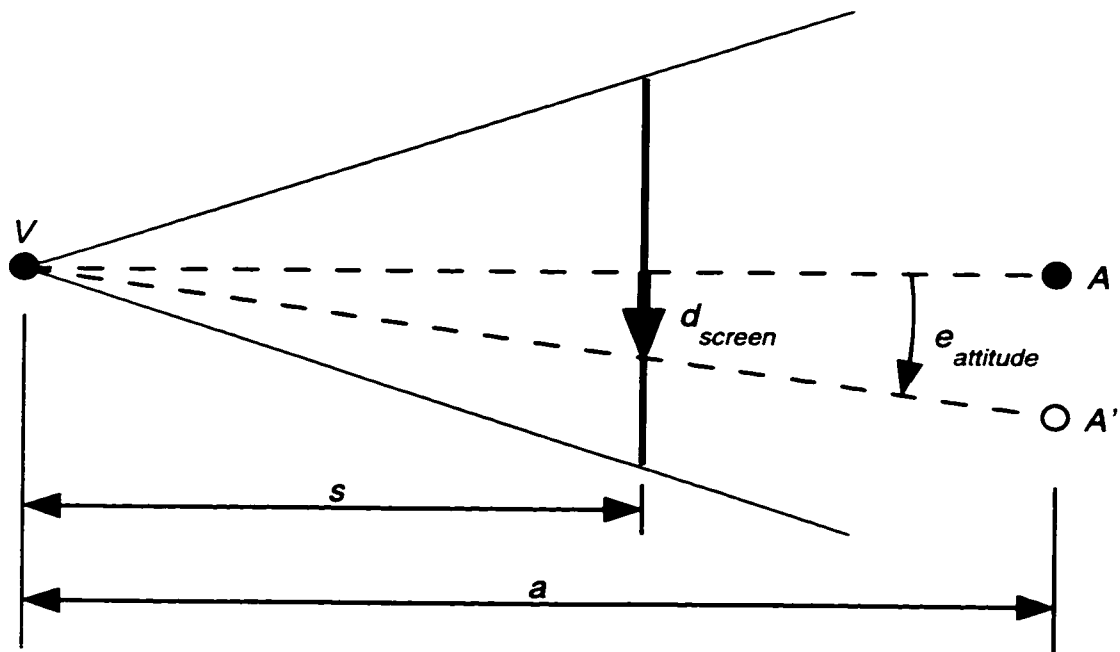


Figure 3.2 Effect of Attitude Error on Onscreen Position

This has the effect of moving point A to point A' in the viewer's reference frame. The onscreen error d_{screen} is

$$d_{screen} = s \tan(e_{attitude}) \quad (3.4)$$

where $e_{attitude}$ is measured in radians. For small errors and objects near the center of the projection,

$$d_{screen} \propto e_{attitude} \quad (3.5)$$

Onscreen error is nearly proportional to attitude error (except for very wide-angle projections), with the proportionality constant determined by the projection geometry. Onscreen error *does not* depend on the distance to the object. Note that for attitude errors that are rotations about the boresight direction, the entire displayed image rotates on the screen. The onscreen error in this case is proportional to the distance of a point from the center of the screen. Aircraft roll errors therefore have increasingly detrimental effects as display screens become larger.

Position errors behave differently. Introducing a position sensor error $e_{position}$ into the eyepoint location effectively translates the object position from A to A'' in viewer coordinates as shown in Figure 3.3. In this case

$$d_{screen} = s \frac{e_{position}}{a} \quad (3.6)$$

or

$$d_{screen} \propto \frac{e_{position}}{a} \quad (3.7)$$

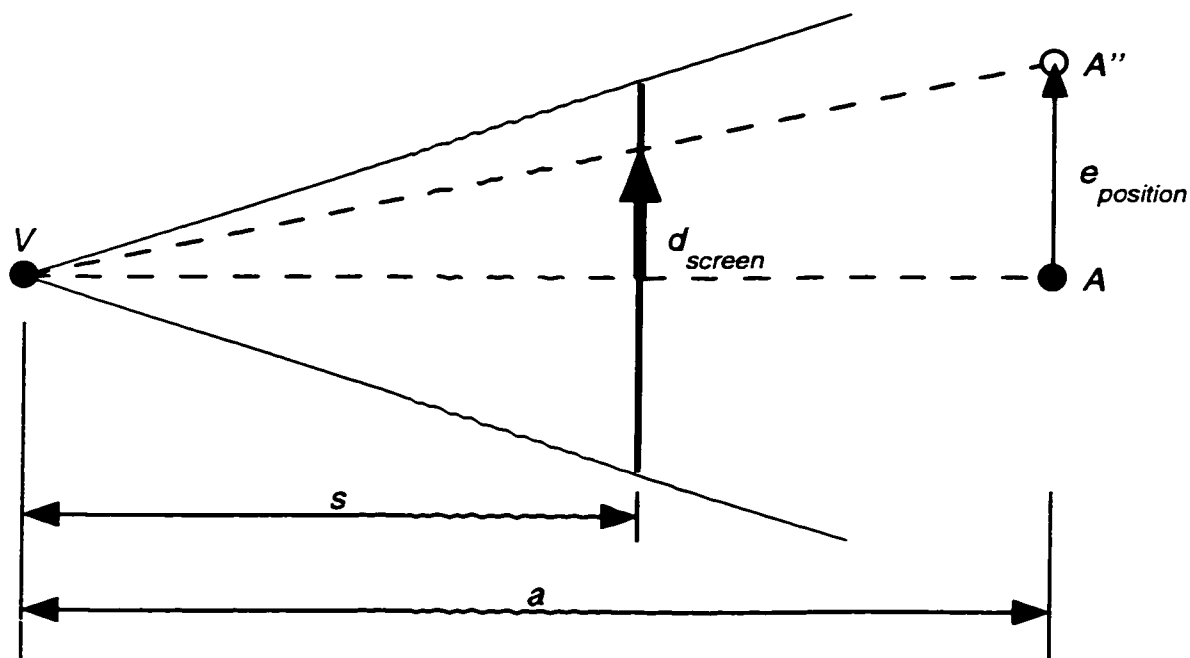


Figure 3.3 Effect of Position Error on Onscreen Position

For position errors, the onscreen error *does* depend on the distance to the object, with closer objects producing larger errors. Far-field objects (such as a mountain or distant airport) are hardly affected by 100-m sensor errors. However, as objects move into the near field (such as runway markings, airport features, or hoops the aircraft is flying through), even a 2-m error can become noticeable. Note that an object's onscreen position is not affected by the positioning error component along the line of sight to the object.

The relationships developed here allow guidelines to be established for sensor selection. First, assume some nominal distance to objects in the scene is known. Given the system's attitude accuracy, a corresponding positioning accuracy can be found that results in equivalent worst-case onscreen errors. Increasing overall system cost to gain better positioning accuracy beyond this point may have diminishing returns. Conversely, given a positioning accuracy and the knowledge that objects will remain in the near field

(typically not the case for aviation), a suitable complementary attitude accuracy range may be calculated.

Second, given the position and attitude errors in a system, one can establish a *critical distance* $a_{critical}$ at which positioning and attitude errors have similar effects:

$$d_{screen} \approx s e_{attitude} \approx s \frac{e_{position}}{a_{critical}} \quad (3.8)$$

$$a_{critical} \approx \frac{e_{position}}{e_{attitude}} \quad (3.9)$$

Beyond this critical distance, attitude errors dominate; within the critical distance, position errors dominate. This heuristic argument is useful to understanding a balanced sensor configuration.

Considering the WAAS positioning accuracy of 2 m and the integrated GPS/inertial attitude system's pitch and heading accuracy of 0.25 deg, the prototype's critical distance was approximately 460 m. Flying down the center of the displayed tunnel, the distance to the tunnel hoops when fully expanded to the edge of the display was approximately 100 m, indicating that positioning errors dominated the onscreen error at this point. On rollout and taxi over painted markings, position sensor jitter was more noticeable than attitude errors.

Sensing requirements may be relaxed as task domain requirements allow. For example, in the case of enroute navigation far from the ground, positioning accuracy is less critical than attitude accuracy. Stand-alone GPS may be viable for this application, despite the fact that $a_{critical}$ is higher than for DGPS.

Chapter 4:

Algorithms

This chapter outlines Tunnel-in-the-Sky definition, guidance, and display algorithms that were driven by incoming sensor data. The segmented flight path definition method is discussed in Section 4.1. Section 4.2 discusses the model of the earth's geoid shape that enabled the computer-generated virtual world to match the real world. Section 4.3 describes fast transformation algorithms for guidance on curved paths. A technique for minimizing numerically induced display jitter is described in Section 4.4. The algorithms created for this effort ran at the display framerate (up to 30 Hz) and were therefore focused on minimizing computational burden for use on low-cost embedded computer hardware.

4.1 Segmented Flight Path Representation

Typical flight management computers represent a flight plan as a series of waypoints. The aircraft flies from one waypoint to another, turning toward the next one as each waypoint is passed. Sophisticated systems have “turn anticipation” that allows

the aircraft to smoothly transition from one active waypoint to the next with minimal overshoot in turns, even though turning transients are not normally represented in the flight plan explicitly. A fundamentally different representation of all straight *and* turning portions of the flight path was required for the Tunnel-in-the-Sky display. This explicit definition was needed for efficient realtime retrieval of tunnel information used to generate continuous predictor symbology on curved paths.

The tunnel flight path was described as a series of path segments and waypoints that could be linked to form an arbitrary trajectory such as the one shown in Figure 4.1. These segments were curved with a constant turn radius and changed altitude with a constant climb or descent gradient. (Straight and level segments were simply a degenerate case of the general segment type.) Data describing the waypoints between segments was also stored to permit backward compatibility with conventional waypoint-based procedures. The internal functions used to set up the flight path at system startup were also used to process the guidance data in real time.

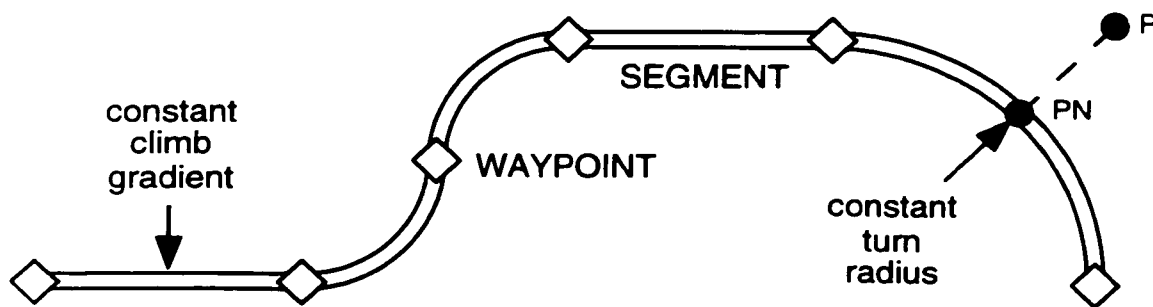


Figure 4.1 Linked Segment Flight Path Description (Overhead View)

The turn radius depended on the approach airspeed. For the Piper Dakota test aircraft with an approach speed of 95 kts, a 950-m turn radius was typical. A radius of 1500 m was used for the 120-kt Beechcraft Queen Air. Using a coordinated turn assumption (where TAS is true airspeed):

$$\text{roll angle} = \tan^{-1} \left(\frac{TAS^2}{r_{turn} g} \right) \quad (4.1)$$

This resulted in roll angles of approximately 15 deg for both aircraft. (This is in fact how the turn radii were chosen. The goal was to keep roll angles less than 30 deg, with a 15-deg margin for gust and crosswind corrections.) This explicit method of path description allowed operation on much more compact paths (the size of a typical airport traffic pattern) than allowed by conventional instruments.

4.2 Geoid Earth Model

Flight simulators commonly model the earth as a flat plate, greatly simplifying navigational computations and the description of flight paths curved in three dimensions. A Cartesian coordinate system is attached to the earth at a convenient spot, typically an airport reference point, to create a flat plate coordinate system as shown in Figure 4.2. This technique has been extended to Tunnel-in-the-Sky flight demonstrations that remain close to the reference airport.

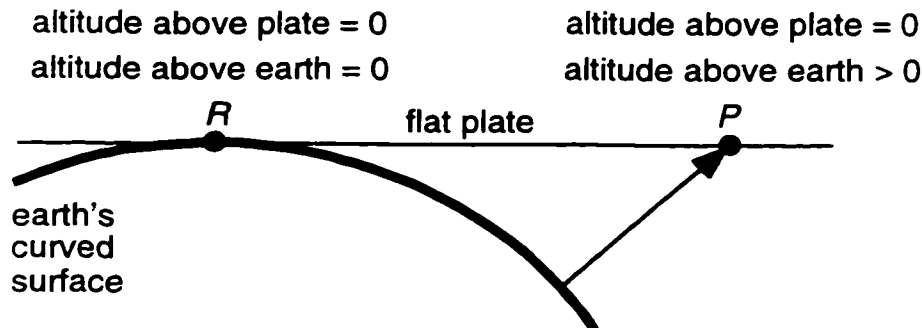


Figure 4.2 Flat Plate Earth Model

Away from the reference point, however, the flat-plate model diverges from the earth's curved shape. At the flat plate reference point *R* in Figure 4.2, altitudes above the flat plate and the earth's surface are equal. Moving away from the reference point, the earth's true surface "falls away" (quadratically at first) from the flat plate. Altitude above

the earth at point P becomes greater than altitude above the flat plate. The result is that the computer-generated world presented on the display begins to disagree with the real world seen by the pilot.

Altitude measured by the barometric altimeter also diverges from flat plate altitude since atmospheric pressure is created by the earth's gravity field and curved surface. This is noticeable to a pilot cross checking a Tunnel-in-the-Sky display with a barometric altimeter - a standard practice when crossing the outer marker beacon on an ILS approach. For example, if a flat plate model were used for the ILS approach at Salinas, California, the initial approach fix "check altitude" printed on the approach plate would be in error by 127 ft at 12 nm. This exceeds the 75-ft allowable altimeter error for light aircraft.

To alleviate the problem, the flat plate reference point can be switched periodically when altitude errors grow to a specified level. This requires additional computational overhead and transformation of data at the switch points. Perhaps more important, the algorithmic complexity of such a scheme poses software integrity risk. The algorithms described in the next section show that this risk may be avoided at minimal computational expense. The system tradeoff identified here (simplicity of a flat-earth model versus accuracy of a curved earth model) was thus turned into an easy decision.

Given the advantages of a curved earth model, the question became "which curved earth model?" The answer was dictated by an additional requirement. The computational language of 3-D graphics is based on Cartesian coordinates and matrix manipulations. Since practical systems will require global coverage, the Earth-Centered, Earth-Fixed (ECEF) coordinate system was the logical choice for internal data representation. Practical systems will also have to conform to standards for accuracy and

compatibility with legacy instruments and data. Much of the existing aviation survey data (e.g. navigation aids and runway ends) was generated with altitude referenced to mean sea level (MSL). Future systems will need to use the language of latitude, longitude, and altitude familiar to pilots. The additional requirement, then, was that the system be able to transform efficiently and accurately between computer-centric ECEF and pilot-centric latitude, longitude, and MSL altitude.

The simplest curved earth model, a sphere, does not model the earth's oblate shape. Altitudes computed from ECEF coordinates can have gross errors of over 21 km if not corrected for the earth's "equatorial bulge." An ellipsoid model incorporates this feature and results in altitudes usable for many navigation tasks. The ellipsoid defined by the 1984 World Geodetic System (WGS-84) is incorporated into nearly all GPS receivers [DMA91].

Irregularities in the earth's shape and mass distribution cause an undulation of mean sea level (the surface of zero gravitational potential) relative to the WGS-84 ellipsoid. This lumpy shape is referred to as the earth *geoid*. It is this surface to which geodetic altitudes and almost all altitudes used in operational flying and aviation survey are referenced.

The largest values of *geoid undulation* (the geoid height above the WGS-84 ellipsoid model) are around 100 m - very large compared to the allowable errors for precision instrument approaches. Clearly, an earth geoid model must therefore be employed in erecting a practical algorithmic framework for operational systems. In practice, the geoid model used was only slightly more complicated than the WGS-84 ellipsoid itself, requiring one additional correction step described in Subsection 4.3.1. The undulation lookup model was based on values tabulated in [DMA91].

4.3 Realtime Segment Computations

Navigation and guidance computations were performed on a segment-by-segment basis. This required determining the active path segment and then generating guidance cues relative to this segment. Pre-computation of relevant quantities along with careful algorithm design enabled realtime navigation on curved paths over the earth's geoid surface.

Determining the Active Segment

At the beginning of a frame of data, the first step was determining which straight or curved segment the airplane was on. Each segment had its own reference point (typically at the beginning of that segment) and segment coordinate system (locally level and aligned with the initial segment heading). To determine if the aircraft was on a candidate segment, the position was transformed into segment coordinates. A limit check determined whether the aircraft was on the candidate segment. If not, the next segment in sequence was tried.

Since they were used many times each second, the coordinate transformations were performed using optimized algorithms. Subsection 4.3.1 discusses fast transformation of the airplane ECEF position into segment coordinates and transformation of guidance symbol locations from segment coordinates back into ECEF coordinates. All path computations were performed in geodetic coordinates with one exception described in Subsection 4.3.2.

Generating Guidance Commands

All further guidance calculations were performed in the segment coordinate system. For each frame of navigation data, the point nearest the aircraft on the stored trajectory (called the *nominal point*) was found. In Figure 4.1, for example, *PN* is the

nominal point closest to aircraft position P . Guidance symbology was then generated based on the desired state at this nominal point. This information was transformed back into ECEF coordinates before display.

Representing the Tunnel

Positions of vertices describing the tunnel hoops were calculated at system startup in a local coordinate system for each segment and then transformed to world-referenced ECEF coordinates for storage. Drawing of these vertices in realtime is discussed in Section 4.4.

4.3.1 Geodetic Path Segments

Figure 4.3 shows an exaggerated view of a descending glideslope from point P to point S with a constant angle α_1 between the path and the local horizontal. The path therefore curves with the earth's geoid shape. (Note that an ILS glideslope is actually straight, requiring special treatment as described in Subsection 4.3.2.) For very long straight and level segments, the geodetic segment algorithms allowed paths to maintain constant barometric altitude as is customary for cruising flight. A flat plate approximation would have required that long segments be broken into many small segments, needlessly raising computational complexity.

This subsection describes efficient transformations between ECEF coordinates, geodetic coordinates (latitude, longitude, geoid-referenced altitude), and segment coordinates. To minimize the floating-point math burden, any data that could be pre-computed at system startup was stored on a per-segment basis for realtime retrieval.

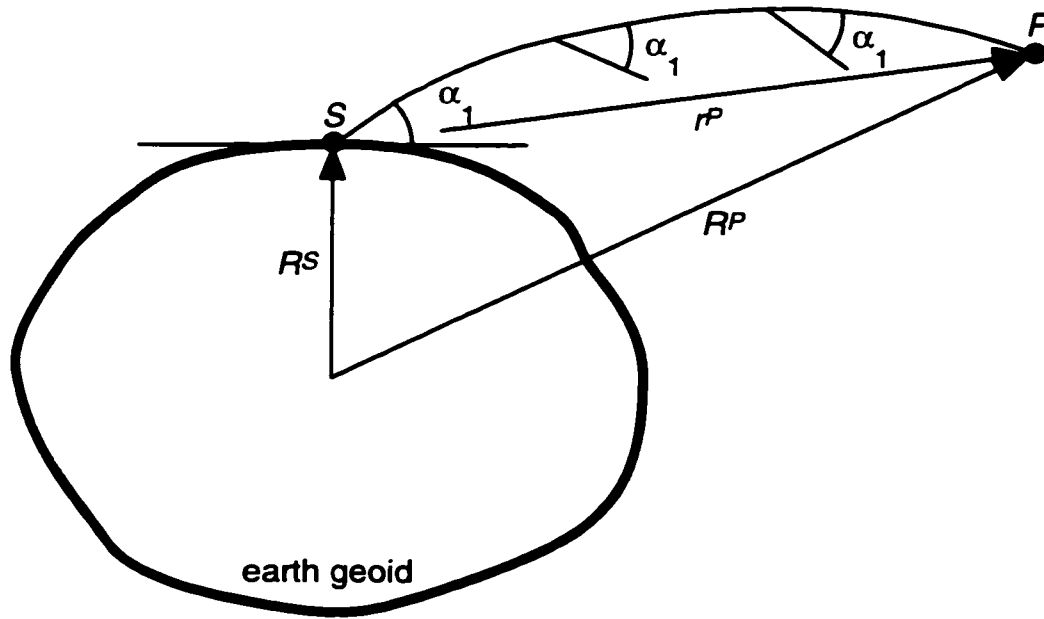


Figure 4.3 Geodetic Path Segment

Transforming From ECEF to Segment Coordinates

The first step in transforming the sensor-derived ECEF airplane position R^P was a standard conversion to WGS-84 ellipsoidal coordinates:

$$lat^P, lon^P, A_{ellipsoid}^P = f(R^P) \quad (4.2)$$

where

$$\begin{aligned} lat^P &= \text{geodetic latitude of } P \\ lon^P &= \text{geodetic longitude of } P \\ A_{ellipsoid}^P &= \text{height of } P \text{ above WGS-84 ellipsoid} \end{aligned}$$

Using a lookup table, this was then corrected for geoid undulation U to find the height above the geoid:

$$A_{geoid}^P = A_{ellipsoid}^P - U(lat^P, lon^P) \quad (4.3)$$

$$LLA^P = \text{geodetic coordinates of } P = lat^P, lon^P, A_{geoid}^P \quad (4.4)$$

Since the segment reference points S were known at system startup, their geodetic coordinates LLA^S were pre-computed using their ECEF positions R^S .

The transformation to find aircraft position in segment coordinates r^P was based on the latitude, longitude, and altitude difference of P and S :

$$r^P = {}_{seg}X_{lla}(LLA^P - LLA^S) \quad (4.5)$$

where the pre-computed 3x3 matrix ${}_{seg}X_{lla}$ was the transformation from (latitude, longitude, altitude) coordinate directions to segment coordinate directions. The transformation incorporated the following effects:

- 1) Scaling factors in latitude and longitude (from degrees to meters),
- 2) A scaling factor of $\cos(lat^S)$ in the east-west direction, and
- 3) A rotation to align with initial true heading for the given segment.

(${}_{seg}X_{lla}$ was not orthonormal due to the two scaling factors)

It was the step in equation (4.5) that “warped” the segment coordinates over the curved earth. With the airplane position determined in segment coordinates, further guidance computations (described in Chapter 5) could be performed as though the segment coordinate system were Cartesian.

Transforming From Segment to ECEF Coordinates

Once the position in segment coordinates r^G of the guidance symbol G was found, it was converted back to ECEF coordinates using the reverse transformation:

$$LLA^G = {}_{lla}X_{seg}r^G + LLA^S \quad (4.6)$$

$$lat^G, lon^G, A_{geoid}^G = LLA^G \quad (4.7)$$

Where $_{lla}X_{seg}$ was calculated and stored at system startup. The geoid model was again used to find the ellipsoidal coordinates of the guidance symbol:

$$A_{\text{ellipsoid}}^G = A_{\text{geoid}}^G + U(\text{lat}^G, \text{lon}^G) \quad (4.8)$$

These were finally converted to world-referenced ECEF coordinates using the inverse WGS-84 ellipsoid transformation of equation (4.2) above:

$$R^G = f^{-1}(\text{lat}^G, \text{lon}^G, A_{\text{ellipsoid}}^G) \quad (4.9)$$

The guidance information R^G was thus resolved in world-referenced ECEF coordinates as required by the graphics algorithms.

4.3.2 Cartesian Path Segments

All path segments were handled as above with one exception. In some instances it was desirable for the tunnel to exactly match an ILS approach path both horizontally and vertically. This path was defined by localizer and glideslope radio beams that extended outward and upward from the runway in a straight line. By design, geodetic path segments followed the curve of the earth's surface. If such a method were used to define an ILS final approach segment, the displayed tunnel and emitted radio beam would diverge far away from the runway. Since an important operational goal was for perfectly flown Tunnel-in-the-Sky approaches to result in zero deviation on the aircraft's existing instruments, a method was required for specifying segments that *do not* curve with the earth's surface. Such a path is shown in Figure 4.4.

In these instances, a local Cartesian (or flat plate) system was defined. Calculating the airplane position in segment coordinates r^P was simpler, not requiring a conversion to geodetic coordinates:

$$r^P = {}_{seg}C_{ecef}(R^P - R^S) \quad (4.10)$$

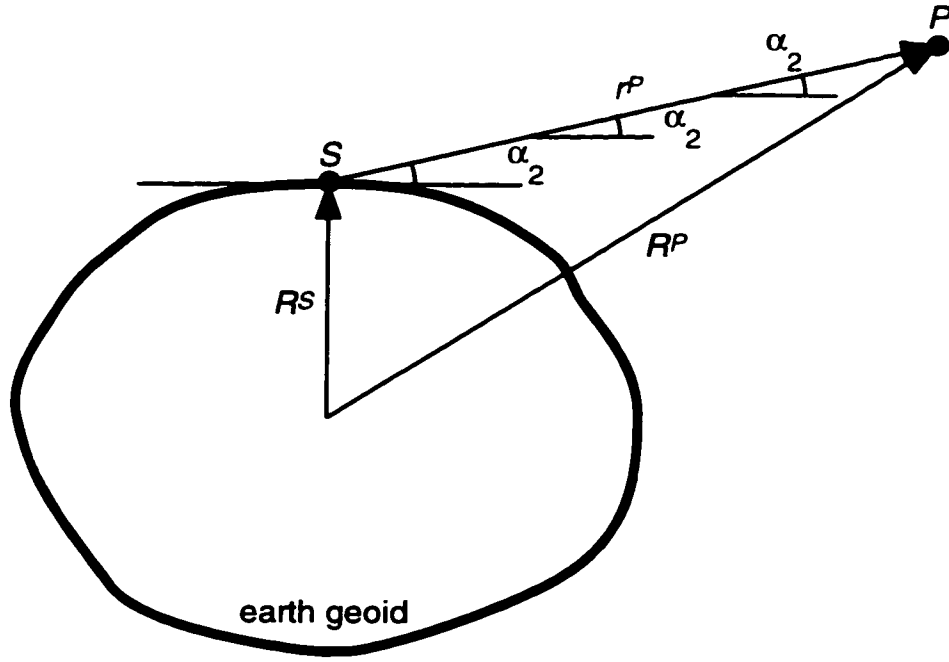


Figure 4.4 Cartesian Path Segment

Guidance information in segment coordinates r^G was then calculated. This was finally converted back into world coordinates R^G using:

$$R^G = {}_{ecf}C_{seg} r^P + R^S \quad (4.11)$$

Since the forward transformation matrix *was* orthonormal, ${}_{ecf}C_{seg}$ was simply the transpose of ${}_{seg}C_{ecf}$. Appropriate quantities were pre-computed and stored as with geodetic segments.

4.4 Compensation for Numerically Induced Jitter

It is common for flight simulators to require large dynamic range for internal representation of floating point numbers. If position is represented in ECEF coordinates, values range from nearly -7×10^6 m to $+7 \times 10^6$ m, roughly the radius of the earth. However, aircraft position must be represented to within tens of centimeters to avoid visual jitter of near-field objects. This is beyond the approximately seven significant

figures that can be represented by single-precision (32-bit) floating point numbers. Double-precision (64-bit) storage and computation should therefore be used for these quantities. However, much of the low-cost consumer 3-D software and hardware employs single-precision arithmetic for speed. PC simulation software can avoid jitter problems by using simplified flat plate world models. As noted above, operational displays forgo this luxury since the real and computer-generated worlds must match over large distances. The following method allowed double-precision sensor fusion and navigation algorithms to yield accurate results with commodity 3-D rendering systems.

A major step in turning stored data into points, lines, and polygons displayed on the screen is 3-D coordinate transformation. Consider the point A shown in Figure 4.5 (this could be one vertex of a hoop in the tunnel or an element of guidance symbology):

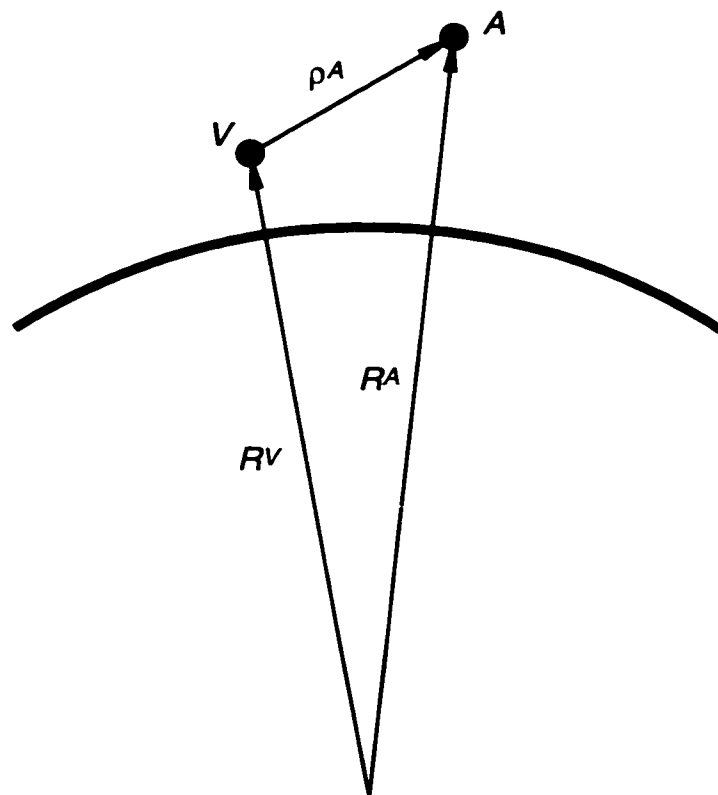


Figure 4.5 Viewer and World Coordinate Systems

Point A's ECEF position R^A must be transformed into a viewer coordinate system located at the display eyepoint V as introduced in Chapter 3. Generating this vector ρ^A requires a translation to the ECEF viewpoint location R^V and a rotation based on the aircraft attitude, ${}_{view}C_{ecef}$.

$$\rho^A = {}_{view}C_{ecef}(R^A - R^V) \quad (4.12)$$

These are exactly the quantities provided by the sensor fusion algorithms discussed in Chapter 3. In practice this translation/rotation is performed as one computation in the 3-D graphics pipeline.

$$\begin{bmatrix} \rho^A \\ 1 \end{bmatrix} = \begin{bmatrix} {}_{view}C_{ecef} & -{}_{view}C_{ecef}R^V \\ 0 & 1 \end{bmatrix} \begin{bmatrix} R^A \\ 1 \end{bmatrix} \quad (4.13)$$

The 4x4 *modelview* matrix on the right side is normally calculated once per frame [Neider93]. Vertex locations R^A in ECEF are then right multiplied one at a time to produce locations ρ^A in viewer coordinates. The fourth vector element (called the *homogeneous coordinate* and normally set to one) allows addition and subtraction to be performed within the context of optimized matrix multiplication. Each ρ^A undergoes further perspective and screen transformations on its trip through the graphics pipeline until finally ending up on the screen as pixels.

The vector ρ^A may only be a few tens of meters long for objects near the aircraft, such as a nearby tunnel element or predictor symbol. The vectors R^V and R^A are very large, on the order of earth radius. Since the rotation matrices have unity norm, the result of equation (4.13) is a small number found by differencing two large vectors, ${}_{view}C_{ecef}R^A$ and ${}_{view}C_{ecef}R^V$. On powerful machines this math can be done in double-precision arithmetic, but it challenges the single-precision range used by low-cost systems.

Chapter 3 described how sensor jitter introduces errors into the graphics transformation matrices, and that this manifests itself as jerkiness on the screen. Numerical error introduced in ρ^A by exceeding the available numerical precision causes errors that look similar to sensor jitter. Trial single-precision implementations of the Stanford Tunnel-in-the-Sky display suffered from noticeable visual jitter. A method was needed to perform critical computations in double precision, while letting the dedicated graphics software and hardware operate in single-precision optimized for speed and low cost.

The solution was to introduce a local coordinate system centered at point L as shown in Figure 4.6. The local system was completely predefined by its origin (located at R^L in ECEF coordinates) and transformation matrix ${}_{ecef}C_{local}$. Instead of storing vertex locations in ECEF, locations referenced to the local system r^A were used for realtime graphics.

By using small vectors r^A for the right multiplication of each vertex, the differences of large quantities could be eliminated. First it was noted that

$$R^A = R^L + {}_{ecef}C_{local} r^A \quad (4.14)$$

or in the 4x4 matrix notation used by the graphics pipeline:

$$\begin{bmatrix} R^A \\ 1 \end{bmatrix} = \begin{bmatrix} {}_{ecef}C_{local} & R^L \\ 0 & 0 & 0 & 1 \end{bmatrix} \begin{bmatrix} r^A \\ 1 \end{bmatrix} \quad (4.15)$$

Substituting this into equation (4.13) gives

$$\begin{bmatrix} \rho^A \\ 1 \end{bmatrix} = \begin{bmatrix} {}_{view}C_{ecef} & -{}_{view}C_{ecef}R^V \\ 0 & 0 & 0 & 1 \end{bmatrix} \begin{bmatrix} {}_{ecef}C_{local} & R^L \\ 0 & 0 & 0 & 1 \end{bmatrix} \begin{bmatrix} r^A \\ 1 \end{bmatrix} \quad (4.16)$$

which yields

$$\begin{bmatrix} \rho^A \\ 1 \end{bmatrix} = \begin{bmatrix} \text{view } C_{ecef} \text{ ecef } C_{local} & \text{view } C_{ecef} (R^L - R^V) \\ 0 & 1 \end{bmatrix} \begin{bmatrix} r^A \\ 1 \end{bmatrix} \quad (4.17)$$

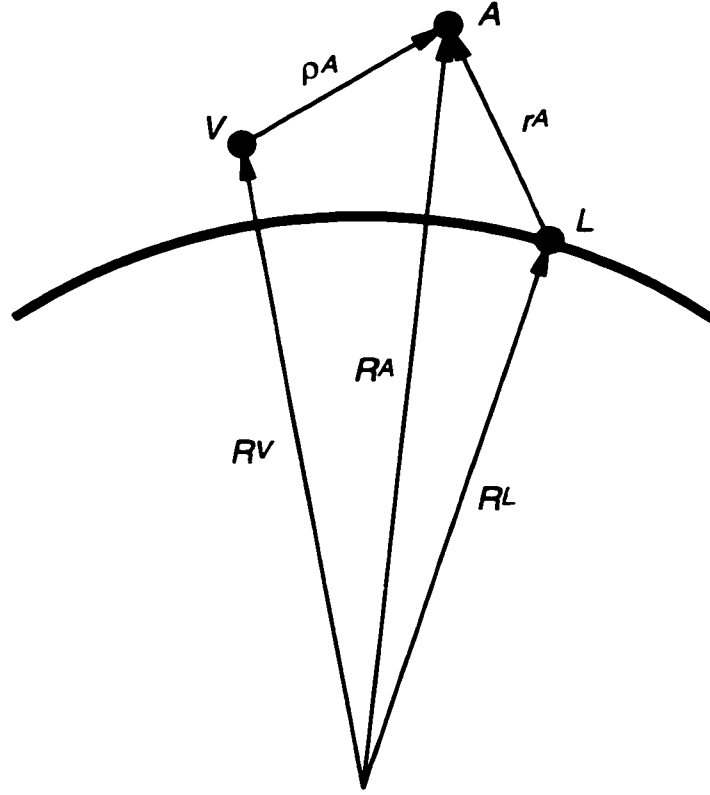


Figure 4.6 Addition of a Local Coordinate System

The 4x4 matrix on the right side of equation (4.17) was computed once per frame in double precision by custom software. The critical difference of large vectors ($R^L - R^V$) thereby retained the precision necessary to prevent visible onscreen errors. The per-vertex matrix multiplications involving r^A were then handled in single-precision by the optimized (off-the-shelf) graphics pipeline.

Loss of precision would only result when r^A became large, on the order of several hundred km. This could be easily handled by using several local coordinate systems on

very long flights; keeping the local origins within a few hundred kilometers of each other would prevent visible jumps as the reference point was switched. No realtime penalty need be incurred since all values of r^A are computed and stored upon path generation. This scheme would not significantly add to the computations required for an inflight re-routing since the number of reference points would be far smaller than the total number of computed vertices.

The decomposition of steps leading to equation (4.17) allowed isolation of the math that must be done in double precision from that which could be left to the single-precision graphics. Computing the double-precision matrix incurred negligible overhead since it was reused many times per frame. As with the previously described earth geoid navigation algorithms, the system tradeoff of computation time for numerical (and visual) accuracy was made easily bearable by employing algorithms appropriate for low-cost hardware.

Chapter 5:

Display Design

This chapter describes development of the Stanford Tunnel-in-the-Sky display. The overriding design philosophy is outlined in Section 5.1. Section 5.2 describes the display in its final configuration while Section 5.3 discusses the original configuration and evolution with extensive flight testing. Section 5.4 describes the low-cost hardware used at various stages of system development.

5.1 Design Philosophy

The purpose of the Tunnel-in-the-Sky display was to enhance situational awareness while increasing aircraft utility. This was achieved with improved path-following accuracy and reduced workload. Extensive use was made of previous display format work to allow focus on implementation and operational issues.

The display had to be easy to learn to fly. Flight training in general - and instrument training specifically - are time consuming barriers to widespread use of

personal aircraft. For airlines, initial and recurrent pilot training are significant costs of doing business. Making the display intuitive reduced the need for training and memorization of how it should be used. This substitution of what [Norman89] calls “knowledge in the world” (which uses natural mappings to simplify interpretation) for “knowledge in the head” (which needs to be memorized and practiced) is a fundamental premise of perspective flight displays.

Related to making the display easy to learn was making it easy to *relearn*, that is, easy to come back to after a period of pilot inactivity. The instrument flying skills of scanning, manual attitude flying, and cockpit resource management must be used frequently to retain at a safe level. It is therefore difficult for most pilots to maintain their instrument currency, thus limiting the utility of instrument training for the private pilot. Reducing the need for rote skills was considered an important goal of the design.

Many of today’s familiar instrument concepts were retained on the Tunnel-in-the-Sky display. The fewer new ideas the pilot had to learn, the better. The display can accordingly be viewed as a combination of conventional primary instruments, 3-D path guidance, and external objects the pilot would see on a sunny day.

The space on an aircraft instrument panel has been called the most valuable real estate in the world. A final overriding principle in using it wisely was to avoid clutter - to make every pixel count. Design of the display was a compromise between including enough information for the pilot to perform the flying task and preventing excess clutter. A good design maximizes the accessibility of the relevant information and minimizes content that detracts from what is important. This follows the principle of Data-Ink Maximization for printed charts put forth in [Tufte83], which states that the amount of ink used to represent information other than data should be minimized. The “Keep it simple, stupid” objective is especially relevant for general aviation with its limited

emphasis on cockpit rigor and minimal space for cockpit instrumentation. (The test display had fewer than 20 sq. in. of area available, while new airline aircraft have *multiple* displays of 48 sq. in. or larger.) Keeping symbology to a minimum had the additional benefit of reducing computational requirements, a significant advantage for the low-cost hardware employed.

5.2 Display Elements

The final Tunnel-in-the-Sky display configuration used for this effort is shown in Figure 5.1. The various display elements are explained in the Subsections that follow.

5.2.1 Frame of Reference

Choice of reference frame is fundamental for spatial information displays. Nearly all aircraft horizon references and attitude indicators employ an *inside-out* frame of reference, meaning that the aircraft symbol remains stationary with respect to the instrument panel while the ground/sky artificial horizon pitches and rolls in the aircraft frame. The inside-out artificial horizon thereby matches the view seen out the window. An *outside-in* instrument moves the aircraft symbol around on a fixed ground/sky background.

Both formats have been shown to be workable in Tunnel-in-the-Sky simulations [Wickens89]. A single display may combine inside-out and outside-in cues. Russian attitude indicators make use of *split* cues with pitch depicted inside-out and roll displayed outside-in. As might be guessed, Russian pilots transitioning into western aircraft have reported confusion.

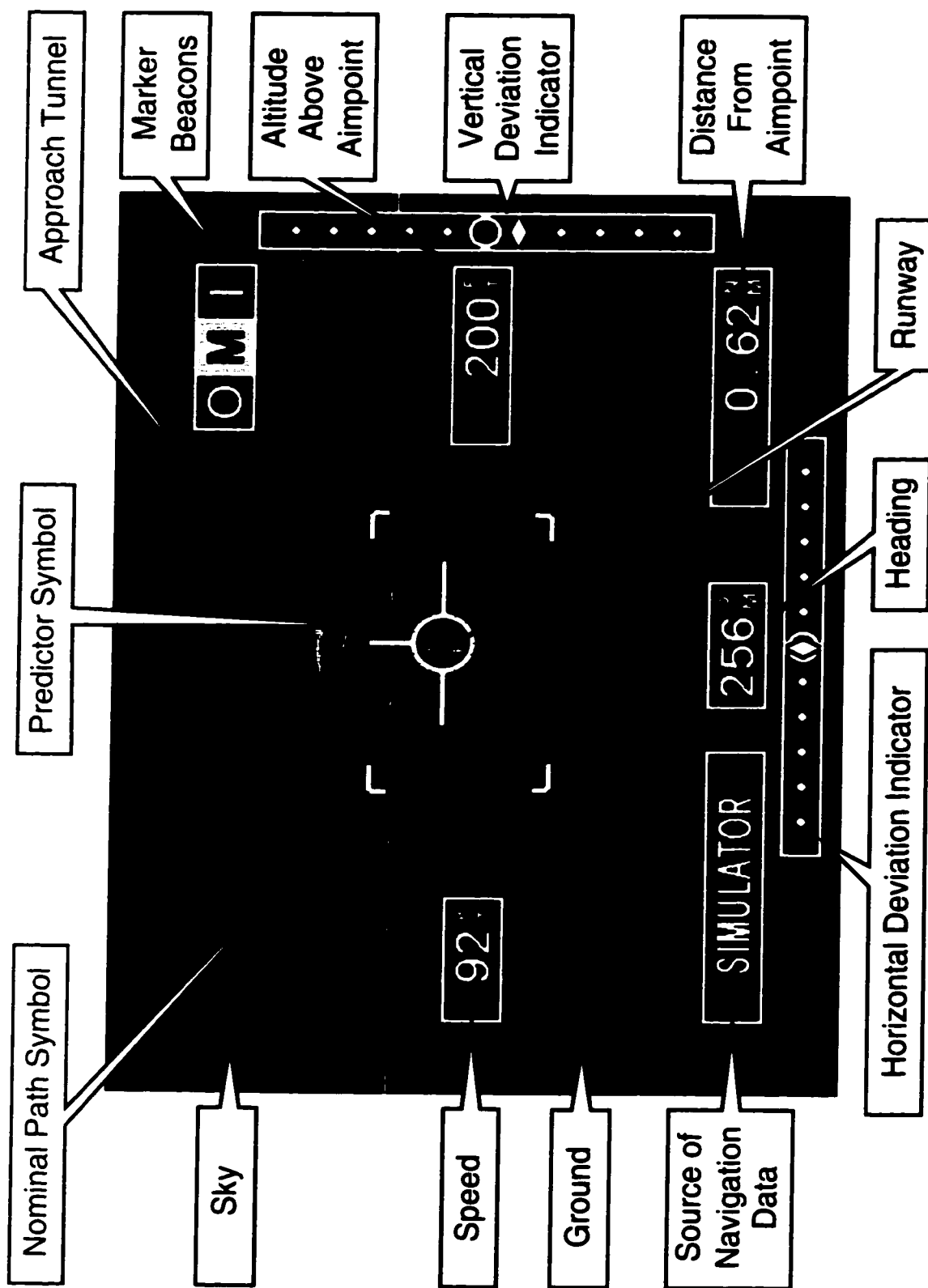


Figure 5.1 Final Stanford Tunnel-in-the-Sky Display Configuration

Displaying perspective symbology on the attitude indicator requires an additional choice of forward reference. Options include heading-forward, track-forward (or velocity vector-forward), or hybrids thereof. [Theunissen97] reports on simulator experiments with a velocity vector-aligned reference frame. This format may be useful for stabilization in the presence of crosswinds.

Despite possible benefits of outside-in cues, they are currently outweighed by the negative implications of abandoning the overwhelming standard ingrained in nearly all pilots. Therefore, the Tunnel-in-the-Sky frame of reference was chosen to be inside-out, or *egocentric*. Visually acquiring the runway after breaking out of clouds on instrument approach was aided by using exactly the same reference as the view directly out the front of the aircraft, i.e. heading forward. Reusing the inside-out standard can also exploit pilots' previous training for recovery from unusual attitudes.

The display background depicted the ground in brown, the sky in blue, and the horizon line in white to provide standard attitude indicator information. The perspective field of view was 40 deg vertical by 50 deg horizontal allowing for +/- 20 deg of pitch to fill the frame vertically, similar to a standard primary flight display.

The field of view included a runway with centerline dashes to provide motion cues and ease the critical transition from instrument to visual references. A control tower was also depicted off to the side of the runway. Other features could have been added, such as taxiways, roads, and water, but at some computational expense. Although roll and pitch scales have been implemented on the display, they were not used for the tests documented here. For categories of aircraft larger than the test aircraft used, these become important quantities for accurate display. The display of terrain is discussed in Subsection 5.2.4.

5.2.2 Tunnel Depiction

The tunnel extended in front of the aircraft to give the pilot a preview of the trajectory ahead. This trajectory preview benefited situational awareness by helping the pilot plan future actions. For example, if the pilot saw a turn coming up on approach, he could choose to communicate with ATC, lower flaps or gear, or make a power reduction before starting the turn. To use an analogy from control system theory, this preview injected *feedforward* information into the control loop.

This mode of managing control workload to plan for procedural tasks is called *error neglecting control*. By enabling accurate estimates of Time-to-Wall Crossing (introduced by [Theunissen94]), Tunnel-in-the-Sky displays allow the pilot to deliberately shift attention away from compensatory control. Error neglecting control gives the pilot time to perform other cockpit chores along with awareness of when full attention must be returned to active compensatory control. This ability to think ahead and manage priorities is beneficial to situational awareness, even for an airline crew acting as supervisory controller of an autopilot.

Although previous researchers used rectangular hoops or channels with an open top, the tunnel hoops for this work had a pentagonal shape with a slight “rooftop.” This shape was designed to provide a confirming up/down indication with the additional benefit of a line-up cue for lateral deviation. For instrument approaches, the approach path was depicted in green and the missed approach path in magenta as shown in Figure 5.1. The hoops were banked in turns at an angle appropriate to the aircraft’s true airspeed and coordinated turn radius.

The hoops were 100 m wide by 60 m tall, with the size chosen through investigation of previous literature, piloted simulation, and flight testing. It was shown in [Theunissen95] that control activity decreased and errors increased (although not

significantly) with increasing tunnel size. Since a major goal was reducing workload, a large tunnel width of 100 m was chosen to allow the pilot to spend more time in an error neglecting control mode. The tunnel height was made smaller than its width because vertical accuracy is typically more critical on final approach.

The straight and curved path segments were drawn with an in-track hoop spacing of 200 m. For the groundspeeds achieved with the two test aircraft, this resulted in hoop passage every 3 or 4 sec. Additional comments on choice of hoop spacing are made in Subsection 5.3.2.

No lines were drawn connecting corners of one tunnel hoop to the next. Although the splay angle formed by these lines with the vertical has been identified as important in extracting cross-track error [Theunissen97], they were omitted specifically to reduce clutter in the critical central area of the display. The success of the display without these corner lines suggests that pilots perceived this emergent cue without the dots' being connected onscreen.

When the aircraft began outside the tunnel or left it for some reason (e.g. for traffic spacing at the control tower's request), the pilot visually guided the aircraft into the displayed tunnel. Although on-demand generation of back-to-tunnel paths has been demonstrated, it was not employed here. Certification of such schemes is complicated by the fact that verified terrain information will be required to ensure that the spontaneously generated path clears terrain. Pre-defined procedures, in contrast, can be verified and certified before the flight.

5.2.3 Predictive Guidance Symbolology

Guidance symbology similar to that introduced in [Grunwald81] and [Grunwald84] led the pilot through the tunnel. The predictor and guidance symbols were

driven by fundamentally *kinematic* processes with dynamics not explicitly modeled, allowing the guidance scheme to apply to light airplanes generically. This augmentation to the tunnel depiction provided intuitive guidance with the added advantages of trajectory preview and enhanced spatial awareness.

Flight Path Predictor

A white *predictor symbol* shaped like a circle with wings displayed the aircraft's predicted position $\Delta t = 3.5$ sec in the future (Δt is called the *predictor time*). This predicted position was estimated using the current position, velocity, and acceleration vectors:

$$\mathbf{r}_{predictor} = \mathbf{r}_{aircraft} + (\Delta t)\mathbf{v}_{aircraft} + \left(\frac{\Delta t^2}{2}\right)\mathbf{a}_{aircraft} \quad (5.1)$$

One advantage of DGPS navigation was that it provided accurate velocity measurements as well as position. In Chapter 3 it was noted that acceleration was not measured. Therefore $\mathbf{a}_{aircraft}$ was inferred using roll angle:

$$magnitude(\mathbf{a}_{aircraft}) = \frac{\mu}{a_{earth}^2} \tan(\phi) \quad (5.2a)$$

$$azimuth(\mathbf{a}_{aircraft}) = \psi_{true} + 90^\circ \quad (5.2b)$$

$$elevation(\mathbf{a}_{aircraft}) = 0^\circ \quad (5.2c)$$

where μ is the WGS-84 earth gravitational parameter, a_{earth} is the WGS-84 earth equatorial radius, ϕ is roll angle, and ψ_{true} is true heading. The magnitude of $\mathbf{a}_{aircraft}$ was based on the assumption of a coordinated turn. The azimuth formula had the effect of directing the horizontal acceleration vector in the roll direction (note that left turns produced a negative magnitude). In light aircraft, vertical accelerations are typically smaller than horizontal ones and thus were not taken into account by this model. If

vertical acceleration were deemed important, a pitch rate gyro could be used to estimate this quantity in the absence of an accelerometer.

Equation (5.1) is a parabolic form linear in powers of Δt . More complex circular models have also been employed that extrapolate the aircraft's future path as a segment of a circle. This scheme is discussed in [Grunwald85] along with higher-order predictor models that incorporate additional aircraft states.

Guidance Symbolology

The guidance source, called the *nominal path symbol*, consisted of four corner tick marks representing the aircraft's desired position in 3.5 sec as if it were flying perfectly down the center of the tunnel. The tick marks were referenced to the nominal point (introduced in Chapter 4) on the tunnel closest to the aircraft position. With previous research as a starting point, the predictor time of 3.5 sec was tuned empirically to give acceptable performance with light airplanes. Larger aircraft with slower dynamics benefit from longer prediction times [Grunwald96a].

Flying the Display

From the pilot's point of view, the guidance task was simply to fly the predictor symbol into the center of the four tick marks. This task was very similar to flying with a flight director since the higher derivatives of position driving the predictor symbol (velocity and lateral acceleration) provided lead compensation. [Theunissen97] points out that while the mathematics may be similar, the tunnel is better because it permits separate awareness of the position and orientation errors. A flight director displays only a composite error signal based on these two quantities.

5.2.4 Other Information

Scales at the bottom and right of the display presented flight path deviations in the manner of standard ILS needles. A field of five dots either side of center was traversed by a diamond shaped pointer to show lateral and vertical errors on straight final approach segments. As with an ILS, the sensitivity of these tapes was typically 6 deg full-scale laterally and 1.4 deg full-scale vertically [FAA-AIM90]. A set of ILS marker beacon indicators was displayed at the upper right corner of the screen. These GPS-driven indicators were lit when the aircraft flew over the outer, middle, and inner marker beacons on an ILS approach. For airports with an installed ILS, the beamwidths and marker beacon positions were taken from an FAA database to match existing nav aids. A textual readout displayed the source of positioning information, e.g. WAAS, ILS, Coast Guard DGPS, or simulator.

Groundspeed (readily available from DGPS), heading, and altitude above the runway aimpoint were presented in the form of textual readouts at the left, bottom, and right of the display respectively. The textual format was chosen because a moving tape format would have required too much graphics processing. (This is no longer an issue as of this writing.) As described in Chapter 3, additional pitot and static pressure sensors would permit display of airspeed.

As noted previously, terrain was not depicted on the display for several reasons. First, low-cost graphics hardware available at the start of the project was not suitable for drawing complex terrain databases at high refresh rates. The power to do this with consumer video boards has become available only recently. Second, there isn't yet a standard high-integrity terrain database for aviation, although work described in Chapter 8 is proceeding in this area. Some Tunnel-in-the-Sky demonstrations have utilized lines extending downward from the hoops to the terrain (called *goalposts* in the literature). In

the absence of a high-integrity terrain database, goalposts were not drawn on the prototype display. Additional tradeoffs between terrain awareness and display clutter are areas of active research.

Most importantly, this work focused on *procedural safety* for instrument procedures. The premise is that if an instrument procedure is designed with adequate terrain clearance, then a system that allows the pilot to fly the procedure easily and correctly will enhance safety. (In the rare event that the aircraft ventures outside the tunnel, awareness of threats such as terrain becomes critical. *Safety through threat awareness* is the subject of a different research thrust.) Pilots who have flown the Tunnel-in-the-Sky display (without terrain) say that it is a quantum leap ahead of today's methods for flying instrument approaches.

5.3 Evolution of Display in Response to Pilot Evaluations

The final Tunnel-in-the-Sky display format evolved through a continuous process of software development, piloted simulation, and flight testing. Usability issues were often not understood until flight testing in a bouncing cockpit flooded with bright sunlight. This effort's operational orientation uncovered real-world design concerns that have not historically been noticed in the comfort of laboratory simulations.

An early display version flight tested on a Piper Dakota in 1995 is shown in Figure 5.2. This used a custom-written set of 3-D graphics routines since an industry standard for 3-D graphics didn't yet exist for PCs. Graphics were displayed at a low 320x240-pixel resolution to minimize video memory bandwidth requirements. Predictor guidance symbology was not included; instead, a triangular yellow "own-aircraft" symbol was fixed at the center of the display. Pilots were told simply to "fly the yellow symbol through the hoops." Evolutionary improvements to this initial display are described below.

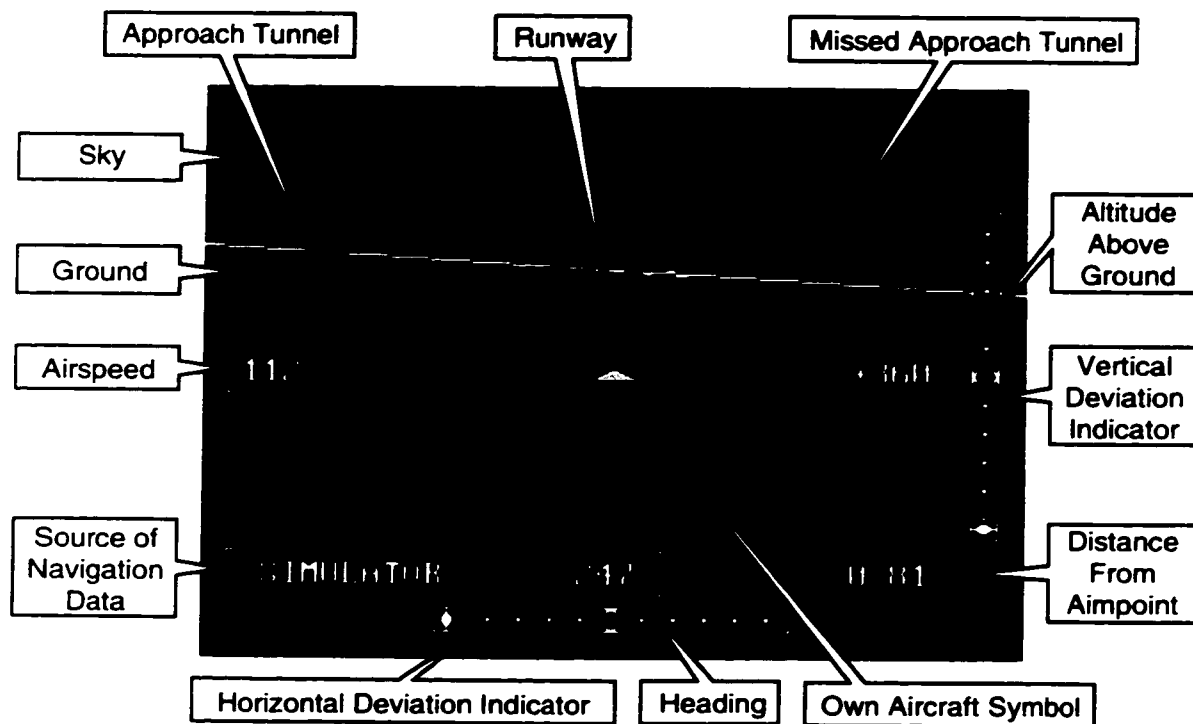


Figure 5.2 Initial Stanford Tunnel-in-the-Sky Display Configuration

5.3.1 Added Horizontal and Vertical Deviation Indicators

The horizontal and vertical deviation indicators were not present in initial testing. Pilots who flew the display on a simulator unanimously requested more information on path-following error. Once near the center of the tunnel, test subjects commented that it was difficult to assess small deviations from the desired flight path, especially in the vertical direction. Although they easily guided the aircraft through the tunnel, they wanted raw deviation information similar to an ILS indicator. Adding ILS-style indicators provided a familiar link to current instrumentation and a direct display of flight path errors. Discovering this issue in initial piloted simulation avoided unnecessary flight test expense.

5.3.2 Tightened Hoop Spacing

Hoops were spaced 500 m apart on the initial display to limit the number of hoops drawn by the graphics hardware. In simulated turning flight, pilots complained that they could see only one or two hoops of the turn before it curved out the side of the display. Therefore, on curving segments the spacing was reduced to 200 m to allow more hoops to be displayed for better curved trajectory preview. Spacing was kept at 500 m on straight segments to maintain a reasonable graphics framerate.

5.3.3 Added Predictor Guidance Symbology

In describing the tracking strategy used without the predictor symbol, pilots said they attempted to fly the own-aircraft symbol through one of the next hoops in the tunnel. This resulted in ambiguity over which of the next few hoops the pilot should try to fly through. It was in response to this feedback that predictor symbology similar to that described in [Grunwald84] was added. From the pilot's perspective, the pursuit tracking task became unambiguous: fly the predictor symbol into the middle of the nominal path tick marks.

5.3.4 Moved Guidance Symbology into Central Field of View

The four corner tick marks of the nominal predictor symbol were initially sized 100 m wide by 60 m tall, the same as the tunnel hoops. With a predictor time of 3.5 sec, this located the marks more than halfway to the edge of the display. Simulator pilots commented that they had to "scan" the display to locate first the predictor position, then the tick marks, etc. The corner tick marks were simply spaced too widely to allow for easy pilot assessment of whether the predictor was centered within them. To enable the pilot to see the predictor and nominal path tick marks simultaneously, the corner tick mark frame was drawn 50 m wide and 30 m tall, exactly half the tunnel dimensions.

These dimensions are used in Figure 5.1, although the visual effect is difficult to infer from a static picture.

In 1996, dedicated 3-D graphics capability was added to the Tunnel-in-the-Sky prototype. The hardware was driven by the OpenGL graphics software library that had recently become available for the PC. This provided greater processing power and allowed more graphical elements to be drawn. The faster hardware permitted reduction of hoop spacing on straight segments to 200 m to match the curved segments. The graphics hardware also featured line antialiasing to eliminate jaggedness. A more-realistic gradient horizon (found in many flight simulators) was programmed using the Gouraud shading feature. Figure 5.3 shows the display after this hardware was installed.

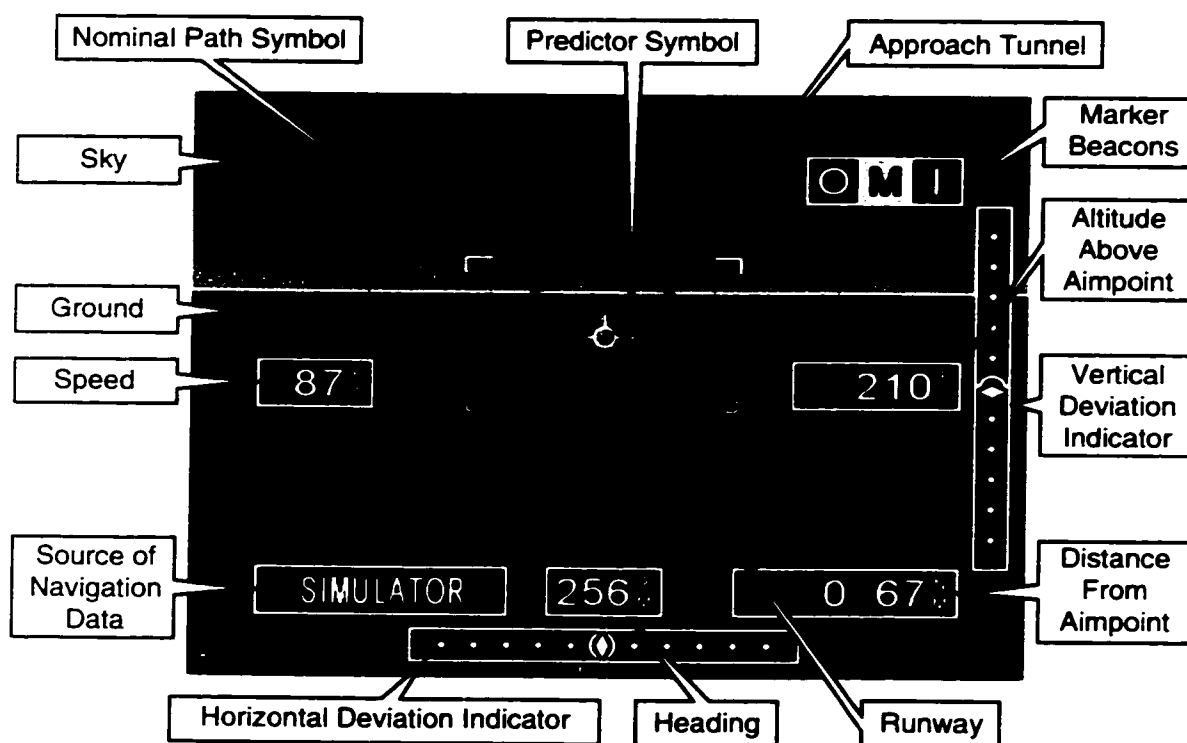


Figure 5.3 Intermediate Stanford Tunnel-in-the-Sky Display Configuration

5.3.5 Eliminated Gradient Horizon and Increased Contrast

Although the display in Figure 5.3 was flyable on the simulator in the laboratory, it didn't work as well in the actual flight environment. Initial flight testing of the display in a Beechcraft Queen Air took place late on a sunny afternoon. The bright sun and angle of incidence in the cockpit caused washing out of the display. The late-afternoon turbulence shook the airplane, making the symbology difficult to read. The predictor was especially hard to see against the light background of the gradient-shaded blue sky. The light background decreased contrast and also washed out the light green and magenta of the tunnel hoops. All display elements therefore became harder to see near the center of the display where they were most important. To make the symbology more accessible, the color gradient in the blue sky was removed. The brown ground and blue sky colors were darkened for increased contrast. The green and magenta hoop colors were also lightened to increase contrast with the ground/sky background. (This would be less of a problem in airliner cockpits with deeper glareshields and smaller relative window area. The bubble canopy of a military fighter presents even more difficult problems with display brightness and contrast.)

5.3.6 Increased Symbol Size and Added Shadowing

To further make the predictor, corner tick marks, and tunnel hoops stand out on the display, the line width of these symbols was increased. (Although thinner lines looked "cleaner" in printed material and on the laboratory simulator display, they were difficult to interpret in the aircraft cockpit.) The size of the predictor symbol was also enlarged for easier visibility.

To further increase the ease of extracting this information in the glare and turbulence, black shadowing was added to make the symbols stand out from the horizon display as a distinct layer of symbology. The need to trade away pleasing aesthetics for

instant readability was revealed only by extensive flight testing in high-workload situations such as traffic pattern work.

5.3.7 Decluttered Center of Display

Initial display versions drew all the tunnel hoops at the same intensity. When flying through long straight segments of tunnel, pixels would fill the center of the display as perspective effects concentrated the hoop images. This created the effect of a mass of green at the display center. [Theunissen97] reduced this problem by drawing hoops beyond a specified distance ahead of the aircraft at a reduced intensity. The technique adopted for this effort simply stopped drawing hoops beyond a distance of 4 km from the aircraft. This had the advantage of reducing graphics processing requirements, which could become large for long procedures.

By the time the Stanford Tunnel-in-the-Sky display had evolved into the final configuration of Figure 5.1, it incorporated feedback from 25 flight tests, 110 instrument approach procedures, 7 pilots, and 2 aircraft. Subtle shading effects had been removed and delicate symbols had been made more ponderous. This final configuration appeared relatively simple compared to previous Tunnel-in-the-Sky demonstrations, but it was *easy to fly*, tested for *real-world operations*, and based on *low-cost* hardware detailed below.

5.4 Display Hardware

Keeping the prototype cost down meant using consumer computer technology as it became available. This was also true of the decision to use AMLCD flat panel displays rather than something more exotic. Although some previous Tunnel-in-the-Sky research has focused on HUD implementations, this approach was not taken due to the prohibitive

expense and installation requirements of HUDs for small aircraft. Development of low-cost HUDs (notably for the automobile industry) may change this situation in the future.

Initial Configuration

The initial hardware platform, first flown on the Piper Dakota in 1994, was an 80486-based laptop with DOS as the operating system. 3-D graphics software was custom-written for this purpose because dedicated graphics hardware was still too expensive. The graphics chipset had no 3-D acceleration capabilities, and display framerates were typically 12 Hz or 15 Hz. The copilot held the laptop computer up to the right side of the instrument panel. The 9.5-inch diagonal transfective display was easy to read in the brightly-lit cockpit, but it was limited to grayscale images.

Flight Computer Upgrade

In 1995, the computer was upgraded to a ruggedized 90-MHz Pentium PC outfitted with a 64-bit graphics card (but with no 3-D acceleration). To position the display as close to the pilot as possible, a 5.5-inch diagonal AMLCD color video monitor was fixed to the glareshield of the test aircraft. Display on the 320x234-pixel monitor required a video scan conversion and an attendant loss of display sharpness. The transmissive backlit display proved difficult to read in bright sunlight.

Accelerated 3-D Graphics

In 1996, the operating system was upgraded to Windows NT to take advantage of the emerging selection of low-cost 3-D graphics boards for the PC. OpenGL 3-D graphics functions were accelerated by the GLiNT 300SX video chipset that implemented parts of the rendering pipeline in hardware. All lines on the display were drawn with antialiasing, a standard feature of commercial glass cockpit avionics that prevents jaggedness. The display framerate was typically 15 Hz. A ruggedized sunlight-

readable 6.4-inch diagonal AMLCD with 640x480 resolution was mounted in the right side of the Piper Dakota instrument panel. In bright light, the display was easily visible from the right seat, but it was difficult for the pilot to read across the cockpit.

Change of Test Aircraft

In 1997, with the change to a Beechcraft Queen Air test aircraft, the graphics board was once again upgraded, reflecting the rapid development and price drops in this arena. A PC video card based on the GLiNT 500TX chipset was installed to increase the framerate to 20 Hz. Based on the 10 Hz position sensor update rate and the 20 Hz framerate, maximum total system latency for displayed images was estimated to be 150 msec. The 6.4-inch diagonal AMLCD monitor was mounted in the instrument panel to the left of the heading indicator – close enough to the center of the pilot's scan to serve as the primary flight display. This configuration, combining accelerated 3-D graphics with a centrally located display, provided a capable platform for the bulk of the flight test program.

The cost of the final prototype hardware in 1997 (not including the specialized GPS attitude receiver) was less than \$25,000. With the prices of enabling hardware components going down, a complete system cost of \$20,000 seems a reasonable target for large-scale future commercialization.

Chapter 6:

Piloted Simulation Tests

Piloted simulation was integral to development of the Tunnel-in-the-Sky display. It was used initially to validate software architecture and low-level algorithms. The simulator was flown extensively before the first flight tests, and ongoing improvements were always refined in simulation before additional flying. This paradigm allowed for rapid prototyping and efficient use of limited flight test resources. Section 6.1 describes the simulator itself while Sections 6.2 through 6.6 describe experiments performed on the simulator. Section 6.7 summarizes the piloted simulation results.

6.1 Experimental Simulator

A PC-based IFR procedures simulator was used throughout this work. The simulator was customized by the manufacturer to produce serial output in a packet format identical to that of the GPS equipment used in flight testing, allowing flight hardware to be used in the lab with minimal reconfiguration. (Different configurations for testing and actual use make for unpleasant systems engineering surprises!) Since the simulator's

runway database was based on real-world information in Jeppesen-Sanderson's NavData database, the Tunnel-in-the-Sky display performed exactly as it did in flight with GPS data.

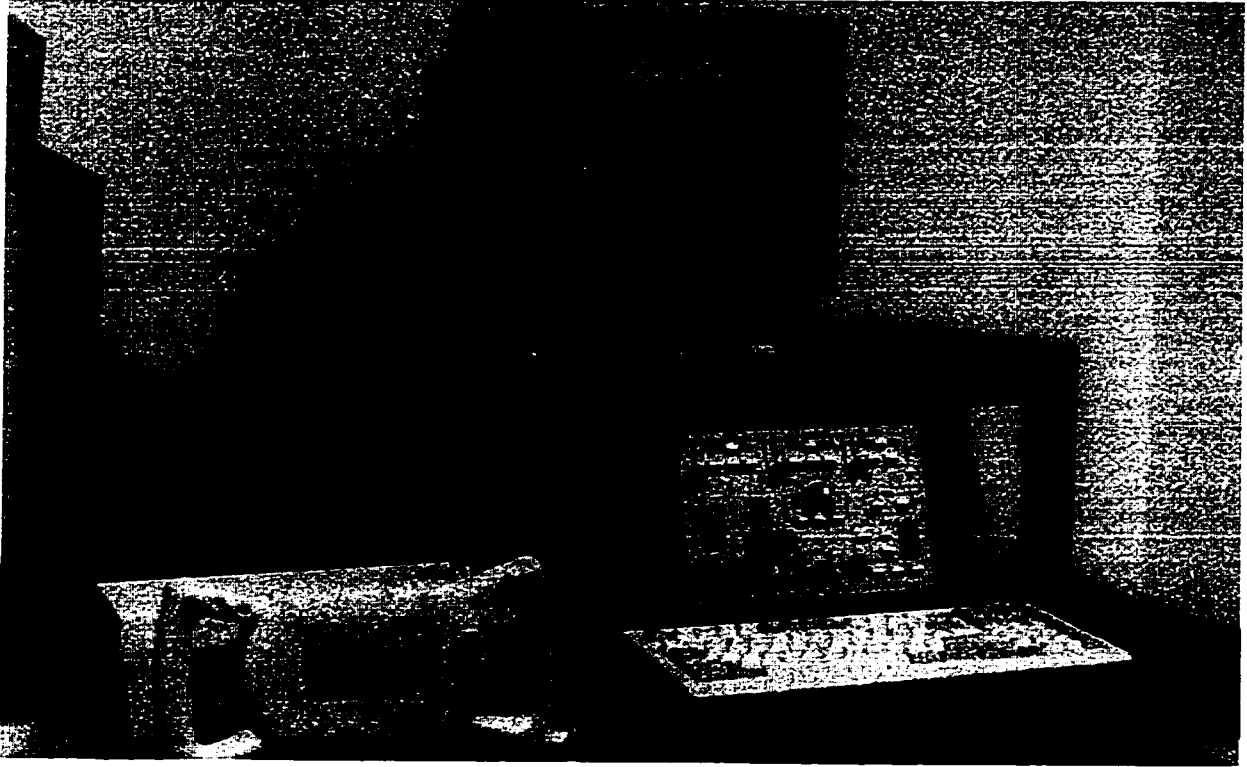


Figure 6.1 Experimental Simulator Setup

As shown in Figure 6.1, a control yoke and console were used to adjust power, trim, flaps, and landing gear, making keyboard use unnecessary. The simulator instrument panel included an attitude indicator, heading indicator, altimeter, airspeed indicator, and vertical speed indicator. The flight dynamics emulated those of a high-performance single-engine aircraft. The landing gear of the simulator was left down during these tests to closely parallel operation of the fixed-gear Piper Dakota test aircraft.

6.2 Methodology

The primary quantitative measure gathered during simulation was Flight Technical Error. Since NSE is relatively small for DGPS systems, measurements of FTE are an excellent estimate of TSE. (TSE and FTE were, in fact, equal for the simulator since it had perfect knowledge of the aircraft state.) Recalling from Chapter 2, reduction of TSE was one of the high-level goals of this Tunnel-in-the-Sky project. Making low TSE easy to achieve can aid situational awareness with today's procedures, while reduced TSE on tomorrow's complex procedures can increase aircraft utility.

Three pilots were involved in these tests. This small test subject pool and the amount of testing performed were not intended to provide results of statistical significance. Quantitative workload was also not measured, as it was felt that subjective observations would be more useful during early development than a highly focused study of the human-machine interface. The trials were used instead to focus system development and lower costs of the operational flight test program.

6.3 Straight-In Approaches with Varying Winds

The objective of this experiment was to verify that the initial display design would be operationally useful for ILS approach procedures flown in the Piper Dakota. An additional goal was to demonstrate advantages of the Tunnel-in-the-Sky display for missed approach procedures.

Procedure

Simulator tests consisted of approach and missed approach procedures for runway 25R at Livermore, California. The simulator pilot was an 800-hour Private Pilot with approximately 70 hours of instrument time. The pilot flew six runs using the Tunnel-in-the-Sky display and six using the standard ILS needle display introduced in Chapter 2.

Six different wind conditions were used as shown in Table 6.1. Although “light” turbulence was selected on the simulator, the pilot commented that it behaved more like moderate turbulence based on flight experience. The Tunnel-in-the-Sky format was that shown in Figure 5.2. The order of display type and wind condition was randomized to mitigate systematic learning effects. A one-hour training session was given on use of the simulator and displays.

Table 6.1 Wind Conditions for Straight-In Approaches

Wind Direction [deg magnetic]	Wind Speed [kt]	Condition
256	0	calm
166	15	90° left crosswind
211	15	45° left crosswind
256	15	wind down runway
301	15	45° right crosswind
346	15	90° right crosswind

An overhead view of the procedures flown for this test is shown in Figure 6.2. Each run started with the aircraft 11 km from the runway, 2 km to the left of centerline, and below the 2.9-deg glideslope. (This glideslope angle was determined through flight testing at Livermore airport and is expressed relative to local horizontal determined from the WGS-84 ellipsoid.) The initial aircraft heading was 285 deg magnetic to make an approximate 30-deg intercept with the 256-deg magnetic runway heading. The pilot flew straight ahead to intercept the runway centerline and then turned left towards the runway. Upon glideslope intercept, a descent was commenced to stay on the glideslope. The pilot

was instructed to execute a missed approach at the decision height (DH) of 200 ft above ground level approximately 1 km from the runway. The missed approach procedure consisted of climbing straight ahead to 700 ft and then initiating a climbing right turn. This turn was stopped on a heading of 060 deg magnetic. Conventional missed approach procedures are specified on the approach plate as a series of textual instructions.

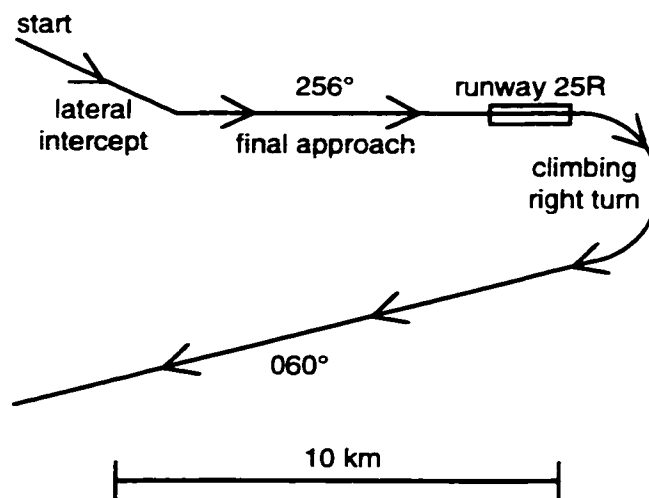


Figure 6.2 Overhead View of Straight-In Test Procedure

Results

Figure 6.3 shows vertical FTE on the straight-in portion of the twelve approaches from 7.5 km to 2 km from touchdown. (Data recording stopped at 2 km in preparation for the missed approach procedure.) The aircraft moves from left to right on the plot. The Tunnel-in-the-Sky display approaches (represented by solid curves) show generally smaller path following error than the ILS needle display runs (represented by dashed curves). Vertical root-mean-square (RMS) FTE for the Tunnel-in-the-Sky display was 14.2 m compared to 27.5 m for the ILS needle display over the entire distance. At the left side of the plot, the ILS needle runs show a trend towards being low. Since the runs began with the aircraft below the glidepath, this suggests that the pilot was often slow in completing the vertical glideslope intercept. (This is typical of ILS operations and not

problematic; accuracy near DH is of greater concern.) The angular nature of the ILS would be expected to lower FTE nearer the runway.

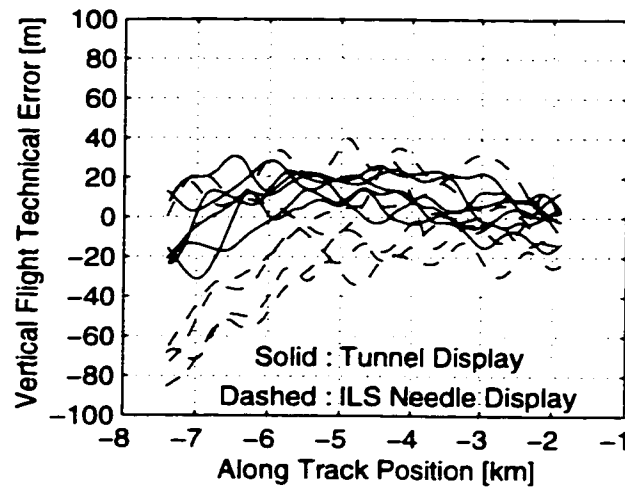


Figure 6.3 Vertical FTE on Straight-In Approaches

Lateral (cross-track) FTE on final approach is presented in Figure 6.4. The Tunnel-in-the-Sky runs contain smaller average lateral FTE of 37.1 m RMS FTE compared with 85.9 m RMS FTE for the ILS needle runs. The ILS needle runs exhibit more oscillation or “hunting” for the correct horizontal path, while the Tunnel-in-the-Sky runs appear smoother.

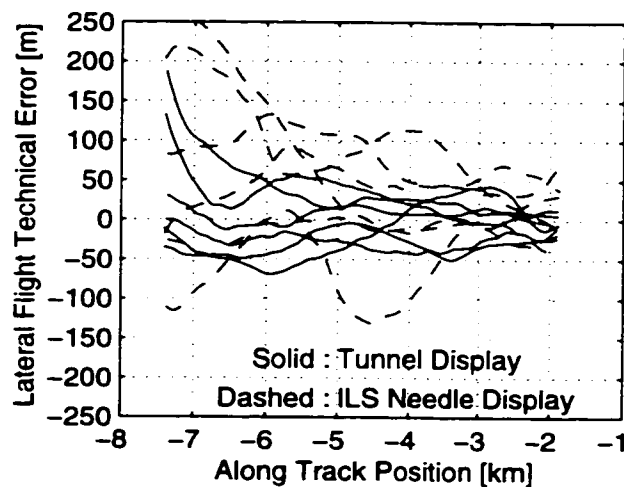


Figure 6.4 Lateral FTE on Straight-In Approaches

Figure 6.5 shows an overhead view of the lateral intercept made to the runway centerline and reveals interesting behavior associated with this inbound turn maneuver. The ILS needle runs exhibit overshoot and undershoot as the pilot tried to smoothly intercept the localizer. After intercept, additional hunting for the lateral path is evident. The Tunnel-in-the-Sky runs exhibit fewer tendencies towards overshoot and undershoot, and show that the pilot achieved smoother lateral intercepts when confronted with varying wind conditions.

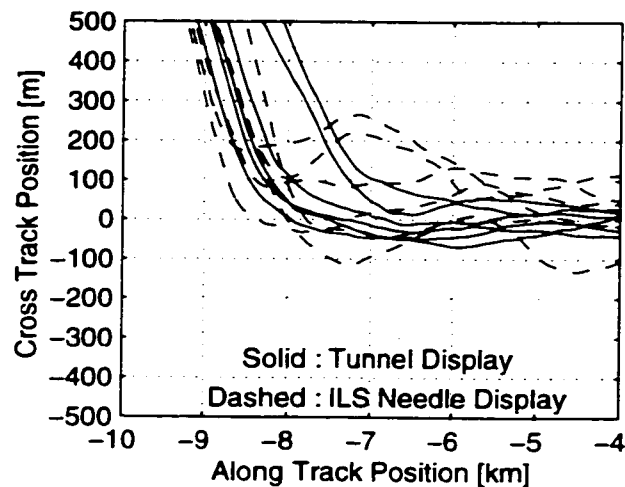


Figure 6.5 Lateral Flight Path Intercept on Straight-In Approaches

An overhead view of all twelve approaches is shown in Figure 6.6. On such a large scale, lateral deviations on the approach are difficult to see; however, the missed approach segments look quite different. The curving missed approaches using the Tunnel-in-the-Sky display collapse onto one thick trace, demonstrating that the pilot was able to repeat the curving flight path with each of the various wind conditions. The missed approaches flown in the conventional manner show scatter due to different wind conditions and different turn initiation points. Since the pilot consistently ended the right turn at 060 deg magnetic, the varying winds and starting points caused different ground tracks for each run.

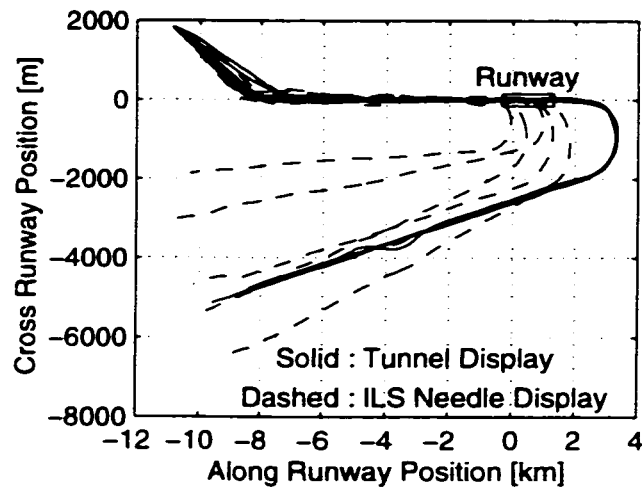


Figure 6.6 Overhead View of Straight-In Approaches

Discussion

On approach, lateral and vertical FTEs using the Tunnel-in-the-Sky display were approximately half as large as those using the ILS needle display. When flying with the Tunnel-in-the-Sky display, the pilot commented that he had more difficulty assessing vertical errors than lateral ones. This resulted in addition of vertical and horizontal deviation indicators to the bottom and right side of the display.

The Tunnel-in-the-Sky display appeared to allow smoother transitions between flight conditions than the ILS needle display. For example, the runway centerline intercept was performed smoothly without overshoot or undershoot. The hunting for the runway centerline with the needle display was probably influenced by the subject pilot's low instrument time (70 hr); a highly experienced and skilled instrument pilot would likely have flown smoother approaches. This highlights one of the key findings of this research: that the Tunnel-in-the-Sky allowed pilots to fly accurate approaches even when recent experience or instrument training was less than optimal.

On the curving missed approach - with altitude and heading simultaneously changing - the pilot was able to easily follow cues for starting and ending these maneuvers. Climbs and descents were made easier since the pilot had positive cues (rather than printed instructions) for capturing and maintaining an altitude or climb/descent gradient. As expected, missed approaches flown in the conventional manner showed scatter due to different wind conditions. This uncertainty requires approach designers to specify large obstacle clearance areas when setting up conventional missed approach procedures [FAA-TERPS93].

Of more importance than reducing FTE, it appears that the Tunnel-in-the-Sky display gave the pilot the 3-D path awareness needed to accomplish tasks accurately and smoothly.

6.4 Curved and Segmented Approaches

These experiments were performed after initial Tunnel-in-the-Sky flight tests. The objective was to increase path complexity in preparation for flight tests of curved and segmented instrument approaches. Such GPS-enabled approaches are expected to lower instrument minimums and increase utility at airports currently limited by terrain on the approach and missed approach paths.

Procedure

Two pilots flew curved and segmented approaches with missed approach procedures that brought the aircraft back to the start of the approach. Pilot A was a student pilot with only 1.5 hours (one lesson) of flight time - literally as inexperienced as a test subject could be and still be a pilot. Pilot B was an instrument-rated Private Pilot with 210 hours of flight time and 70 hours of instrument time.

Both pilots flew the two procedures with four different wind conditions (shown in Table 6.2) for a total of eight approaches per pilot. The order of approach type and wind condition was randomized. Power was adjusted to produce an airspeed of 90 kt at all times, and a “light” turbulence setting was used. The Tunnel-in-the-Sky format with predictor symbology was that shown in Figure 5.3. A one-hour training session was given on the use of the simulator and Tunnel-in-the-Sky display.

Table 6.2 Wind Conditions for Curved and Segmented Approaches

Wind Direction [deg magnetic]	Wind Speed [kt]	Condition
256	0	calm
166	15	90° left crosswind
256	15	wind down runway
346	15	90° right crosswind

The curved approach, shown as flown by the pilots in Figure 6.7, began with the aircraft on a wide base leg at a 90-deg angle to the runway. After a short straight segment, the pilot made a 90-deg right turn (800 m radius) and finally rolled out onto a straight final approach. The segmented approach, shown as the pilots flew it in Figure 6.10, also began on a wide base leg. A series of three 30 deg right turns (800 m radius) brought the aircraft onto final approach. Both approaches began approximately 1000 ft above the runway and continuously descended at 3 deg. Approximately 200 ft above the runway, the pilots were told to execute a missed approach. Power was applied and the pilot transitioned from flying through the green approach tunnel to following the magenta missed approach tunnel. The missed approach climbed straight ahead, made a 150-deg

right turn, a long straight leg, and finally a 120-deg right turn to bring the aircraft back to the approach path. The missed approach leveled out 1,000 ft above the runway.

Both approaches along with their missed approach trajectories were extremely compact compared to procedures in current use. For example, the straight final approach segments were both about 2 km long, compared with approximately 11 km (6 nm) for a typical ILS procedure. The procedures were deliberately made small to explore the capabilities of the Tunnel-in-the-Sky display. Following these paths with reference to conventional light aircraft instruments would have been virtually impossible due to the number of flight path changes required in a short time period.

Results

Figure 6.7 shows an overhead view of data from the curved procedures flown by both pilots. The figure contains eight traces, from both pilots flying with four wind conditions each. All eight ground tracks lie very close to each other, forming a thick trace on the graph despite the varying wind conditions.

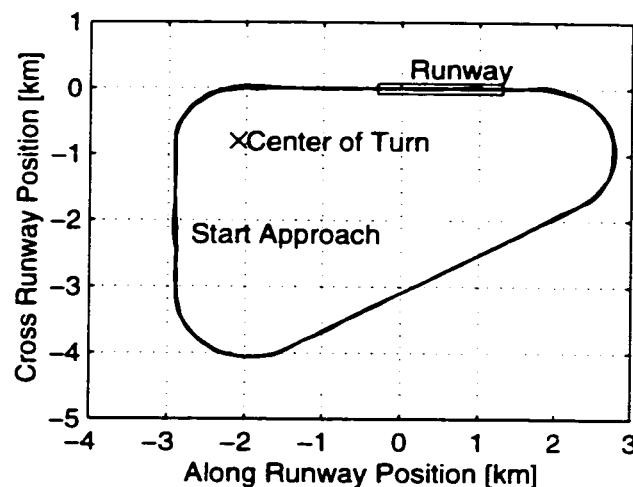


Figure 6.7 Overhead View of Curved Approaches (Pilots A and B)

Each trace in Figure 6.7 begins at the “Start Approach” label, continues clockwise to the runway, onto the missed approach, and then back to the beginning of the approach.

Figure 6.8 shows lateral and vertical FTE for pilot A on the curved approach with the four wind conditions. The curved approach is “flattened out” onto the page so that the aircraft moves from left to right. The beginning and end of the turn are indicated. RMS FTE values for pilot A were 6.6 m lateral and 4.7 m vertical. Maximum errors were less than 20 m in both dimensions. (The upturn in vertical FTE at the end is a pull-up to the missed approach.) Figure 6.9 presents the same information for pilot B. RMS FTE values for pilot B were 11.8 m lateral and 6.7 m vertical. Pilot B’s errors just after the turn initiation tended towards the inside of the turn.

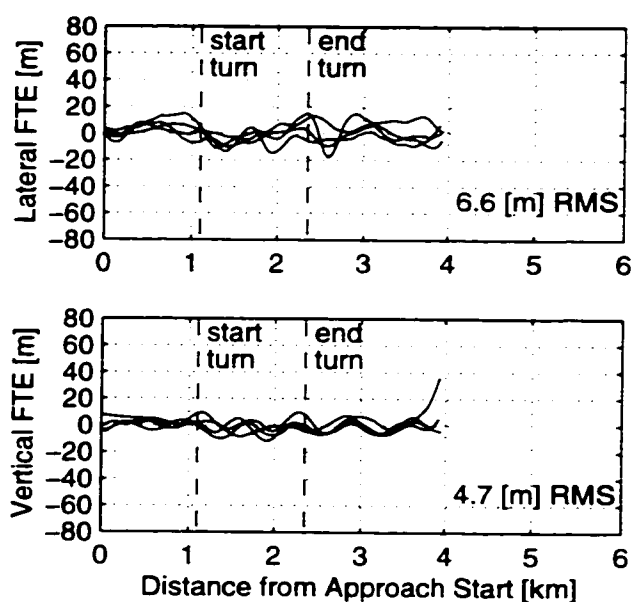


Figure 6.8 FTE on Curved Approaches (Pilot A, Student Pilot)

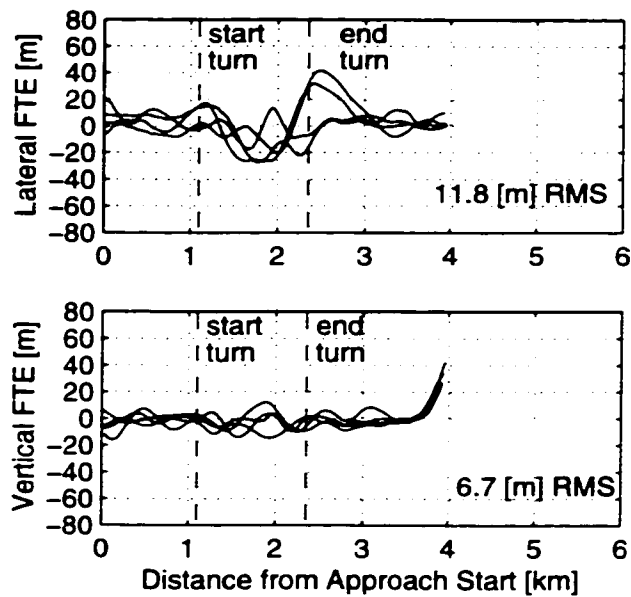


Figure 6.9 FTE on Curved Approaches (Pilot B, 210-Hour Instrument Pilot)

Figure 6.10 shows an overhead view of the segmented approaches and missed approaches flown by both pilots. Again, all eight ground tracks lie very close to each other, except for a small deviation noticeable at the first turn of one of the traces.

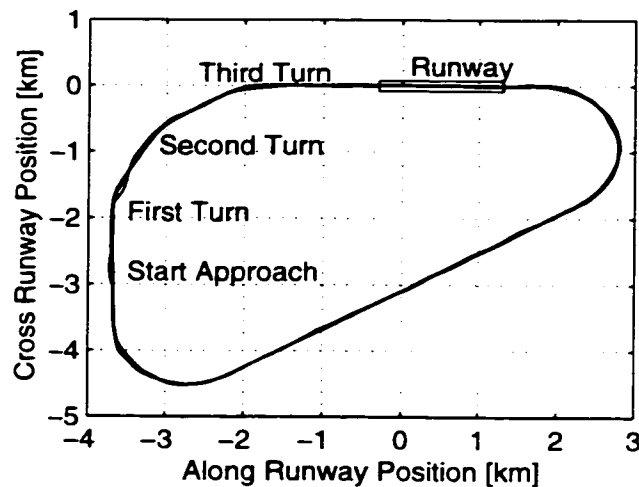


Figure 6.10 Overhead View of Segmented Approaches (Pilots A and B)

Figure 6.11 displays FTE for pilot A on the segmented approach with the four wind conditions. Again, the segmented approach is “flattened out” onto the paper with

the beginnings of the three turns indicated. RMS FTE values for pilot A were 6.5 m lateral and 4.2 m vertical. Maximum errors were less than 20 m in both dimensions.

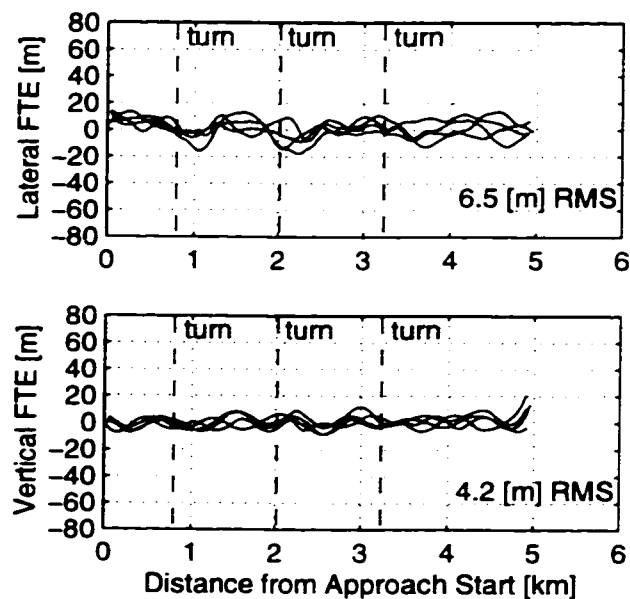


Figure 6.11 FTE on Segmented Approaches (Pilot A, Student Pilot)

Figure 6.12 presents the same information for pilot B. RMS FTE values for pilot B were 13.2 m lateral and 9.8 m vertical. One event at the first turn produced errors of approximately 70 m to the right (inside of turn) and approximately 50 m below the desired path.

Discussion

FTE for pilot A was consistently smaller than FTE for pilot B, an unexpected result since pilot B had more flight hours and an instrument rating. Pilot B's experience with real aircraft dynamics may actually have made it more difficult to adapt to the simulator dynamics. Training effects may also account for the difference.

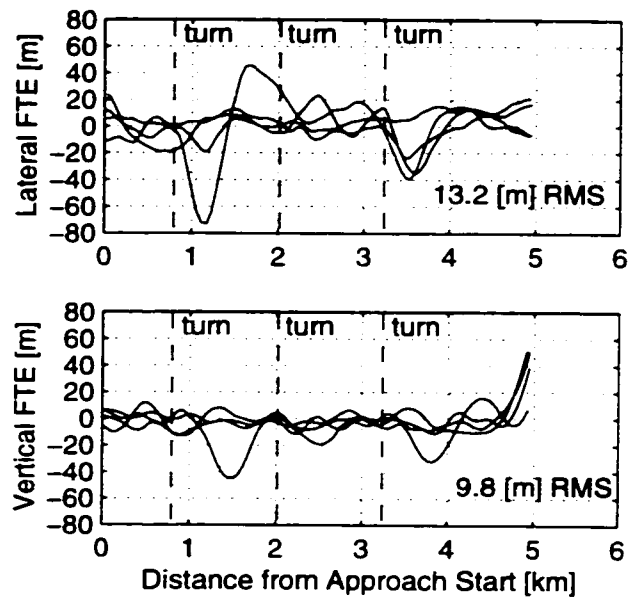


Figure 6.12 FTE on Segmented Approaches (Pilot B, 210-Hour Instrument Pilot)

It should be remembered, however, that the path-following errors for both pilots were relatively small compared to typical values using conventional instruments [Knox93]. It should also be emphasized that minimizing FTE is not an end in itself. The tunnel display appeared to give the pilots the situational awareness they needed to accomplish these complex flying tasks. Both pilots were able to follow the intended trajectories with none of the “hunting” for the correct path typically seen when using a conventional ILS display in varying wind conditions.

Neither pilot complained of lack of vertical situational awareness as had been noted before addition of predictor symbology to the Tunnel-in-the-Sky display. FTE on these complex procedures was smaller by a factor of two or three compared with the straight-in approach tests. However, comparison of the straight-in approaches with this experiment can only be anecdotal. The former used no predictor symbology and involved an initial intercept of the tunnel, while the latter began and ended inside the tunnel using a predictor display.

Both pilots produced repeatable ground tracks despite varying wind conditions. This reinforces the notion that accurately flown complex approaches and missed approaches can increase utility of airports currently limited by instrument approach capabilities.

6.5 ILS Approaches Flown by a Student Pilot

This non-quantitative experiment investigated whether there was a difference in learning to fly an ILS approach with conventional instruments versus the Tunnel-in-the-Sky display.

Procedure

Pilot A (the student pilot who flew the curved and segmented approaches) was given a half-hour of instruction in the use of conventional round-dial instruments (including the ILS needle display) for flying straight-in ILS approaches. The pilot then flew 11-km straight in approaches with a 3-deg glideslope and no wind. Four approaches were flown - two with the Tunnel-in-the-Sky predictor display pictured in Figure 5.3 and two with the ILS needle display.

Results

Attempting to fly the ILS using conventional needles did not produce encouraging results. On the first ILS approach, the aircraft drifted so far off course laterally that it was displaced 1.5 km (0.8 nm) from the runway centerline when it crashed into the ground. On the other ILS needle approach, the vertical FTE reached 880 m (1900 ft) *above* the glideslope! Using the Tunnel-in-the-Sky display, the pilot was able to bring the aircraft into position for a safe landing at the 200-ft DH on both approaches. FTE was similar to pilot A's performance flying curved and segmented approaches.

Discussion

Asking a student pilot to learn to fly ILS approaches in only half an hour was an impossible request; it typically takes many hours of flying before this can be done safely. In contrast, the Tunnel-in-the-Sky display allowed this low-time pilot to quickly become proficient at flying the procedure, with successful results the very first time. The ease with which the student pilot learned to fly using the Tunnel-in-the-Sky implies that it will be easier for infrequent instrument pilots to maintain proficiency with the display. A light-aircraft passenger assisting an incapacitated pilot would also appreciate this contribution to safety.

6.6 Skywriting with GPS

A final test was performed to investigate the Tunnel-in-the-Sky display's ability to guide a pilot along extremely complicated curved flight paths. Pilot A (the student pilot) was shown a path with a series of left and right turns with bank angles up to 45 deg. The entire procedure, which did not include any climbs or descents, took about 7 min to fly at a speed of 90 kt. The predictor display format was that shown in Figure 5.3. The resulting ground track is shown in Figure 6.13. If the aircraft is imagined as a skywriter with a smoke system, it is evident that the student pilot spelled "gps" solely by instrument reference! Accurate flight path control was thereby demonstrated by a student pilot on a path far more complex than any conventional instrument flight procedure. Flying this path in an aircraft is described in Chapter 7.

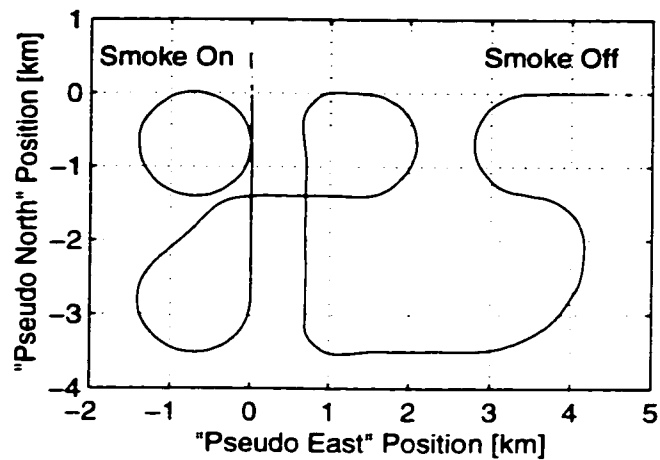


Figure 6.13 Skywriting with GPS (Piloted Simulation)

6.7 General Discussion

Throughout this effort, piloted simulations produced valuable focus to display evolution and flight testing. Simulator trials demonstrated that the Tunnel-in-the-Sky display allowed pilots to fly repeatable straight and curved ground tracks, even in varying wind conditions. Pilots made smooth path intercepts and generally had very good awareness of flight paths curved in three dimensions. The ability to fly curved, segmented, and precise missed approaches can increase utility at terrain- or traffic-bound airports.

The 1.5-hour student pilot flew straight-in, curved, and segmented approaches after only an hour of training. The complex skywriting path was also flown with no difficulty. Attempting to fly an ILS approach with minimal training and standard needle instruments produced the expected (and unacceptable) result. These results suggest that Tunnel-in-the-Sky displays will be useful in initial and recurrent instrument training.

Chapter 7:

Flight Tests

This chapter documents low-cost flight testing of the Tunnel-in-the-Sky display. The small single and twin piston-engine aircraft used are introduced in Section 7.1, and Section 7.2 outlines the quantitative and qualitative methods used in assessing test results. Sections 7.3 and 7.4 deal with initial and expanded flight test experiments, each designed to investigate a specific potential benefit of Tunnel-in-the-Sky displays. Section 7.5 documents *tunnel overlay approaches* intended to coexist with existing instrument approaches. A database of path-following error properties was developed for curved and straight flight segments and is described in Section 7.6. Conclusions for the operational and human-machine interface pillars of this work are summarized in Section 7.7.

7.1 Flight Test Aircraft

The goal of flying the Tunnel-in-the-Sky display in a variety of operational conditions dictated that the aircraft had to be inexpensive to operate. This led to the choice of the two piston-engine airplanes described below.

7.1.1 Piper Dakota

Initial flight testing was performed on the Piper Dakota shown in Figure 7.1. Representing the smallest and lowest-cost class of aircraft on which advanced avionics research could be performed, this fixed-gear aircraft had four seats and a 235-hp engine. Cruise speeds ranged from 125 kt to 145 kt, and ILS approach speeds ranged from 90 kt to 100 kt.

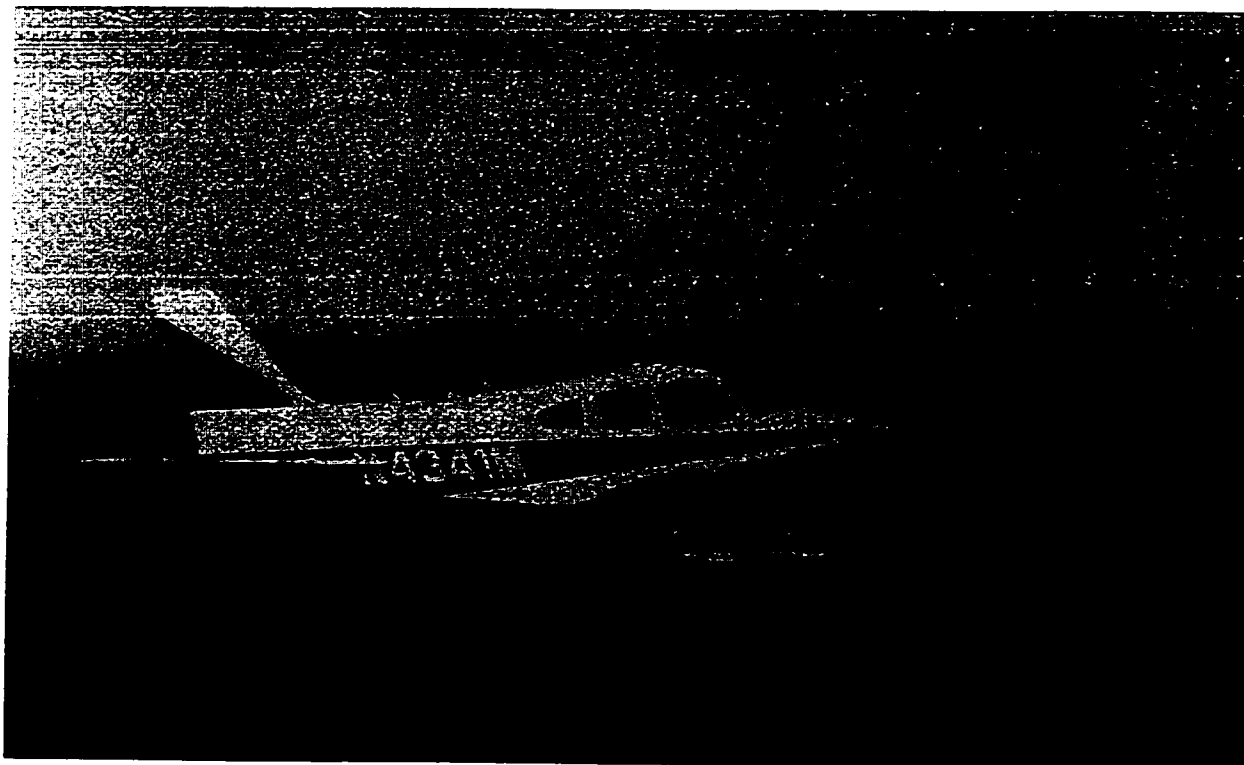


Figure 7.1 Piper Dakota N4341M Test Aircraft

Computers and GPS sensors were mounted on a wood pallet in the rear baggage compartment, and inertial instruments were mounted on a stable frame built into one of the rear seats. The 5.5-inch diagonal display used for these initial tests was attached to the center of the glareshield.

Two pilots flew the tunnel display in the Dakota, one an 800-hour Private Pilot with approximately 70 instrument hours, and the other a 210-hour Private Pilot with approximately 70 instrument hours.

7.1.2 *Beechcraft Queen Air*

The test aircraft was later changed to a 1965 Beechcraft BE65 Queen Air, a twin piston-engine aircraft capable of carrying two pilots and six passengers. The Queen Air shown in Figure 7.2 had a cruise speed of 160 kt and approach speeds ranging from 120 kt to 140 kt. These higher speeds were more representative of transport aircraft than the Piper Dakota's. The Queen Air's engines were quite noisy - a fact that became relevant during flight testing

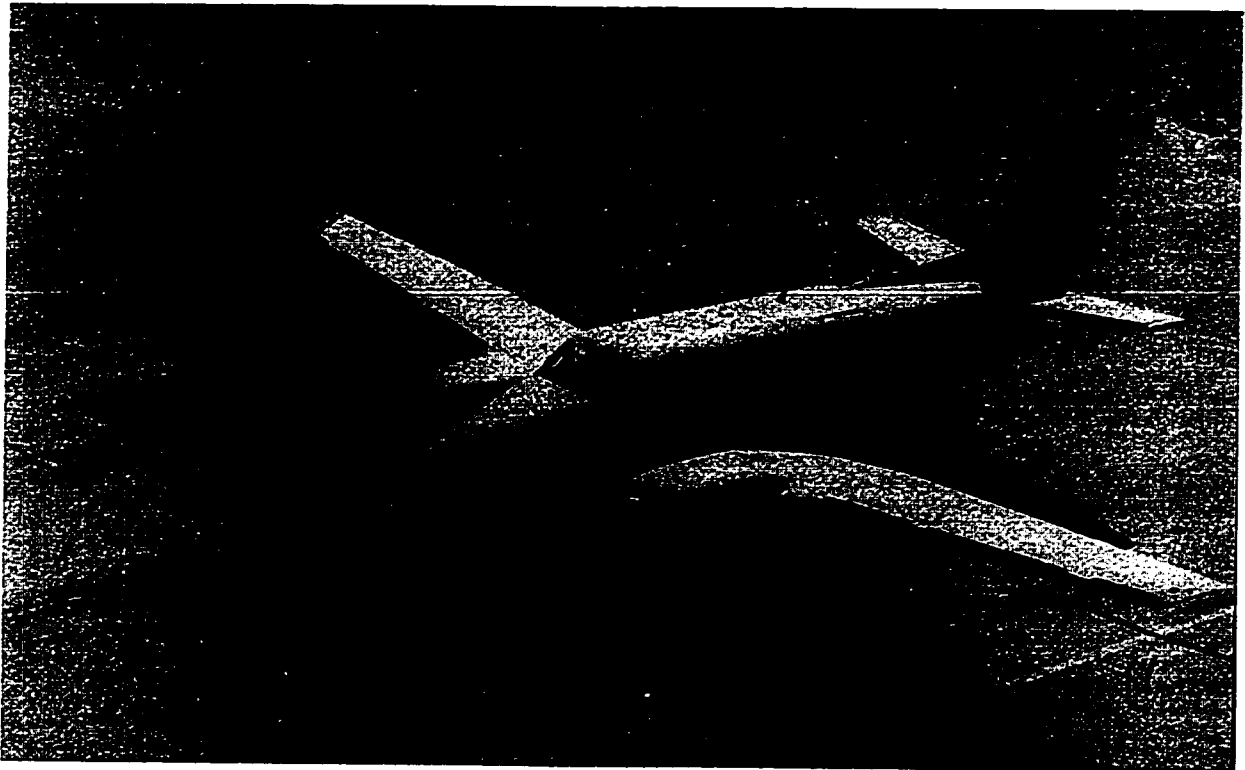


Figure 7.2 Beechcraft Queen Air N6890Q Test Aircraft

The aircraft carried a power system, GPS antennas, and two equipment racks (one for the Tunnel-in-the-Sky system and the other for WAAS receiver hardware). The display was positioned to the left of the pilot's heading indicator and below the airspeed indicator, as shown in Figure 7.3.



Figure 7.3 Queen Air Instrument Panel with Tunnel-in-the-Sky Display

A total of seven pilots flew the Tunnel-in-the-Sky display in the Queen Air, ranging from a 210-hour Private Pilot to a 15,000-hour Airline Transport Pilot. One test subject performed most of the Queen Air flying presented here. This Commercial Pilot had approximately 3,000 hours of flight time.

7.2 Methodology

A primary project goal was lowering Total System Error to improve utility and situational awareness. Since navigation “truth” data was not available in flight, TSE

could not be measured directly. The quantity measured during flight tests was FTE, the difference between measured and desired position. As mentioned in Chapter 3 however, the high accuracy of WAAS measurements implies that FTE is an excellent approximation of TSE.

Iterative refinement of the display relied on pilot feedback from real-world testing. Quantitative workload was not measured due to the significant complexity of estimating this variable in operational conditions. Pilots were closely observed and asked for subjective opinions on workload and operational issues. Limited flight test resources forced a tradeoff between statistical significance and breadth of experience. At this early stage of technology development, it was felt that a focus on qualitative factors would be more valuable than one or two large datasets.

Each of the seven test pilots typically had an hour of simulator training before flying the aircraft using the display. No practice runs were flown in the aircraft; the first trajectories flown were production data runs. All tunnel procedures were hand flown. (The Queen Air was not even autopilot-equipped.) All procedures were performed in visual meteorological conditions except for five ILS approaches flown through clouds. Experiments were always performed with a properly qualified safety pilot monitoring the test subject. During experimental procedures the test pilot did not look outside the cockpit, relying only on the Tunnel-in-the-Sky display for flight path information. The test subject typically wore view-limiting glasses to simulate instrument flight conditions.

7.3 Initial Flight Testing

Initial flight tests performed on the Piper Dakota were designed to explore Tunnel-in-the-Sky operational aspects on simple straight-in approaches.

7.3.1 Straight-In Approaches

First flight of the system took place at Truckee, California on 21 June 1995. The follow-on testing described here occurred at Livermore, California in September 1995. DGPS positioning data for the straight-in approaches was provided by WAAS, with WAAS corrections sent through a datalink antenna mounted on a hangar at Livermore Airport. Since the integrated GPS/inertial attitude system described in Chapter 3 had not yet been developed, attitude was assumed to be straight and level with runway heading. The pilot therefore had to include the aircraft's installed attitude and heading indicators in his scan for attitude stabilization. The test subject was the 800-hour Private Pilot who flew the first simulator tests.

Procedure

Straight-in approaches were flown to runway 25R at Livermore. In addition to the Tunnel-in-the-Sky display format, a conventional ILS needle format could be generated by the flight computer and was used for comparative test runs. The pilot occasionally looked outside the cockpit to spot nearby aircraft called out by the control tower. Winds at Livermore were reported from 240 deg magnetic at 16 kt.

The aircraft began each approach approximately 10 km from the runway, 3 km to the right of centerline, and 2,000 ft above ground level. The pilot then turned onto final approach to intercept the 2.9-deg glideslope from below. Upon glideslope intercept, the pilot began a descent that continued down to near the DH of 200 ft. Four approaches are documented here, two flown using the Tunnel-in-the-Sky display and two flown with the ILS needle display.

Results

Figure 7.4 shows vertical FTE on the four approaches from 7.5 km until 2 km before touchdown, moving from left to right. (Data recording was stopped at 2 km in anticipation of the missed approach pull-up.) The vertical RMS FTE has the same order of magnitude for both displays (13.2 m for the Tunnel-in-the-Sky display, 19.4 m for the ILS needle display). One of the ILS needle runs exhibits a vertical deviation of more than 50 m above the glideslope.

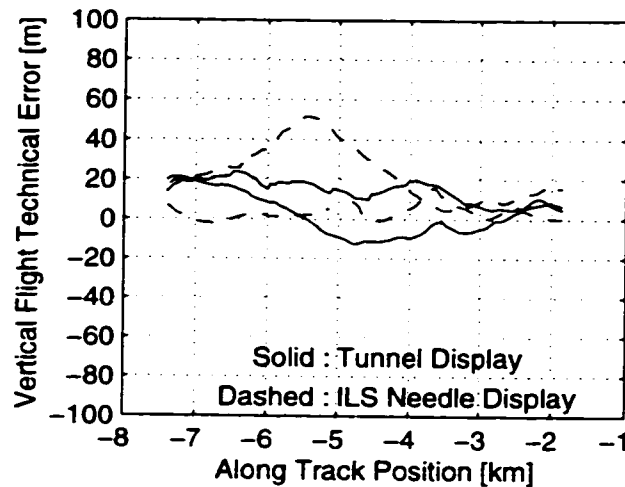


Figure 7.4 Straight-In Approaches Vertical FTE

Lateral RMS FTE, shown in Figure 7.5, is comparable for the two displays (28.0 m for the Tunnel-in-the-Sky display, 33.0 m for the ILS needle display).

Figure 7.6 presents an overhead view farther out on the approach where three of the four runway centerline intercepts were already completed. The fourth (an ILS needle run shown as a dashed trace) exhibits a runway centerline overshoot of almost 0.5 km. This is noted here because of its relatively large magnitude.

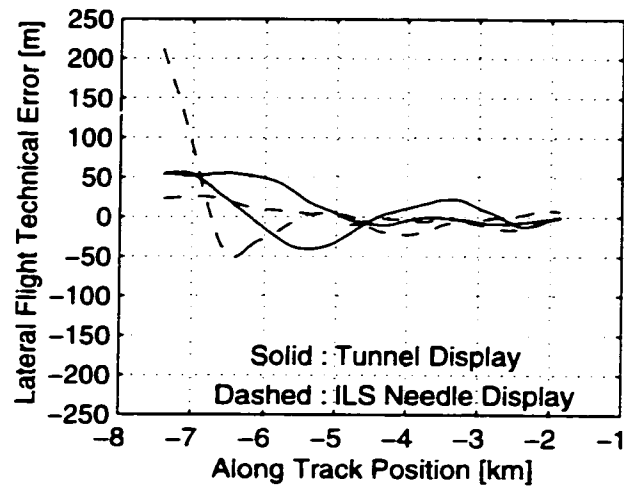


Figure 7.5 Straight-In Approaches Lateral FTE

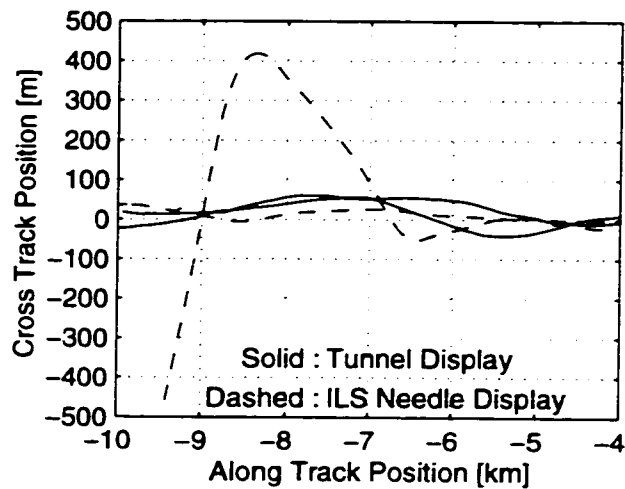


Figure 7.6 Overshoot Using ILS Needles for Lateral Flight Path Intercept

Discussion

This limited data was useful for initial confirmation of the Tunnel-in-the-Sky display's usability. Close-in FTE histories do not suggest any reason to believe that path-following performance was markedly different for the two displays. FTE was larger than that observed in subsequent flight testing, most likely due to the lack of dynamic attitude data. The pilot remarked that vertical deviations were more difficult to assess than lateral

ones, a result also seen in the piloted simulations of Chapter 6. These comments resulted in addition of deviation indicators and predictor symbology to the display.

It appeared that large deviations were more likely to occur with the ILS needle display than with the Tunnel-in-the-Sky display. Examples of this included the vertical FTE deviation and lateral intercept overshoot seen in the data. The Tunnel-in-the-Sky display seemed to permit identification of incipient deviations and enabled the pilot to correct for these conditions.

That this early Tunnel-in-the-Sky implementation had a perceived benefit over the needle display is interesting since it did not integrate all primary flight information onto a single display. Critical attitude data had to be obtained by scanning other instruments. It may be that the perspective position and rate cues from the fixed-attitude Tunnel-in-the-Sky display were more easily interpreted than the same information displayed using ILS needles.

7.3.2 Approaches with GPS as the Sole Sensor

On 2 May 1996, the first known flight of a Tunnel-in-the-Sky display driven solely by GPS for position and attitude was performed at Palo Alto, California. Positioning data came from a receiver capable of simultaneous WAAS and Integrity Beacon Landing System (IBLS) operation [Lawrence96]. A long-baseline GPS antenna array (two on the wingtips, one on the fuselage, and one on the tail) supplied GPS attitude information at 10 Hz. Fifteen straight-in approaches were made using this equipment. WAAS positioning was used on approach until approximately 250 ft altitude, when overflight of the pseudolites resulted in sub-decimeter accuracy from IBLS. These flights were conducted in a busy traffic pattern and thus did not provide enough approach data to identify meaningful FTE trends.

7.4 Expanded Flight Operations

The next set of experiments was designed to extend the system's capability in challenging conditions on the Beechcraft Queen Air. These tests were performed at Moffett Federal Airfield in Mountain View, California, chosen for its long runways (8125 ft and 9200 ft) and lack of air traffic. The WAAS datalink antenna was located on top of the Moffett control tower. In addition to the 3,000-hour Commercial Pilot who flew most of these tests, the 15,000-hour Airline Transport Pilot flew portions of the experiments documented in Subsections 7.4.1 and 7.4.2. By the time these tests occurred, developmental flight testing had led to increased contrast, thickness, and shadowing for the central display elements.

7.4.1 Curved and Segmented Approaches

Procedure

The segmented approaches shown in Figure 7.7 began just over 3 nm (nautical miles) from the runway aimpoint on an extended left base leg for runway 32L. Descending with a flight path angle of 3 deg, a series of three 30-deg left turns brought the aircraft onto a 2-nm final approach. Low approaches were flown at 120 kt airspeed with the aircraft making a left climbing turn to rejoin the downwind leg and tunnel.

Shorter curved approaches were also flown with the aircraft turning onto final approach 1.5 nm from the runway. Figure 7.9 shows two of these that, for reasons explained below, did not follow the procedure exactly.

Results

The segmented approaches were flown with a high degree of accuracy: RMS FTE was 52.7 ft lateral and 50.7 ft vertical and is plotted in Figure 7.8. In fact, the horizontal

flight track repeatability caused a number of noise complaints to the airport operations office because the airplane was flying over the exact same houses each time!
(Subsequent flight tests were planned to minimize noise exposure.)

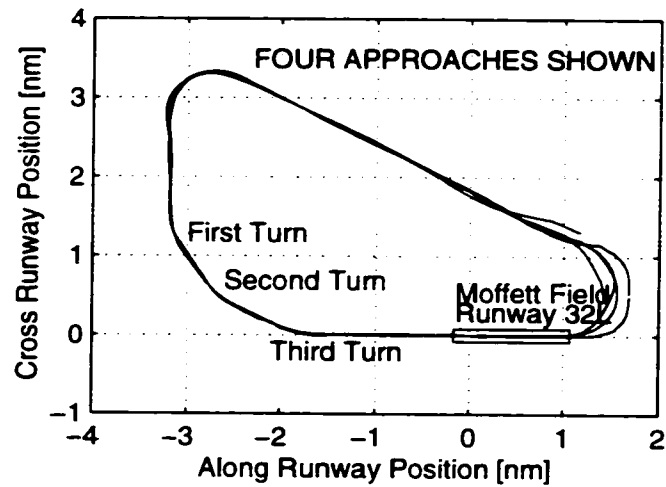


Figure 7.7 Segmented Approaches

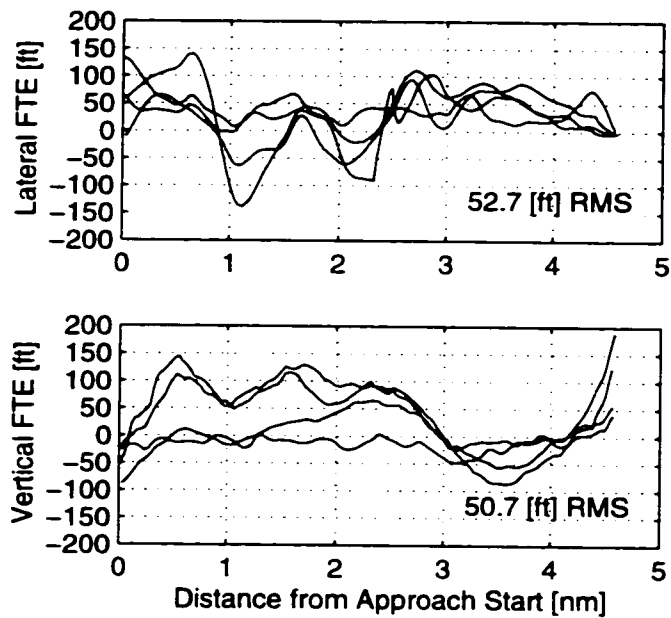


Figure 7.8 FTE on Segmented Approaches

Figure 7.9 shows two curved approach runs that were interrupted by traffic sequencing commands from the control tower. In the first case, the tower commanded a left 360-deg turn to ensure separation from another aircraft. It was decided to continue this data run with the pilot flying the turn by reference to the Tunnel-in-the-Sky display's artificial horizon. When the curved tunnel reappeared on the display after most of the turn was complete, the pilot smoothly merged into the tunnel and continued the approach. On another occasion, the tower instructed the pilot to cut short the turn from base leg to final approach. This required the pilot to leave the curved tunnel on base leg, "cut the corner," and then rejoin the approach less than a mile from the runway. Both of these deviations, the 360-deg turn and the shortened turn, were executed easily by the pilot indicating good 3-D situational awareness of the aircraft's position relative to the curved flight path. Although such low-altitude maneuvers are not possible with normal instruments, they illustrate potential capabilities of WAAS and Tunnel-in-the-Sky displays.

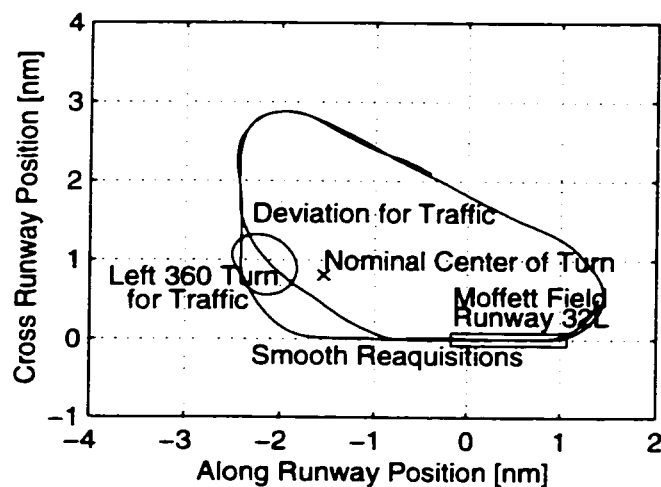


Figure 7.9 Curved Approaches

Discussion

The high accuracy and ease with which curved and segmented procedures were flown confirms the feasibility of complex procedures that could increase airport utility while maintaining or improving safety. The pilot was able to accommodate deviations for traffic and smoothly reenter the approach tunnel when needed. The experiments discussed in this section are not proposed as routine instrument flight operations. Rather, they were designed to demonstrate the capabilities of the system under challenging circumstances.

7.4.2 Flying Traffic Patterns on Instruments

To explore the Tunnel-in-the-Sky display's ultimate capability for guidance on tight, high-workload procedures, it was used to fly traffic patterns *on instruments*. A traffic pattern is a standardized rectangular path around a runway for procedural traffic separation. The patterns employed here had straight upwind and downwind legs joined by 180-deg turns representing the crosswind and base legs. For compactness, the Queen Air turn radius was reduced to 1,250 m from the usual 1,500 m. The turn from base leg to final approach ended 1 nm from touchdown, keeping the final approach segment short to minimize noise exposure. Several of the traffic patterns flown to runways 32L and 32R are shown in Figure 7.10.

Since the Tunnel-in-the-Sky display aircraft was once again enabling repeated ground tracks over the same houses, the Moffett Field operations office received noise complaints from residents near the base leg of the runway 32R pattern. The right traffic pattern was therefore moved 0.75 nm closer to runway 32R to permit a greater threshold crossing height, putting more of the base leg close to the airport. Several of these patterns are shown in Figure 7.11. No further noise complaints were received.

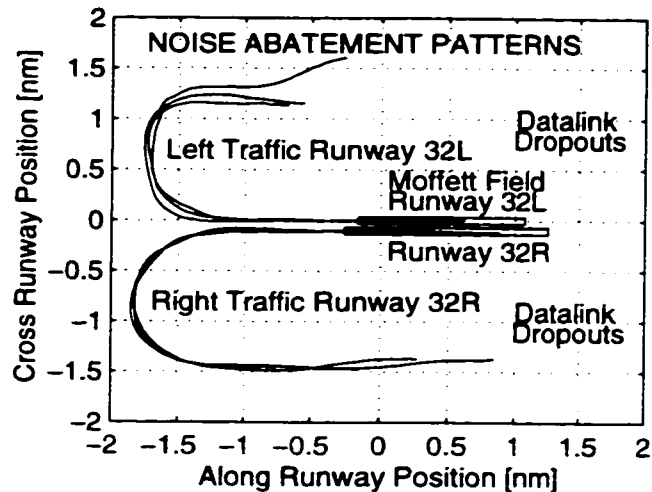


Figure 7.10 Traffic Patterns Flown on Instruments

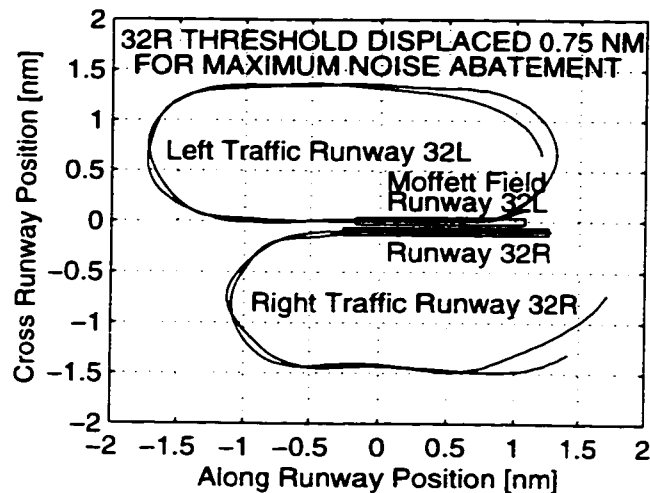


Figure 7.11 Tight Traffic Patterns on Instruments

This experiment demonstrated the flexibility offered by DGPS navigation and advanced flight displays. DGPS provided positioning on the downwind legs where an ILS signal (and even that of a Microwave Landing System) cannot provide useful data. The traffic patterns kept the pilot busy between watching the display, manipulating the controls, communicating with the tower, and performing pre-landing checks. Since a good deal of visual attention in the traffic pattern is directed at the runway, the Tunnel-in-the-Sky display was unable to convey important off-axis visual cues. This experiment

was not intended to suggest that traffic patterns should be flown on instruments. It merely demonstrated the pilot's ability to perform complex tasks while maintaining awareness of dynamic factors. One could not conceive of flying these procedures with needle-based displays.

7.4.3 Skywriting Using GPS

This demonstration repeated the skywriting experiment flown by the student pilot in simulation. The ground track flown near Santa Cruz, California is shown in Figure 7.12. During the fifteen minutes of data collection, WAAS datalink contact was briefly lost three times. The outages occurred due to distance from the datalink transmit antenna (at Moffett Field) and shading of the receive antenna by aircraft structure. During these periods, positioning information on the Tunnel-in-the-Sky display contained gross errors. When this happened, the pilot was simply instructed to keep the aircraft in the current turn while the datalink was recovered. The pilot would then rejoin the tunnel when datalink contact was reestablished.

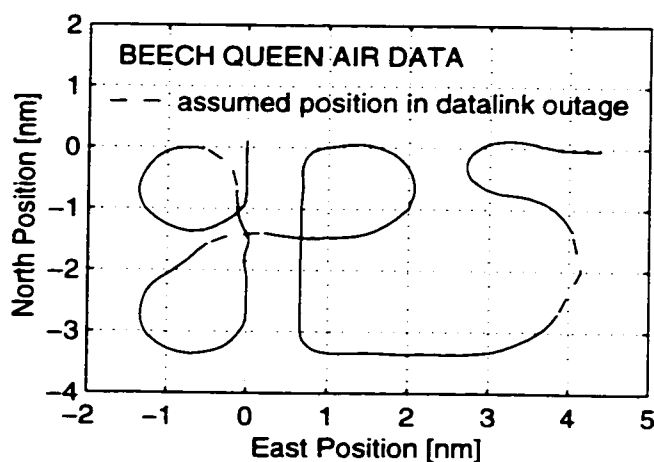


Figure 7.12 Skywriting with GPS (Beechcraft Queen Air)

Even with the datalink outages, the letters “gps” are clearly recognizable (although backward to people on the ground!). The pilot later stated that he was able to

fly through the outages while remembering the trajectory preview information from the display. The display clearly enabled persistent situational awareness of the complex curved path. The complexity of this path far exceeds that of standard instrument procedures, but suggests promise for specialized applications such as photogrammetry.

7.5 Operating Within the Current Airspace System

This section documents three flight experiments - each intended to demonstrate one way in which WAAS or LAAS and a Tunnel-in-the-Sky display can improve real-world operations within the current Air Traffic Control (ATC) system. The first experiment addressed a major current operational problem introduced in Chapter 2, Controlled Flight Into Terrain (CFIT). The other two addressed future applications not yet discussed: closely spaced parallel approaches and noise abatement.

A series of tunnel “overlay approaches” was designed on top of existing ATC procedures. Simply flying through the hoops on the Tunnel-in-the-Sky display satisfied the horizontal and vertical limitations designated on the published approach plate. From ATC’s point of view, the procedures looked like the ones they see every day, although they may have noticed that the pilots flew them more accurately than usual! Since a paradigm shift to Tunnel-in-the-Sky flying may take many years, any immediate ability to use the technology within today’s system is valuable.

The 3,000-hour Commercial Pilot flew these overlay procedures on the Beechcraft Queen Air. For all of these experiments, the WAAS datalink antenna was located on top of the Moffett Field control tower.

7.5.1 Precision Approaches for a Non-Precision Airport

As introduced in Chapter 2, Controlled Flight into Terrain (CFIT) continues as a major accident category for air carrier and light aircraft. The increased workload of non-

precision approaches augments the risk of CFIT accidents. For this experiment, the Tunnel-in-the-Sky system added positive vertical guidance to a non-precision approach to enable long, stabilized descents to the runway.

Existing Published Approach Procedure

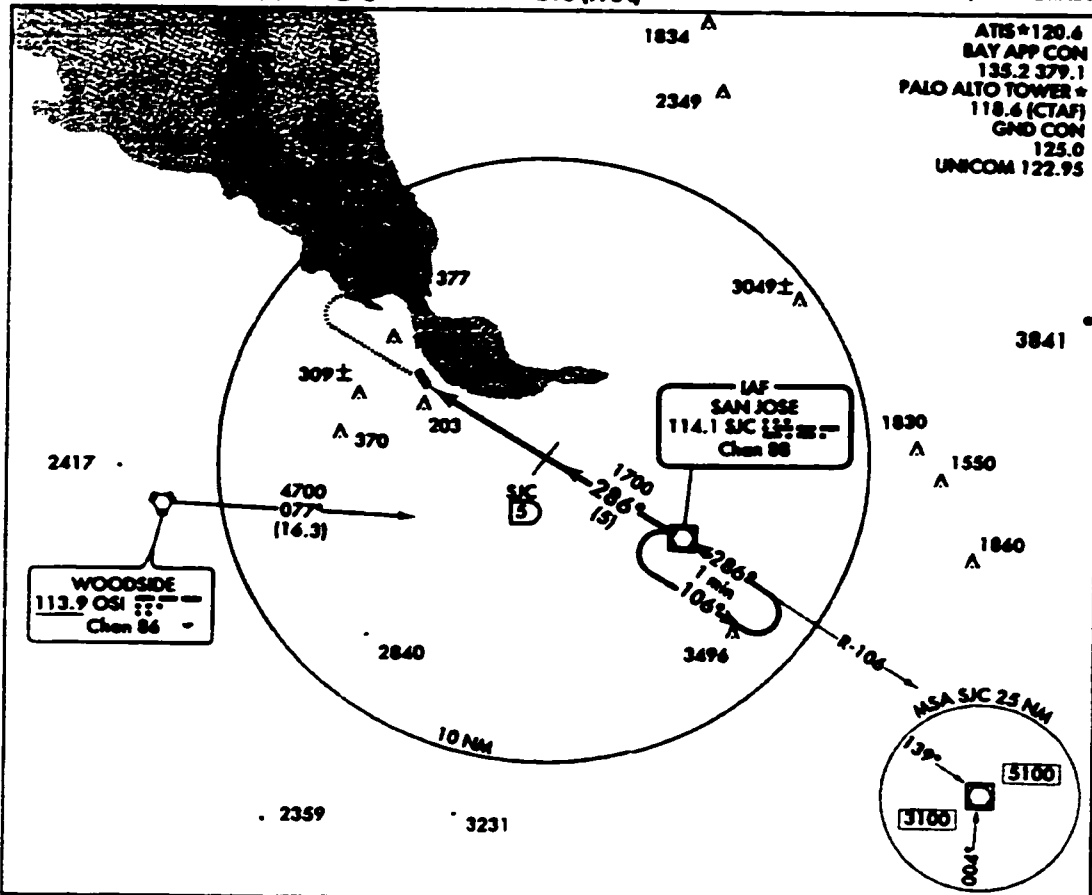
The nominal profile for the (non-precision) VOR/DME approach to runway 30 at Palo Alto, California is shown on the approach plate (Figure 7.13) and as a dashed trace on Figure 7.14. The published approach begins with the aircraft outside the San Jose VOR at 3,000 ft above mean sea level (ft MSL). As soon as the aircraft passes over the VOR inbound, the pilot can legally descend to the “stepdown altitude” of 1,700 ft MSL. Starting this descent requires changes in power and pitch accompanied by pilot workload (configuration change #1). During the descent, there is no electronic vertical guidance; the altimeter provides the only indication of whether the aircraft is above the relevant minimum descent altitude (MDA). The actual path followed through space depends on descent rate, airspeed, winds, and aircraft weight. On reaching the MDA of 1,700 ft, the pilot must level out (configuration change #2). The aircraft flies inbound level at 1,700 ft until 4.5 nm from touchdown (5 nm DME from the San Jose VOR). At this stepdown fix the pilot begins another descent (configuration change #3). The pilot descends to the final MDA of 460 ft MSL and levels out (configuration change #4). Pilots of light aircraft are trained to make a relatively rapid descent to the MDA, allowing more time there to visually acquire the runway. Unfortunately, this also increases the chance of descending below the MDA. When the aircraft is finally in a position to make a normal approach to landing, the pilot may descend (configuration change #5) to the runway. The timing and altitudes associated with the configuration changes are critical - misinterpreting the correct MDA for the current approach segment can result in flying below MDA and impacting terrain.

304

VOR/DME RWY 30

PALO ALTO AIRPORT OF SANTA CLARA COUNTY (P.A.O.)
AL-9216 (FAA) PALO ALTO, CALIFORNIA

PALO ALTO, CALIFORNIA

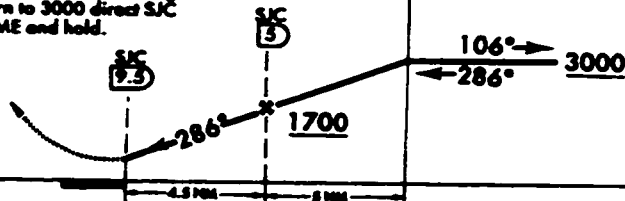


MISSED APPROACH
Climb to 1000 then climbing
right turn to 3000 direct SJC
VOR/DME and hold.

VOR/DME

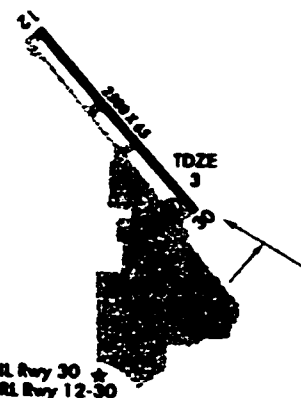
One Minute Holding Pattern

ELEV 3



CATEGORY	A	B	C	D
S-30	460-1	457 (500-1)	NA	
CIRCLING	460-1 457 (500-1)	540-1 537 (600-1)	NA	
SAN JOSE INTL. ALTIMETER SETTING MINIMUMS				
S-30	500-1	497 (500-1)	NA	
CIRCLING	500-1 497 (500-1)	580-1 577 (500-1)	NA	

When control tower closed, use San Jose tail altimeter setting.
Circling not authorized SW of Rwy 12-30.



Knots	40	90	120	150	180
Miles per hour					

Figure 7.13 VOR/DME Approach Plate for Palo Alto, California Runway 30

Tunnel Overlay Procedure

To create positive vertical guidance for this approach, a glidepath was extended from the runway touchdown point to the stepdown fix 4.5 nm from touchdown (5 nm DME from the San Jose VOR). This resulted in a glidepath angle of 3.55 deg, close to the standard angle of 3 deg. The glidepath was then extended further back along the approach until reaching 3,000 ft MSL, the published initial altitude for the approach. This occurred approximately 8 nm from touchdown. Finally, an initial approach segment was added that crossed San Jose VOR at 3,000 ft. The result was a precision glidepath that satisfied the minimum altitude requirement at the stepdown fix while avoiding the many configuration changes of the VOR/DME approach.

Results

Figure 7.14 shows a profile view of the approach flight data. The thick trace is an approach flown using the usual course deviation needle and altimeter technique. This conventional approach exhibits transients near the configuration changes while the pilot trimmed the airplane. Since the aircraft never descended below MDA according to the cockpit barometric altimeter, the apparent descents below MDA are most likely due to barometric altimeter error. By fitting a straight line to the measured ground track, approximate lateral RMS FTE was determined to be 295.7 ft for the conventionally flown approach.

The two thin traces represent approaches using the Tunnel-in-the-Sky display. These were performed with average lateral RMS FTE of 21.1 ft and average vertical RMS FTE of 27.3 ft. Maximum deviations from the tunnel centerline were 53.4 ft lateral and 57.1 ft vertical. Both tunnel approaches clearly followed a long, stabilized descent profile that arrived at the stepdown fix with the desired 1,700-ft MSL altitude. The pilot

stated (subjectively) that the tunnel approaches were much easier to fly than approaches using the CDI needle, DME, and altimeter.

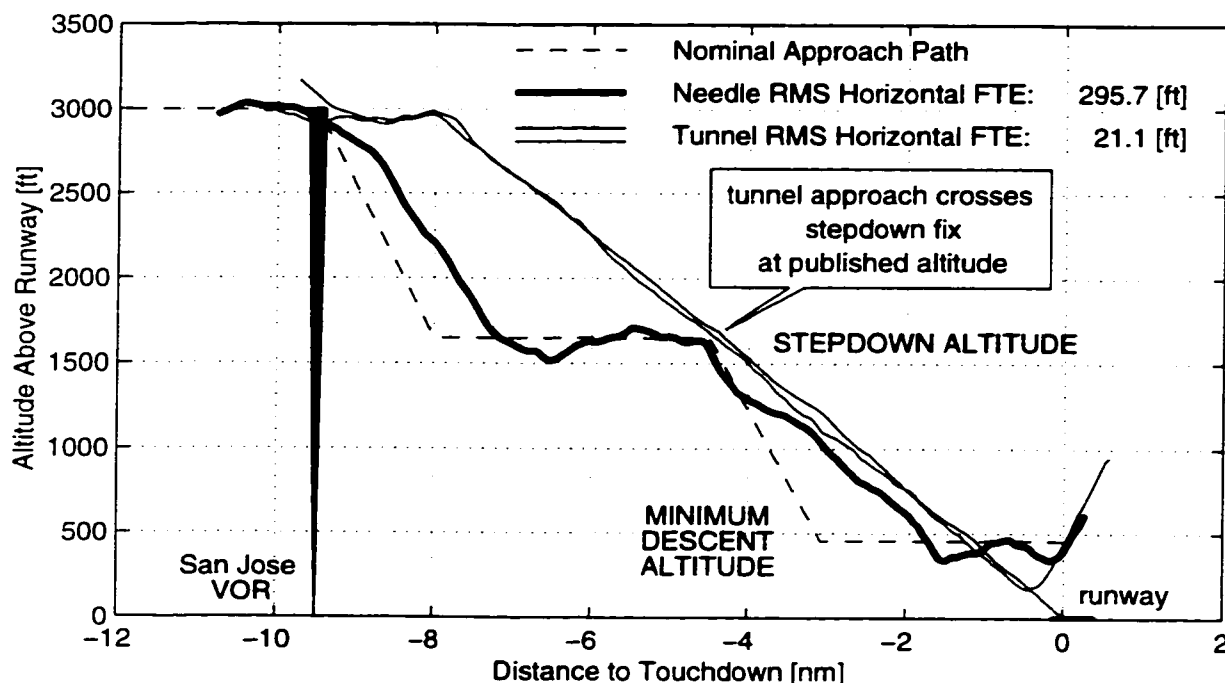


Figure 7.14 Profile View of Palo Alto VOR/DME Approach

Discussion

A high level of path-following accuracy was achieved with the Tunnel-in-the-Sky display compared to conventional instruments. By eliminating unnecessary aircraft configuration changes and inherent workload, the requirements of certified non-precision approaches can be satisfied with the safety of precision approaches. Eliminating non-precision approaches altogether would provide major safety benefits for all classes of aircraft.

7.5.2 Approaches for Closely-Spaced Parallel Runways

Existing communication, navigation, and surveillance systems limit simultaneous instrument operations on closely spaced parallel runways. The lower limit for instrument

runway separation ranges from 2,500 ft to 4,300 ft depending on installed equipment and type of operation. This leaves airports with less than 2,500 ft of runway separation with no alternative but to revert to inefficient single-runway operations during degraded weather conditions. San Francisco International Airport, for example, has only 750 ft of spacing between the parallel runways typically used for landing traffic. Modern sensors and displays may allow for Closely Spaced Parallel Approaches (CSPA) in bad weather. The improved navigation of WAAS and LAAS could ultimately be combined with Automatic Dependent Surveillance - Broadcast (ADS-B) traffic information to give aircrews this new tool. This experiment was intended to demonstrate very accurate lateral approach tracking and situational awareness, two of several capabilities necessary for future instrument CSPA operations.

Existing Published Approach Procedure

The localizer/DME approach to runway 32R at Moffett Federal Airfield, CA uses a radio signal for horizontal guidance and the altimeter to ensure terrain and obstacle clearance. The approach plate is shown in Figure 7.15. The localizer-only non-precision version of this ILS/DME approach has three intermediate stepdown altitudes and a final MDA, resulting in *nine* pitch and power configuration changes on a typical approach.

Tunnel Overlay Procedure

A tunnel approach was overlaid on the existing approach with the ground track matching the localizer beam. Although the experiment's emphasis was on lateral tracking, a vertical glidepath angle of 3 deg was added, allowing a single configuration change at 5,500 ft to establish a stabilized descent to the runway.

97254

154

ILS/DME RWY 32R

AL-410 (NASA)

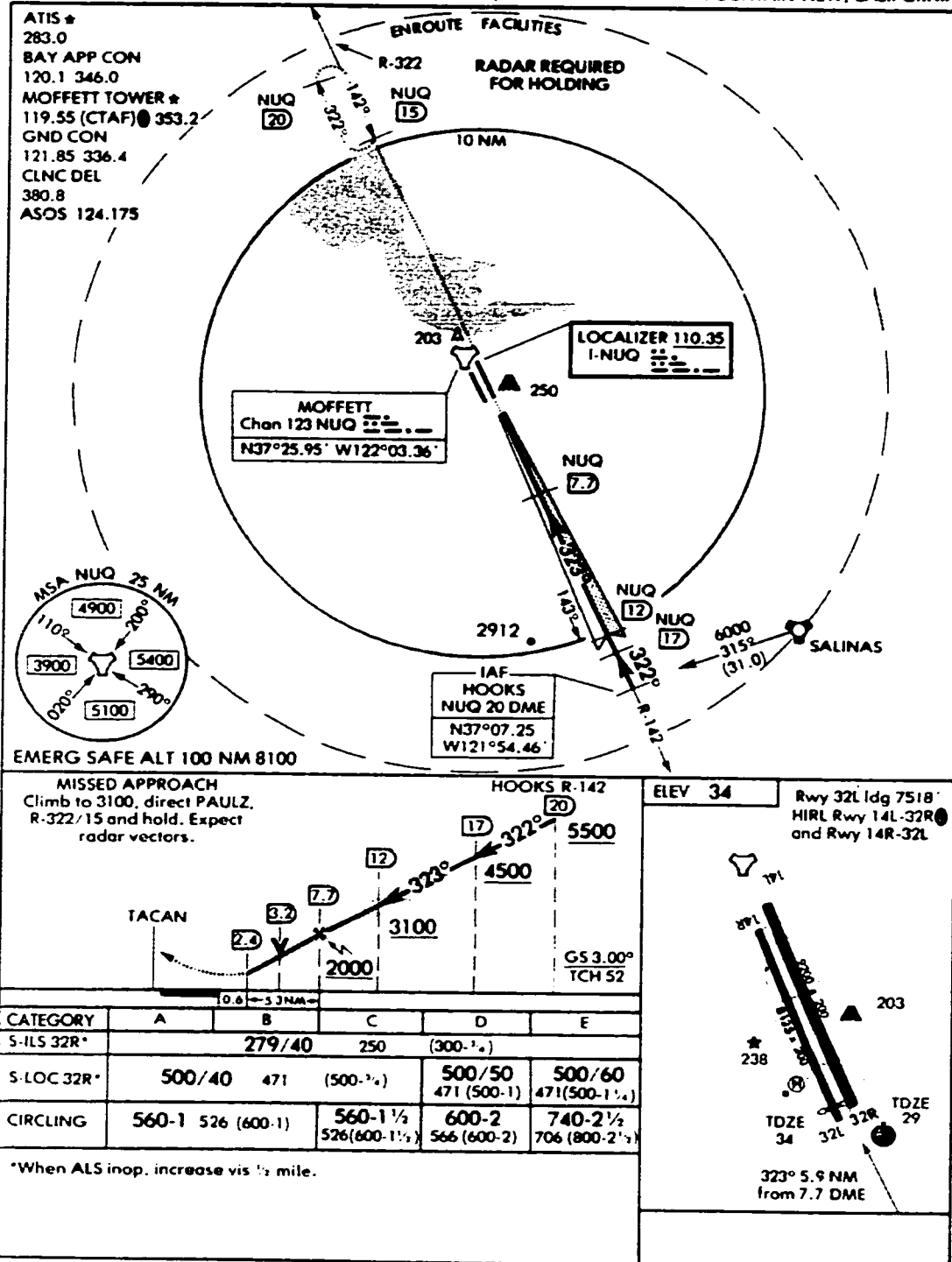
MOFFETT FEDERAL AFLD (KNUQ)
MOUNTAIN VIEW, CALIFORNIA

Figure 7.15 LOC/DME Approach Plate for Moffett Field, California Runway 32R

Results

Figure 7.16 shows an overhead view of the approach flight data. The thick trace portrays an approach made using the conventional localizer needle and altimeter method. Cumulative FTE was calculated over the approach from 20 nm until approximately 0.7 nm before touchdown. For the conventional approach, large cumulative RMS lateral FTE (estimated to be 517.0 ft using the display's DGPS sensor) resulted far from the runway due to the angular nature of the localizer beam.

The thin traces depict three tunnel overlay approaches. The average lateral RMS FTE using the Tunnel-in-the-Sky display was 23.8 ft, far smaller than that for the conventional approach. The pilot stated that the tunnel overlay approaches were very easy to fly.

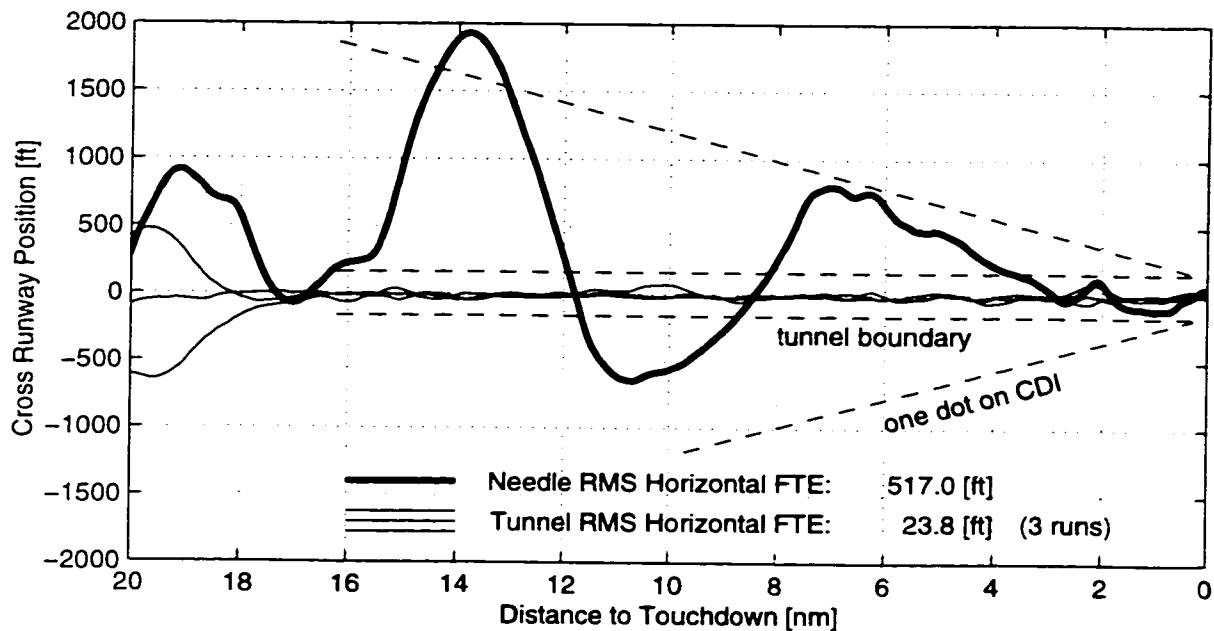


Figure 7.16 Overhead View of Moffett Field LOC/DME Approach

Figure 7.17 shows the profile view. The numerous configuration changes required by the non-precision localizer approach are clearly evident on the thick trace. The three Tunnel-in-the-Sky vertical profiles had an average RMS vertical FTE of 18.4 ft.

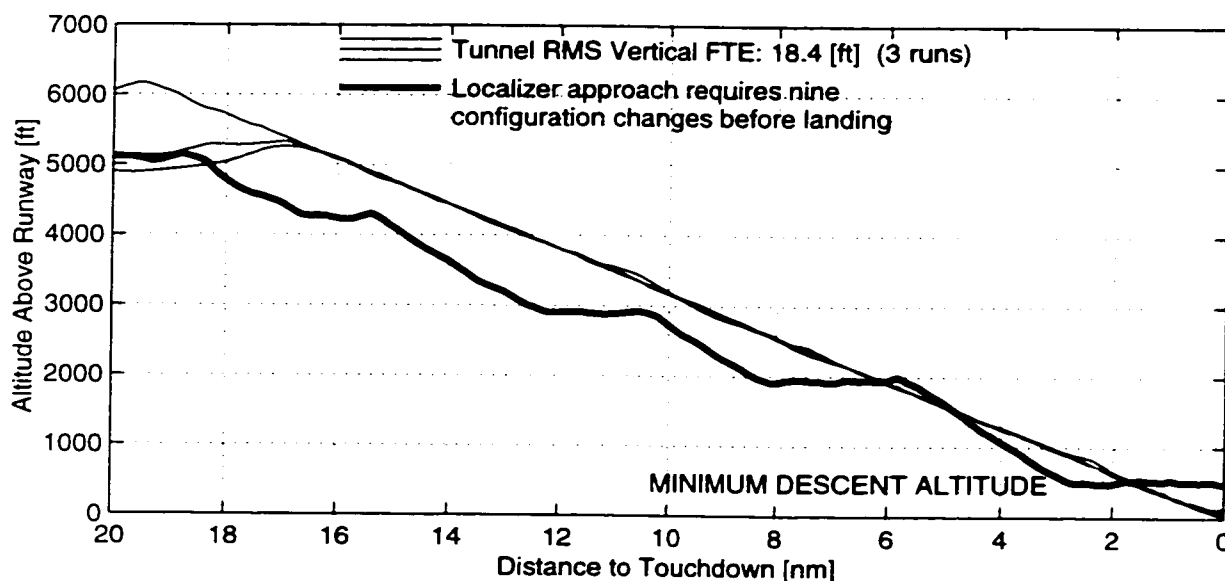


Figure 7.17 Profile View of Moffett Field LOC/DME Approach

Discussion

Despite the dramatic difference in FTE using the two displays, the conventional approach was actually flown quite well by the test pilot. The ground track remained almost entirely within a one-dot range of the course deviation indicator (CDI) needle and thus met the highest standards for certification as an Airline Transport Pilot. Although small needle deviations resulted in large absolute FTE far from the runway, the ground track accuracy is well within specifications for certified approaches. Highlighting the disparity in FTE for the two methods could, on one hand, be considered unfair since the pilot did an excellent job given the angular navigation system used. However, low *Total*

System Error is the performance criterion required for instrument operations to runways only several hundred feet apart.

The large FTE disparity was due mainly to the angular nature of the localizer navaid; the difference in display formats was probably less significant. If DGPS is used to drive a needle display with constant sensitivity (i.e. linear instead of angular behavior), a much lower FTE can be achieved as demonstrated by [Houck99]. However, it appears that the workload required to achieve a given FTE is higher with a needle display than it is for a Tunnel-in-the-Sky display. This could be an important advantage of Tunnel-in-the-Sky displays for CSPA operations: reduced workload for a given level of accuracy in the event that manual control is necessary. Additional situational awareness benefits for CSPA are discussed in Chapter 8.

7.5.3 Noise Abatement Approaches

Aircraft noise is of continuing concern outside of - and therefore within - the aviation community. This expensive problem reduces the utility of the world's airports through restrictions on airport development and nighttime operations. Better engine and nacelle designs have reduced noise footprints considerably over the last several decades, but noise remains a contentious issue. The ability to fly complex flight paths with precision - both horizontally and vertically - can reduce cumulative noise exposure on the ground. Horizontally, the noise footprint can be moved to reduce overflight of the most crowded areas. Flight paths can also be shifted throughout the day to avoid repetitive overflights of the same area. In the vertical dimension, initial approach glidepath angles and power settings can be made more favorable to noise reduction on the ground.

One method for reducing noise (and in some cases maintaining terrain clearance) is to fly approaches at glidepath angles steeper than the standard 3 deg. Since the Instrument Landing System (ILS) glideslope is fixed in space, an aircraft equipped only

with ILS cannot arbitrarily use an off-nominal glidepath. Some flight management systems found in modern turbine aircraft allow for enhanced vertical flight profiles, but most of these rely on standard displays to establish vertical situational awareness. Unless the system includes a profile display, trajectory preview to allow the pilot to plan ahead is absent. Schemes involving one needle for guidance on a variable-slope glidepath or dual needles to represent “outer” and “inner” glideslopes are possible. Neither provides preview for spatial path awareness, however. This test was performed to demonstrate the enhanced spatial awareness on steeper-than-normal glidepaths that can be gained using a 3-D perspective display.

Existing Published Approach Procedure

The ILS approach to runway 32R at Moffett Field was used as a baseline. This procedure had a DH of 250 ft and a 3-deg glideslope.

Tunnel Overlay Procedure

Steep approaches were created that joined up with a standard 3-deg ILS glideslope close to the runway. Beyond 8 nm from touchdown, each approach descended on a normal 3-deg glideslope as seen in Figure 7.18. Approximately 7.5 nm from touchdown, the overlaid approach tunnel leveled off at 2,500 ft MSL. The approach continued until intersecting a 4.5-deg or 5-deg outer glideslope. When this steeper-than-normal glideslope intersected the normal glideslope approximately 2.5 nm from touchdown, the approach tunnel rejoined the 3-deg inner glideslope. This enabled the aircraft to remain high and at low power for reduced noise, but permitted a standard 3-deg descent during the final 2 nm of the approach. The steepest glidepath angle for the Queen Air was limited to 5 deg by engine shock cooling considerations.

Results

Figure 7.18 depicts flight data on these approaches, with an approach flown using the normal 3-deg glideslope displayed for reference. The pilot was able to follow the Tunnel-in-the-Sky display's vertical guidance with no observed difficulty. The vertical RMS FTE was 35.2 ft for the 4.5-deg glideslope, 14.7 ft for the 5.0-deg glideslope, and 12.4 ft for the normal 3.0-deg glideslope. FTE for the 4.5-deg glideslope may have been highest because it was performed first; a more complete set of approaches would be needed to compensate for learning effects. The pilot stated that although it was not difficult to interpret the changes in tunnel slope as they appeared on the display, a stronger cue to these changes would have been useful. For example, a cue 15 sec in advance of the flight path angle changing from level to a 5-deg descent would have helped him plan for changes to flaps, landing gear, and power.

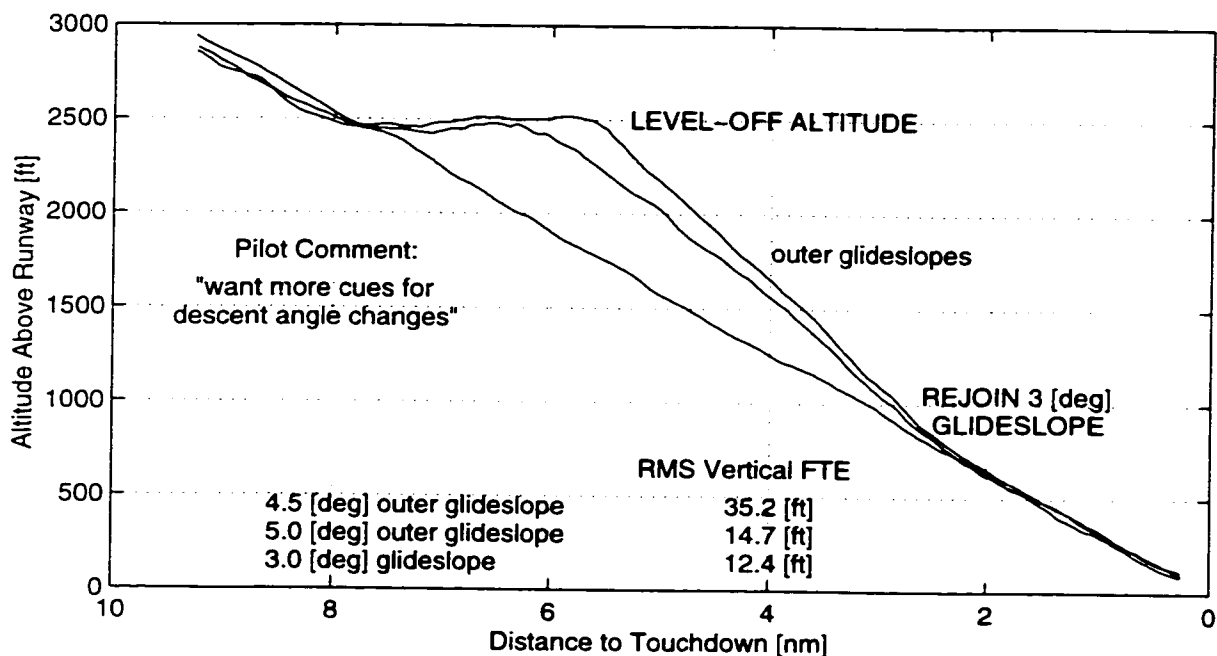


Figure 7.18 Profile View of Moffett Field Noise-Reducing Approaches

Discussion

Enhanced navigation and situational awareness on complex noise-abatement approach and departure procedures could provide significant benefits for aircraft operating in populated areas. This experiment demonstrated Tunnel-in-the-Sky guidance for approaches with changing glidepath angles.

The test pilot's request for stronger vertical cues alludes to one of the accepted advantages of perspective displays - trajectory preview. This is simple to interpret in the case of turns, where the tunnel ahead can be seen turning out the side of the display. However a 2-deg change in glidepath angle produces a much more subtle effect when mapped through perspective projection onto the display. Evidently, the pilot did not recognize such changes in vertical glidepath as easily. The design of augmented cues for glidepath angle changes remains a subject of future study.

7.6 Generating a Prototype Flight Technical Error Dataset

The design of domestic instrument approaches is governed by the United States Standard for Terminal Instrument Procedures (TERPS) [FAA-TERPS93]. The specified criteria include protection envelopes for terrain and other obstructions. These criteria are based partly on the NSE and FTE available with applicable navigation sensor and guidance technology.

The operational flexibility and lower FTE possible with WAAS or LAAS and improved displays could lead to curved approaches and missed approaches with greater utility. However, changing current certification criteria will require flight data to guide these changes. An experiment was flown to generate prototypical data that could be valuable for Tunnel-in-the-Sky procedure criteria. The experiment was flown on the Beechcraft Queen Air with the 3,000-hour Commercial Pilot as the test subject. The

objective was to obtain quantitative results as a model for constructing future statistically significant tests with multiple pilots.

Procedure

A family of trajectories composed of straight and curved segments was flown at 9,500 ft over the San Francisco Bay Area. The turbulence was light during this evening flight. Turns of 30, 60, 90, and 180 deg were flown with radii ranging from 750 m to 3,000 m. The tightest turn radius of 750 m was much smaller than found in normal instrument flying practice (it resulted in a nominal bank angle of approximately 30 deg at 120 kt) but was included to explore the limits of system capability. The patterns were flown with the pilot wearing view-limiting glasses and a safety pilot in the right seat.

Results

The experiment resulted in a database of 76 min flying controlled straight lines and over 30 min in turning flight. The actual flight tracks are shown in Figure 7.19.

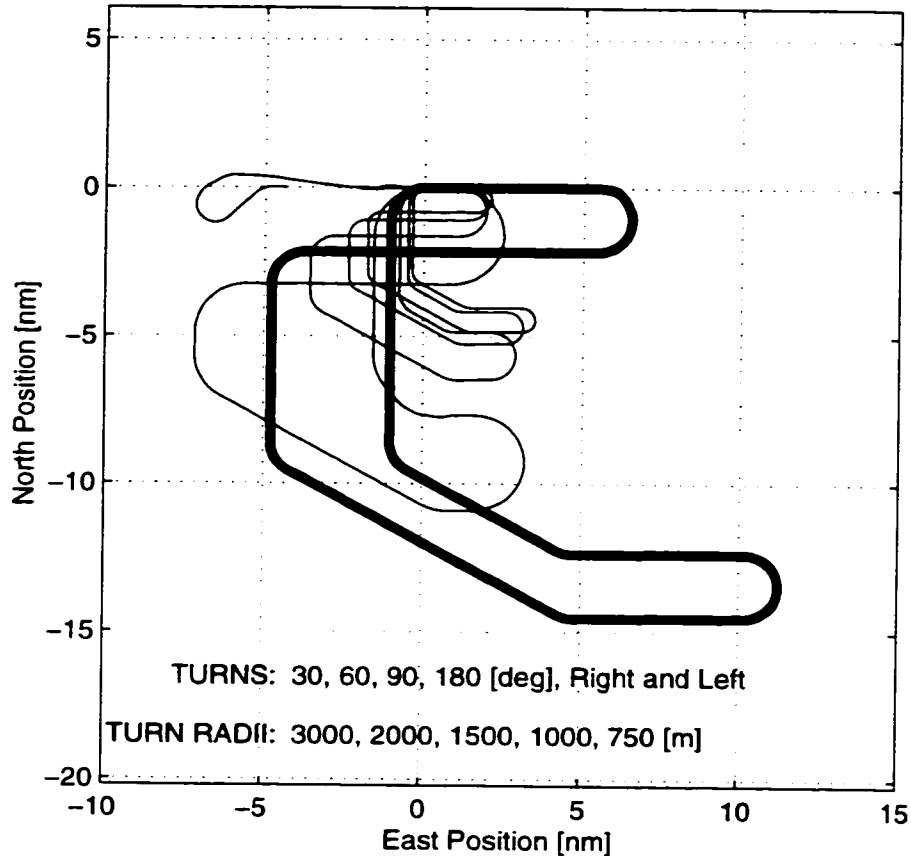


Figure 7.19 Prototype FTE Dataset Patterns (Actual Flight Data)

On straight segments the lateral and vertical RMS FTEs were 21.8 ft. and 11.8 ft. respectively. On curved segments the corresponding average figures were 38.2 ft and 15.8 ft. RMS FTE values and maximum deviations experienced on straight and curved segments are presented in Table 7.1 along with straight-in ILS figures from [Knox93] for comparison. The Tunnel-in-the-Sky accuracy figures obtained are better than typical values for ILS at the DH.

Although it was expected that decreasing the turn radius would result in increased FTE, this was not a strong trend. FTE for the 750-m radius case was less than twice the FTE for the 3,000-m radius turns.

Table 7.1 Prototype FTE Dataset Results

	Lateral RMS FTE [ft]	Lateral MAX FTE [ft]	Vertical RMS FTE [ft]	Vertical MAX FTE [ft]
ILS [Knox93]	187.2		56.8	
ILS at 200 ft [Knox93]	109.7		19.3	
Tunnel Straight (76 min)	21.8	127.9	11.8	57.0
Tunnel Curved (30 min)	38.2	202.6	15.8	89.1

Discussion

As might have been expected, the FTE on curved segments was not as small as that on straight segments of tunnel. However, the *maximum* deviations seen on *curved* segments are of comparable order of magnitude to *RMS* values for the *straight-in* ILS! The data reinforces the trend that Tunnel-in-the-Sky displays can provide excellent path following accuracy with improved ease of use.

Data of this type is expected to be useful in developing database and certification requirements for new procedures that take advantage of Tunnel-in-the-Sky displays. For

this purpose a large statistically significant database using multiple pilots and multiple aircraft will be required.

7.7 General Discussion

The operational flight test program provided a wealth of experience at relatively low cost. This section summarizes some of the specific flight test results, while Chapter 8 presents observations in the context of the entire research effort.

The Tunnel-in-the-Sky display enabled accurate straight-in approaches to be flown with relative ease. Complex curved, segmented, traffic pattern, and skywriting procedures demonstrated the flexibility of the display. Complex procedures were flown with no inflight training, and all pilots who flew with the Tunnel-in-the-Sky display felt it was easy to learn and fly. This ease of use should enhance safety for instrument pilots who are unable to exercise their skills regularly.

The accuracy demonstrated on complex paths suggests that curved approaches and missed approaches can improve the utility of terrain-limited airports. This significant operational benefit can be realized only with improved situational awareness of the aircraft's state and the desired flight path in three dimensions.

The Tunnel-in-the-Sky display generally enhanced situational awareness and allowed pilots to divide attention between procedural tasks and aircraft control. Although not mentioned above, a horizontal situation display (with moving map, weather, traffic, and terrain) would be integral to a cockpit suite designed for high situational awareness.

Tunnel overlay approaches demonstrated that Tunnel-in-the-Sky benefits can be enjoyed today. Introducing precision WAAS vertical guidance and an intuitive display to enhance situational awareness can eliminate the high workload of non-precision

approaches. Doing away with this unnecessary complexity and the associated CFIT risk could provide a major safety benefit for all aviation operators.

Tunnel overlay approaches for parallel runway operations and noise abatement were also demonstrated. Pilots requested enhanced cues for managing changes in glidepath, airspeed, flaps, landing gear, and engine cooling. Overlay approaches were useful enough that in the summer of 1998, two additional overlays were developed and flown at mountainous airports in Alaska (the LDA runway 8 at Juneau and the LDA/DME runway 22 at Petersburg).

An FTE database was generated as a prototype for developing new approach criteria. Average lateral and vertical RMS FTEs were 38.2 ft and 15.8 ft respectively in curved flight. The overall performance of the Tunnel-in-the-Sky display was significantly better than normally achieved with hand-flown ILS procedures, while providing the additional benefit of seamless guidance on straight *and* curved paths.

Clearly, the limited numbers of flight hours and test pilots indicate that the results presented are qualitative. It is hoped that resources may be available in the future to conduct statistically significant multiple-pilot studies. The purpose of this flight test program was to gain a breadth of operational experience to focus further research in this area. These results suggest that the Tunnel-in-the-Sky display can provide significant safety and utility benefits. Future research that balances the human machine interface, implementation, and operations “pillars” will be important to widespread adoption of the technology.

Chapter 8:

Conclusion

This project's dual objectives, increased safety through situational awareness and enhanced utility through flight-path flexibility, were demonstrated using a balanced approach of the three supporting "pillars." Results of piloted simulation and low-cost flight testing are summarized in Section 8.1, and general conclusions are drawn in Section 8.2. Sections 8.3 and 8.4 discuss further work on aviation and non-aviation applications of synthetic vision technology.

8.1 Summary of Results

This project's *low-cost, operationally oriented* approach was validated by a successful flight test program that encompassed operations with two aircraft at six different airports in California and Alaska. A total of 115 Tunnel-in-the-Sky approaches were made, five of which were flown in actual instrument conditions. The results of the test campaigns are summarized below under the pillar headings of human-machine interface, implementation, and operations.

8.1.1 Human-Machine Interface Results

- H-1. Initial piloted simulation tests indicated that the Tunnel-in-the-Sky display reduced FTE to approximately one half that provided by an ILS needle display on straight-in approaches.
- H-2. Pilots uniformly reported that perception and control was most difficult in the vertical dimension with the original display. After the resulting display modifications, lateral and vertical FTE values dropped respectively to approximately 25 and 45 percent of their original values. There were no further reports of difficulty perceiving and controlling small flight path deviations.
- H-3. Flight path deviations were more easily identified with the Tunnel-in-the-Sky display than with conventional instruments, allowing the pilot to correct for errors sooner. The Tunnel-in-the-Sky display allowed separate presentation of position and orientation errors that are normally combined on a flight director display.
- H-4. Flight testing on straight flight paths showed that the Tunnel-in-the-Sky display enabled better path-following accuracy than conventional displays. (Tunnel-in-the-Sky lateral FTE was 21.8 ft versus a 109.7 ft conventional reference; vertical RMS FTE was 11.8 ft versus 19.3 ft.) Additionally, the display enabled accurate following of *curved* paths, a capability lacking in conventional light aircraft instrumentation.
- H-5. Greater accuracy could probably be achieved by further tuning of the guidance algorithms. Two obvious approaches would be tightening the corner tick mark spacing and further quickening of the predictor symbol.

However, accuracy gains would be expected to require greater pilot workload. These parameters must be carefully tuned to the flight operation and aircraft involved.

- H-6. Pilots stated that the display was easier to fly than current instruments, giving them more time to plan for other cockpit events. Reductions in subjective workload were probably due to pilots' use of an error neglecting control strategy.
- H-7. Test pilots learned to fly the Tunnel-in-the-Sky display with almost no training and readily progressed to flying complex flight trajectories by instrument reference. *New pilots flew Tunnel-in-the-Sky approaches more accurately than experienced pilots fly conventional procedures today.* (In fact, the FTE values generated by the 1.5-hr student pilot were less than one third of typical values for trained pilots.)

8.1.2 Implementation Results

- I-1. The prototype Tunnel-in-the-Sky system was successfully and inexpensively operated on small piston aircraft. The form, weight, and power constraints of light aircraft can be met by existing low-cost technologies.
- I-2. A target system cost of \$20,000 appears to be reasonable for commercialization on a large scale. Continuing demand for sensors, displays, and computers will enable rapid improvements in Tunnel-in-the-Sky system cost/performance ratio.

- I-3. The low-cost approach to hardware design resulted in a simple system that allowed for rapid prototyping (a few hours or less) of display improvements and development of new flight procedures.
- I-4. Sensor accuracy, responsiveness, and jitter requirements are determined by the task and the needs of the human sensory system. DGPS (in WAAS or LAAS varieties) and low-cost inertial devices are currently the sensors of choice for Tunnel-in-the-Sky display systems.
- I-5. Accurate modeling of the earth's curved shape is required for the computer-generated environment to correctly match the real world over large geographical areas. Realtime algorithms for curved-path navigation on the earth geoid were developed. The computational cost of geoid modeling was negligible for well-designed algorithms.
- I-6. Ongoing experience and pilot evaluations from flight tests were invaluable to continuous display format improvement. Deviation indicators, predictor guidance, high-contrast symbology, and display decluttering were all added in response to pilot suggestions. Pilots stressed that a complete cockpit suite would include a horizontal navigation display to complement the Tunnel-in-the-Sky display.

8.1.3 Operations Results

- O-1. The Tunnel-in-the-Sky display allowed pilots to fly straight-in, curved, and segmented approaches with high accuracy on the two test aircraft. (RMS FTE segmented approach values were 52.7 ft lateral and 50.7 ft vertical, while values on straight lines were 21.8 ft lateral and 11.8 ft vertical.) With the exception of straight-in approaches, conventional

instruments cannot provide acceptable guidance for these procedures. Straight and curved flight paths produced repeatable ground tracks even in the presence of varying winds. *This flexibility to specify arbitrary 3-D procedures may be the single greatest aviation utility benefit of DGPS.*

- O-2. Experiments showed that lateral and vertical flight path intercepts could be executed more smoothly with the Tunnel-in-the-Sky display than with an ILS needle display. For example, one pilot was able to make a tactical deviation for traffic and still rejoin the curved tunnel approach just before landing. These capabilities were enabled by improved situational awareness of the aircraft's position relative to the desired flight path.
- O-3. By making instrument procedures easier to fly, aircrews can spend more time establishing general situational awareness of aircraft state, terrain, traffic, and weather. Natural, intuitive displays can thereby provide significant safety benefits.
- O-4. Very complex path guidance was demonstrated by a "skywriting" application. Such guidance is expected to be of value in specialized aviation applications described in Section 8.4.
- O-5. Tunnel overlay approaches permit benefits *within today's ATC system*. These approaches integrate seamlessly with current ATC procedures since they are transparent to controllers on the ground.
- O-6. A precision tunnel approach overlaid on a non-precision VOR/DME procedure enabled long, stabilized descents to the runway. This resulted in an order of magnitude decrease in RMS FTE (from 295.7 ft to 21.1 ft) while eliminating unnecessary aircraft configuration changes. *Eliminating*

the situational awareness problems of non-precision approaches may be the single greatest aviation safety benefit of DGPS.

- O-7. Approaches can be flown with high accuracy and low workload that could enable bad-weather *closely spaced parallel approaches*. Cumulative lateral RMS FTE over a long 20-nm final approach was reduced by more than an order of magnitude (from 517.0 ft to 23.8 ft) relative to a conventional localizer needle display.
- O-8. Perspective displays can facilitate complex approach and departure procedures for *noise abatement*. Vertical guidance on steeper-than-normal approaches allowed the pilot to accurately transition to a standard glideslope on short final approach. (Vertical RMS FTE for a 5 deg to 3 deg glideslope transition was only 14.7 ft.) Stronger vertical preview cues would aid in aircraft configuration planning during the approach.
- O-9. A prototype FTE database was collected over 106 minutes of straight and curved flight segments. RMS FTEs on straight segments were 21.8 ft lateral and 11.8 ft vertical, while on curved segments they were 38.2 ft lateral and 15.8 ft vertical. This type of data is expected to be useful in development of certification standards for Tunnel-in-the-Sky procedures.

8.2 Project Conclusions

Integration of GPS, inertial, flat-panel display, and computer graphics technologies resulted in a low-cost Tunnel-in-the-Sky system prototype. *The flight tests of this prototype encompassed the widest known range of procedure types, operational environments, airports, and pilots to date.* Ongoing trends in enabling technologies suggest that Tunnel-in-the-Sky displays may soon become commercially viable for all

aircraft categories. Before certification for use in personal general aviation aircraft or airline transports, however, statistically significant human factors studies will be required.

Increased situational awareness and reduced workload can enhance safety across the entire spectrum of aviation, from light airplanes to highly automated transports. Flexible, accurate navigation along complex flight paths can enhance aircraft and airport utility. Demonstrating these safety and utility objectives benefited from a novel integrated approach that addressed the human-machine interface, implementation technology, and operational issues.

8.3 Related and Future Work

As discussed in Chapter 2, some Tunnel-in-the-Sky researchers have used powerful graphics computers to depict terrain on the display. This information is useful in establishing situational awareness of the surrounding environment. If the aircraft ever leaves the tunnel for some reason, tactical terrain avoidance becomes necessary since procedural safety benefits of being inside the tunnel are lost.

Low-cost graphics hardware that could display realtime terrain was not available when the prototype system was designed. In the meantime, demand for 3-D games and multimedia resulted in inexpensive PC graphics processors that can do this job. [Alter98] describes hardware and software upgrades to the Stanford Tunnel-in-the-Sky system that enabled terrain depiction at low cost. This hardware has since been used to fly complex curved procedures in California and Alaska, with novel terrain depiction and alerting methods being explored.

NASA's Synthetic Vision research program employs two Silicon Graphics Onyx computers for terrain display onboard a Convair NC-131H (the same aircraft as that used

in [Filarsky83]). The Advanced General Aviation Transport Experiments (AGATE) consortium of industry-university-government partners initiated by NASA in 1994 is also working to create a Highway-in-the-Sky (HITS) display for general aviation aircraft. The AGATE display is planned to include terrain.

Terrain databases for commercial use will require certification of accuracy and integrity [Nordwall98]. Such terrain and obstacle data standards are currently in development by RTCA Special Committee 0193 and EUROCAE Working Group 44. An important source of integrity data will be NASA's 2000 Shuttle Radar Topography Mission, which will gather topography measurements over nearly 80% of the earth's surface. Data is expected to be released after a two-year processing period [Scott99]. Issues related to inflight databases (including terrain, airports, and cultural features) are discussed in [Möller94] and [Schiefele97].

Better quantification of pilot workload would be valuable to Tunnel-in-the-Sky researchers. [Regal95] and [Alter99] both measured workload using a secondary task in piloted simulation experiments. Although both experiments determined that the Tunnel-in-the-Sky display lowers workload, statistically significant workload measurements in actual flight conditions would be very useful.

Benefits for Closely Spaced Parallel Approaches (CSPA) and noise abatement are areas in need of further operational testing. Using a datalink such as Automatic Dependent Surveillance-Broadcast (ADS-B), display of traffic approaching the parallel runway could enhance CSPA situational awareness [Jennings99]. Modeling and display of the lead aircraft's probable wake vortex location using in-situ wind measurements would provide the ultimate solution for preserving airport capacity in bad weather. The environmental and human impact of aircraft noise will only increase with urban sprawl and growth in air travel. Departure and approach procedures that benefit from precision

Tunnel-in-the-Sky guidance can reduce community noise exposure. Future work in this area could pay dividends in preserving the ability of aviation operators to fly around the clock. Obviously, operational limitations, traffic mix, local conditions, and - above all - safety must be considered before implementing any new capabilities.

This author cautions against visual realism as an end in itself for synthetic vision displays. Photorealistic depictions of visual scenes will eventually be available at low cost. However, the layperson's desire for stunning realism in computer graphics should not guide the design of aviation displays. A cockpit instrument should display the essential information required to accomplish the desired task; it should not display anything more that would detract from the essential information. To use an analogy from electrical engineering, *the display should maximize signal-to-noise ratio*. In this regard, terrain texturing using satellite imagery, cultural features on the ground, and clouds in the sky should all be scrutinized as display elements. No more visual decoration than is necessary for a particular application should be included.

8.4 Future Synthetic Vision Applications

Flight training is a logical beneficiary of Tunnel-in-the-Sky technology. Perspective displays could aid initial students in learning to fly instrument approach procedures while easing recurrent training requirements for experienced pilots. While Tunnel-in-the-Sky displays coexist with conventional instruments, the perspective display could be used as a training aid for the older needle-based instruments!

Future Air Traffic Management schemes such as Free Flight can derive safety and operational gains by moving beyond the constraints of today's navaid and display systems. These scenarios may require full-time navigation in *four* dimensions (the fourth being time) to make efficient use of airspace, time, and fuel. Helicopters in particular can benefit from 4-D procedures that allow them to mix with fixed-wing instrument traffic.

This increased level of control will make the need for better displays and situational awareness all the more urgent. 4-D capability may be required during gate pushback, taxi, takeoff, enroute cruise, terminal area maneuvering, approach, and final taxi to the arrival gate.

Visual flight corridors are being designated in the United States for small aircraft operating in congested terminal airspace. Following these corridors today requires detailed map reading and communications procedures. Depiction of such corridors on a Tunnel-in-the-Sky display would relieve some of this burden and reduce accidental incursions into busy airspace.

Specialized aviation users may also benefit from the Tunnel-in-the-Sky concept. Any flight operation requiring high positional accuracy or ground track repeatability is a candidate for better flight displays. These include search and rescue, flight testing, flight inspection, remote sensing, aerial pesticide application, aerial fire fighting, and photogrammetry. Pilot training for these missions can also be greatly reduced while accuracy is increased.

Military and non-aviation applications for synthetic vision technology also exist. Control, rendezvous, and teleoperation of land, marine, submarine, and space vehicles are all areas rich with possibility. Wearable computers coupled with unobtrusive sensors and displays will become viable and lead to widespread use of synthetic and enhanced vision.

8.5 Epilogue

A paradigm shift in cockpit instruments will be a complex enterprise. Issues go beyond better display formats to technical constraints, human factors considerations, operational concepts, initial and recurring training, and political skill within the aviation

and regulatory communities. Transferring this technology from research curiosity to commercial viability will require an integrated, systems engineering approach.

The combination of low-cost position and attitude sensors with embedded computer graphics is an undeniably powerful one, and it will eventually be the standard within aviation despite current teething pains. The aircraft guidance application investigated here is but one application of synthetic vision, however, and the technology will probably find its widest use *outside* of aviation. This compelling way of looking at the world will enable people to operate vehicles at new levels of safety and utility.

References

- [Alter98] K. W. Alter, A. K. Barrows, P. Enge, C. W. Jennings, B. W. Parkinson, and J. D. Powell, "Inflight Demonstrations of Curved Approaches and Missed Approaches in Mountainous Terrain," *Proceedings of ION GPS-98*, pp. 1165-1172, Nashville, Tennessee, Sept. 15-18, 1998.
- [Alter99] K. W. Alter and J. D. Powell, "An Investigation into Augmented Flight Display Symbolologies for Precision Instrument Approaches," *Proceedings of the Tenth International Symposium on Aviation Psychology*, pp. 190-196, Columbus, Ohio, May 3-6, 1999.
- [Below97] C. Below, H. von Viebahn, M. Purpus, "Flight Tests of The 4D Flight Guidance Display," *Proceedings of SPIE Enhanced and Synthetic Vision*, pp. 74-80, Orlando, Florida, April 21-22, 1997.
- [Bray81] R. S. Bray and B. C. Scott, "A Head-up Display for Low Visibility Approach and Landing," *Proceedings of AIAA 19th Aerospace Sciences Meeting*, St. Louis, Missouri, Jan. 12-15, 1981.
- [Brooks97] P. E. Brooks, "Our Legacy is Safety on the Road Ahead," *Flightline*, Allied Pilots Association, Arlington, Texas, pp. 16-22, Jul./Aug. 1997.

- [Cohen94a] C. E. Cohen, B. W. Parkinson, and B. D. McNally, "Flight Tests of Attitude Determination Using GPS Compared Against an Inertial Navigation Unit," *Journal of The Institute of Navigation*, Vol. 41, No. 1, pp. 83-97, Spring 1994.
- [Cohen94b] C. E. Cohen, D. G. Lawrence, B. S. Pervan, H. S. Cobb, A. K. Barrows, J. D. Powell, and B. W. Parkinson, "Flight Test Results of Autocoupled Approaches Using GPS and Integrity Beacons," *Proceedings of ION GPS-94*, pp. 1145-1153, Salt Lake City, Utah, Sept. 20-23, 1994.
- [Cramer96] M. R. Cramer, "Operational Considerations in Improving Access to Juneau, Alaska," *IEEE Position Location and Navigation Symposium*, pp. 368-372, Atlanta, Georgia, April 22-26, 1996.
- [CSI98] Communication Systems International, LGBX-PRO DGPS Receiver Reference Manual, Calgary, Alberta, 1998.
- [DMA91] United States Department of Defense, Defense Mapping Agency, *World Geodetic System 1984*, DMA Technical Report 8350.2, Sept. 1991.
- [Dorighi93] N. S. Dorighi, S. R. Ellis, and A. J. Grunwald, "Perspective Format for a Primary Flight Display (ADI) and Its Effect on Pilot Spatial Awareness," *Proceedings of the Human Factors and Ergonomics Society 37th Annual Meeting*, pp. 88-92, 1993.
- [Enge96] P. Enge, T. Walter, S. Pullen, C. Kee, Y. C. Chao, and Y. J. Tsai, "Wide Area Augmentation of the Global Positioning System," *Proceedings of the IEEE*, Vol. 84, No. 8, pp. 1063-1088, Aug. 1996.
- [Enge99] P. Enge, "Local Area Augmentation of GPS for the Precision Approach of Aircraft," *Proceedings of the IEEE*, Vol. 87, No. 1, pp. 111-132, Jan. 1999.
- [FAA-AIM90] United States Department of Transportation, Federal Aviation Administration, *Airman's Information Manual*, 1990.

- [FAA-TERPS93] United States Department of Transportation, Federal Aviation Administration, *United States Standard for Terminal Instrument Procedures (TERPS)*, Third Edition, U.S. Government Printing Office, Aug. 1993.
- [Filarsky83] S. M. Filarsky and G. W. Hoover, "The Command Flight Path Display," *1983 SID International Symposium - Digest of Technical Papers*, pp. 196-197, Philadelphia, Pennsylvania, May 10-12, 1983.
- [Grunwald81] A. J. Grunwald, J. B. Robertson, and J. J. Hatfield, "Experimental Evaluation of a Perspective Tunnel Display for Three-Dimensional Helicopter Approaches," *AIAA Journal of Guidance and Control*, Vol. 4, No. 6, pp. 623-631, Nov.-Dec. 1981.
- [Grunwald84] A. J. Grunwald, "Tunnel Display for Four-Dimensional Fixed-Wing Aircraft Approaches," *AIAA Journal of Guidance, Control, and Dynamics*, Vol. 7, No. 3, pp. 369-377, May-June 1984.
- [Grunwald85] A. J. Grunwald, "Predictor Laws for Pictorial Flight Displays," *AIAA Journal of Guidance, Control, and Dynamics*, Vol. 8, No. 5, pp. 545-552, Sept.-Oct. 1985.
- [Grunwald96a] A. J. Grunwald, "Improved Tunnel Display for Curved Trajectory Following: Control Considerations," *AIAA Journal of Guidance, Control, and Dynamics*, Vol. 19, No. 2, pp. 370-377, March-April 1996.
- [Grunwald96b] A. J. Grunwald, "Improved Tunnel Display for Curved Trajectory Following: Experimental Evaluation," *AIAA Journal of Guidance, Control, and Dynamics*, Vol. 19, No. 2, pp. 378-384, March-April 1996.
- [Hayward97] R. C. Hayward, D. Gebre-Egziabher, M. Schwall, J. D. Powell, and J. Wilson, "Inertially Aided GPS Based Attitude Heading Reference System (AHRS) for General Aviation Aircraft," *Proceedings of ION GPS-97*, pp. 289-298, Kansas City, Missouri, Sept. 16-19, 1997.

- [Hayward99] R. C. Hayward, A. H. Marchick, and J. D. Powell, "Two Antenna GPS Attitude and Integer Ambiguity Resolution Integrity for Aircraft Applications," *Proceedings of ION National Technical Meeting*, San Diego, California, Jan. 25-27, 1999.
- [Houck99] S. W. Houck, A. K. Barrows, B. W. Parkinson, P. Enge, and J. D. Powell, "Flight Testing WAAS for Use in Closely Spaced Parallel Approaches," *Proceedings of ION GPS-99*, Nashville, Tennessee, Sept. 14-17, 1999.
- [Jennings99] C. W. Jennings, K. W. Alter, A. K. Barrows, P. Enge, and J. D. Powell, "3-D Perspective Displays for Guidance and Traffic Awareness," *Proceedings of ION GPS-99*, Nashville, Tennessee, Sept. 14-17, 1999.
- [Kayton97] M. Kayton and W. R. Fried, *Avionics Navigation Systems, Second Edition*, John Wiley & Sons, New York, 1997.
- [Kee91] C. Kee, B. W. Parkinson, and P. Axelrad, "Wide Area Differential GPS," *Journal of The Institute of Navigation*, Vol. 38, No. 2, pp. 123-145, Summer 1991.
- [Kornfeld98] R. P. Kornfeld, R. J. Hansman Jr., and J. J. Deyst, "Single Antenna GPS Based Aircraft Attitude Determination," *Proceedings of the ION National Technical Meeting*, Long Beach, California, Jan. 21-23, 1998.
- [Knox93] C. E. Knox, "Manual Flying of Curved Precision Approaches to Landing With Electromechanical Instrumentation - A Piloted Simulation Study," NASA Technical Paper 3255, 1993.
- [Lawrence96] D. G. Lawrence, "Aircraft Landing Using GPS," Stanford University Ph.D. Dissertation, Department of Aeronautics and Astronautics, Sept. 1996.
- [Möller94] H. Möller and G. Sachs, "Synthetic Vision for Enhancing Poor Visibility Flight Operations," *IEEE Aerospace and Electronic Systems*, Vol. 9, No. 3, pp. 27-33, March 1994.

- [Neider93] J. Neider, T. Davis, and M. Woo, *OpenGL Programming Guide*, Addison-Wesley, Reading, Massachusetts, 1993.
- [Nordwall94] B. D. Nordwall, "Aircraft Radar Used for Precision Approaches," *Aviation Week & Space Technology*, pp. 51, Oct. 17, 1994.
- [Nordwall98] B. D. Nordwall, "Terrain Database Concerns Slow Advanced Cockpit Displays," *Aviation Week & Space Technology*, pp. 58-60, April 20, 1998.
- [Norman89] D. A. Norman, *The Design of Everyday Things*, Doubleday/Currency, New York, 1989.
- [NTSB2000] National Transportation Safety Board, *Controlled Flight Into Terrain, Korean Air 801*, Aircraft Accident Report 00/01, Jan. 2000.
- [Parkinson96] B. W. Parkinson, "GPS Error Analysis," in *Global Positioning System: Theory and Applications*, Vol. 1, B. W. Parkinson and J. J. Spilker Jr. (eds.), pp. 469-483, American Institute of Aeronautics and Astronautics, Washington, D.C., 1996.
- [Parrish94] R. V. Parrish, A. M. Busquets, S. P. Williams, and D. E. Nold, "Spatial Awareness Comparisons Between Large-Screen, Integrated Pictorial Displays and Conventional EFIS Displays During Simulated Landing Approaches," NASA Technical Paper 3467, Sept. 1994.
- [Pervan96] B. S. Pervan, "Navigation Integrity for Aircraft Precision Landing Using the Global Positioning System," Stanford University Ph.D. Dissertation, Department of Aeronautics and Astronautics, March 1996.
- [Proctor94] P. Proctor, "HGS Offers Airlines Safety, Economic Edge," *Aviation Week & Space Technology*, pp. 50-53, Dec. 12/19, 1994.
- [Proctor97] P. Proctor, "Major Airlines Embrace Enhanced GPWS," *Aviation Week & Space Technology*, pp. 46-48, April 21, 1997.

- [Regal95] D. M. Regal and D. Whittington, "Guidance Symbolology for Curved Flight Paths," *Proceedings of the Eighth International Symposium on Aviation Psychology*, Columbus, Ohio, 1995.
- [Reising95] J. M. Reising, M. Liggett, T. J. Solz, and D. C. Hartsock, "A Comparison of Two Head Up Display Formats Used to Fly Curved Instrument Approaches," *Proceedings of the Human Factors Society 39th Annual Meeting*, pp. 1-5, San Diego, CA, October 1995.
- [RTCA98] *Minimum Aviation System Performance Standards for Local Area Augmentation System (LAAS) DRAFT*, Appendix C, RTCA, DO-245, Washington, D.C., Sept. 28, 1998.
- [Sachs98] G. Sachs, K. Dobler, P. Hermle, "Synthetic Vision Flight Tests for Curved Approach and Landing," *Proceedings of the AIAA/IEEE/SAE Digital Avionics Systems Conference*, pp. E51-1 - E51-8, Bellvue, Washington, Oct. 31 - Nov. 7, 1998.
- [Schiefele97] J. Schiefele, L. May, and H. Raabe, "A Concept for Creating In- and Pre-Flight Databases," *Proceedings of SPIE Enhanced and Synthetic Vision*, pp. 99-109, Orlando, Florida, April 21-22, 1997.
- [Scott99] W. B. Scott, "Flight to Radar-Map Earth From Space," *Aviation Week & Space Technology*, pp. 50-53, Sept. 20, 1999.
- [Swenson93] H. N. Swenson, R. D. Jones, and R. Clark, "Flight Evaluation of a Computer Aided Low-Altitude Helicopter Flight Guidance System," *Combat Automation for Airborne Weapon Systems: Man/Machine Interface Trends and Technologies*, AGARD Conference Proceedings No. 520, pp. 28-1 - 28-11, April 1993.
- [Theunissen94] E. Theunissen and M. Mulder, "Open and Closed Loop Control With a Perspective Tunnel-in-the-Sky Display," *Proceedings of AIAA Flight Simulation Technologies Conference*, Scottsdale, Arizona, Aug. 1-3, 1994.

- [Theunissen95] E. Theunissen, "Influence of Error Gain and Position Prediction on Tracking Performance and Control Activity with Perspective Flight Path Displays," *Air Traffic Control Quarterly*, Vol. 3, No. 2, pp. 95-116, 1995.
- [Theunissen97] E. Theunissen, *Integrated Design of a Man-Machine Interface for 4-D Navigation*, Delft University Press, Delft, The Netherlands, 1997.
- [Tufte83] E. R. Tufte, *The Visual Display of Quantitative Information*, Graphics Press, Cheshire, Connecticut, 1983.
- [van Grass91] F. van Grass and M. Braasch, "GPS Interferometric Attitude and Heading Determination: Initial Flight Test Results," *Journal of The Institute of Navigation*, Vol. 38, No. 4, pp. 297-316, Winter 1991-1992.
- [von Viebahn98] H. von Viebahn, "The 4-D Display," *Proceedings of the AIAA/IEEE/SAE Digital Avionics Systems Conference*, pp. E54-1 - E54-7, Bellvue, Washington, Oct. 31 - Nov. 7, 1998.
- [Walter94] T. Walter, C. Kee, Y. C. Chao, Y. J. Tsai, U. Peled, J. Ceva, A. K. Barrows, E. Abbott, J. D. Powell, P. Enge, and B. Parkinson, "Flight Trials of the Wide-Area Augmentation System (WAAS)," *Proceedings of ION GPS-94*, pp. 1537-1546, Salt Lake City, Utah, Sept. 20-23, 1994.
- [Watler81] J. F. Watler Jr. and W. B. Logan, "The Maneuvering Flight Path Display - An Update," *Fifth Advanced Aircrew Display Symposium Proceedings*, pp. 138-162, Patuxent River, Maryland, Sept. 15-16, 1981.
- [Wickens86] C. D. Wickens, "The Effects of Control Dynamics on Performance," in *Handbook of Perception and Human Performance*, K. R. Boff, L. Kaufman, and J. P. Thomas (eds.), pp. 39-1 - 39-60, John Wiley & Sons, New York, 1986.
- [Wickens89] C. D. Wickens, I. Haskell, and K. Harte, "Ergonomic Design for Perspective Flight-Path Displays," *IEEE Control Systems Magazine*, Vol. 9, No. 4, pp. 3-8, June 1989.

- [Wilckens70] V. Wilckens and W. Schattenmann, "Test Results With New Analog Displays for All-Weather Landings," *Problems of the Cockpit Environment*, AGARD Conference Proceedings No. 55, pp. 10-1 - 10-33, March 1970.
- [Yang94] L. C. Yang and R. J. Hansman Jr., "A Human Performance Evaluation of Enhanced Vision Systems for Approach and Landing," *Proceedings of SPIE Image Sensing, Processing, and Understanding for Control and Guidance of Aerospace Vehicles*, Orlando, Florida, April 1994.